Beyond Glucose Control: The Impact of Metformin on the Appetite-Suppressing Metabolite Lac-Phe and Fatty Acid Metabolism in Humans

A dissertation submitted to Trinity College Dublin in candidature for the degree of Doctor of Philosophy

School of Biochemistry and Immunology
Trinity Biomedical Sciences Institute
Trinity College Dublin, the University of Dublin

2025

By Barry Scott

Under the supervision of Prof. David Finlay

Declaration

I declare that this thesis has not been submitted as an exercise for a degree at this or any other university and it is entirely my own work unless otherwise stated in the figure legends.

I agree to deposit this thesis in the University's open access institutional repository or allow the library to do so on my behalf, subject to Irish Copyright Legislation and Trinity College Library conditions of use and acknowledgement.

I consent to the examiner retaining a copy of the thesis beyond the examining period, should they so wish (EU GDPR May 2018).

X 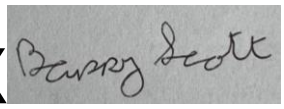

Barry Scott

Summary

Metformin, a widely used first-line treatment for type 2 diabetes (T2D), is known to reduce blood glucose levels, suppress appetite, and exert anti-inflammatory effects. However, despite extensive research on its clinical benefits, the precise molecular mechanisms through which metformin exerts its therapeutic effects remain only partially understood. To address this, we conducted a comprehensive analysis using untargeted metabolomics data from 11 cohorts, employing Liquid Chromatography-Mass Spectrometry (LC-MS) to explore the metabolic alterations associated with metformin treatment. This investigation began with our own in-house cohort, recruited by the lab, and was expanded to include data from 10 additional external cohorts.

Our analysis led us to focus on three primary areas: the impact of metformin on N-lactoyl phenylalanine (Lac-Phe), the relationship between Lac-Phe and feeding, and the effect of metformin on β-hydroxy fatty acids. To understand the relationship between metformin treatment and Lac-Phe levels, we analyzed untargeted metabolomics data from four cohorts—two observational and two interventional. We found a significant elevation of Lac-Phe in the blood of individuals treated with metformin, in both metabolically healthy individuals and those with T2D. This increase was consistent following either a single dose or sustained treatment.

Additionally, we investigated Lac-Phe levels in response to feeding using data from six cohorts—one observational and five interventional. Lac-Phe levels were observed to rise post-prandially under a range of feeding interventions, regardless

of the individuals' metabolic health status. However, interventions involving only glucose, such as the liquid Oral Glucose Tolerance Test (OGTT) or glucose infusion via euglycemic hyperinsulinemic clamp, resulted in only a modest rise in Lac-Phe, implying that the production of Lac-Phe is not solely dependent on caloric content but also on the type and composition of nutrients.

We examined the impact of metformin on β-hydroxy fatty acids across four cohorts—three observational and one interventional. We discovered that metformin treatment significantly increased the levels of these fatty acids, which are intermediates in the β-oxidation of fatty acids. Medium-chain β-hydroxy fatty acids are known to activate the G-protein-coupled receptors HCA3 and GPR84, both of which are involved in inflammatory pathways, with preliminary data suggesting these receptors may also influence appetite regulation. Our findings suggest that metformin may alter multiple metabolic pathways beyond glucose regulation by promoting the accumulation of both Lac-Phe and β-hydroxy fatty acids. This raises the possibility that these metabolites contribute to metformin's broader therapeutic benefits, including appetite suppression and anti-inflammatory effects. The evidence gathered across 11 cohorts underscores the robustness of these findings. Together, they provide new insights into the complex metabolic changes induced by metformin and open new avenues for exploring its mechanisms of action beyond glucose control.

Acknowledgements

Completing this PhD has been a challenging yet incredibly rewarding journey, and it wouldn't have been possible without the support, guidance, and encouragement of many wonderful people.

First and foremost, I would like to express my deepest gratitude to my two supervisors, Dr. Lydia Lynch and Dr. David Finlay. Lydia, thank you for providing me with the opportunity to pursue this research and for your support throughout the process. Your enthusiasm and dedication to science have been a constant source of inspiration. I would especially like to single out Dave, who stepped in at a pivotal moment when I was at a crossroads with my PhD. Without his encouragement and belief in my potential, particularly during a time when his own health was not at its best, I might not have continued on this path. Dave, your unwavering support and exceptional mentorship have made an immeasurable impact on my journey, and for that, I am profoundly grateful.

I would also like to extend a heartfelt thank you to Katie and Karen, who encouraged me to reach out to Dave as a potential supervisor. Without your guidance, I might not have connected with the mentor who would help steer my PhD to completion.

To all the members of both the Lynch lab and the Finlay lab, your camaraderie and support have been invaluable. When I transitioned to the new reading room after changing labs, having Aaron there made all the difference. His presence was both

comforting and energizing, and I always enjoyed our conversations, which brought a sense of familiarity and ease to the new environment. I would particularly like to acknowledge John, the other bioinformatician in the lab, for being a constant sounding board. It was helpful and fun to have someone with whom I could discuss ideas, share the challenges unique to our field. I always enjoyed the conversations.

I must also thank my parents, Jacqueline and Dermot, for their unwavering support throughout the years. Your belief in me has been a cornerstone of my resilience and determination, and I am deeply appreciative of all you have done for me.

To my wife, Caroline, words cannot express how grateful I am for your encouragement to pursue a different path after my career in trading. Your support has been my anchor through this entire process, and I am so thankful for your love and patience. Finally, to my two boys, Isaac and Oscar, thank you for being such a joyful distraction during the busy times. You've brought laughter and light into my life when I've needed it most, and I cherish the balance you've helped me maintain.

Publications

Metformin and feeding increase levels of the appetite-suppressing metabolite Lac-Phe in humans

Barry Scott, Emily A. Day, Katie L. O'Brien, John Scanlan, Grace Cromwell, Aine Ni Scannail, Marie E. McDonnell, David K. Finlay & Lydia Lynch.

Nature Metabolism, 2024.

Uptake of lipids from ascites drives NK cell metabolic dysfunction in ovarian cancer

Karen Slattery, Cong-Hui Yao, John Scanlan, **Barry Scott**, Joseph Patrick Crowley, Orla McGowan, Gavin McManus, Martin Brennan, Katie O'Brien, Kate Glennon, Edward Corry, Ann Treacy, Rafael J. Argüello, Marcia C. Haigis, Donal J. Brennan, Lydia Lynch.

Science Immunology In press.

Metformin elevates medium-chain β-hydroxy fatty acids in the bloodstream independently of diabetic status

Barry Scott, ……., Lydia Lynch & David K. Finlay.

Manuscript in preparation.

Table of Contents

List of Figures

List of Tables

Abbreviations

1,5-AG	1,5-anhydroglucitol
3-HADH	3-Hydroxyacyl-CoA dehydrogenase
β-OH-C10:0	β-hydroxydecanoate
β-OH-C8:0	β-hydroxy octanoate
β-OH-DC-C10:0	β-hydroxysebacate
ADP	Adenosine diphosphate
AFLP	Acute fatty liver of pregnancy
AMPK	AMP-activated protein kinase
ANOVA	Analysis of Variance
ARC	Arcuate nucleus
ATP	Adenosine triphosphate
AUC	Area under the curve
AgRP	Agouti-related peptide
BMI	Body Mass Index
CART	Cocaine and amphetamine regulated transcript
CCK	Cholecystokinin
CNDP1	Carnosine dipeptidase 1
CNDP2	Carnosine Dipeptidase 2
CO2	Carbon dioxide
CPT1	Carnitine palmitoyltransferase 1
CPT2	Carnitine palmitoyltransferase 2
CRT	Centre for Research Training
CSF	Cerebrospinal fluid

Cmax	Maximum serum concentration
DC	Dicarboxylic acid
DPN	Diabetic polyneuropathy
DRE	Digital rectal exam
EDRN	Early Detection Research Network
ER	Endoplasmic reticulum
ESI	Electrospray ionization
ETC	Electron transport chain
ETF	Electron Transfer Flavoprotein
ETFDH	Electron Transfer Flavoprotein Dehydrogenase
FADH2	Flavin adenine dinucleotide (reduced form)
FDG	Fluorodeoxyglucose
FFAR4	Free fatty acid receptor 4
GC-MS	Gas chromatography-mass spectrometry
GDF15	Growth Differentiation Factor 15
GLP-1	Glucagon-like peptide-1
GPCR	G-protein-coupled receptor
GPR81	G-protein-coupled receptor 81
GPR84	G-protein-coupled receptor 84
GTP	Guanosine triphosphate
HCA3	Hydroxycarboxylic Acid Receptor 3
HbA1c	Hemoglobin A1c
IRB	Institutional Review Board
LC-MS	Liquid Chromatography-Mass Spectrometry
LCFA	Long-chain fatty acid

LCHAD	Long-chain 3-hydroxy-acyl-CoA dehydrogenase
LSD	Least Significant Difference
Lac-Phe	N-lactoyl phenylalanine
Lac-Val	N-lactoyl valine
MATE1	Multidrug and toxin extrusion protein 1
MCAD	Medium-chain acyl-CoA dehydrogenase
MCFA	Medium-chain fatty acid
MCT1	Monocarboxylate Transporter 1
MELAS	Mitochondrial Encephalomyopathy, Lactic Acidosis,and Stroke-like episodes
MERRF	Myoclonic epilepsy with ragged-red fibers
MS	Mass spectrometry
MS/MS	Tandem mass spectrometry
MT-TL1	Mitochondrial leucyl-tRNA
MTP	Mitochondrial trifunctional protein
NAD+	Nicotinamide adenine dinucleotide (oxidized)
NADH	Nicotinamide Adenine Dinucleotide (reduced form)
NET	Neutrophil extracellular trap
NHS	National Health Service
NIH	National Institutes of Health
NIHR	National Institute for Health and Care Research
NMR	Nuclear magnetic resonance
NPY	Neuropeptide Y
OCT	Organic cation transporter
OGTT	Oral Glucose Tolerance Test

PET	Positron emission tomography
PKU	Phenylketonuria
PMAT	Plasma membrane monoamine transporter
POMC	Pro-opiomelanocortin
PSA	Prostate-specific antigen
PYY	Peptide YY
Prism	GraphPad Prism
R-squared	Coefficient of determination
ROC	Receiver Operating Characteristic
SCFA	Short-chain fatty acid
SERT	Serotonin transporter
SFI	Science Foundation Ireland
T2D	Type 2 Diabetes
TAME	Targeting Aging with Metformin
TCA	Tricarboxylic acid
UKPDS	United Kingdom Prospective Diabetes Study
UPLC-MS/MS	Ultra-high-performance liquid chromatography tandem mass spectroscopy
VIL1	Villin 1
VLCAD	Very-long-chain acyl-CoA dehydrogenase
m/z	Mass-to-charge ratio
t-test	Student's t-test

Chapter 1 - Introduction

1.1 Metabolism

Metabolism encompasses the broad set of chemical reactions within cells that are essential for maintaining life, providing the energy needed to fuel biological processes and generating the building blocks for cellular structures. These reactions are divided into two main processes: anabolism, which synthesizes large molecules such as proteins and nucleic acids from smaller precursors, and catabolism, which breaks down larger molecules. Catabolic pathways can produce ATP, which serves as the universal energy currency, connecting catabolic and anabolic processes. This ATP is not only essential for biosynthesis but also powers mechanical work, such as muscle contractions, and other cellular activities requiring energy[1].

1.1.1 Glycolysis

One of the central pathways in cellular metabolism is glycolysis, the primary mechanism for breaking down glucose—a key fuel derived from dietary carbohydrates[2]. Glycolysis is a multistep process that converts a single glucose molecule into two molecules of pyruvate[3]. This pathway is tightly regulated both allosterically and transcriptionally by enzymes sensitive to the cell's energy status, ensuring that glycolysis proceeds only when energy or metabolic intermediates are needed[4,5]. Each glucose molecule yields two molecules of ATP and one NADH, providing a modest amount of energy[6].

After glycolysis, pyruvate has two principal metabolic fates in mammals, each contributing to energy production under different conditions. When cells favor aerobic metabolism, pyruvate is converted into acetyl-CoA, a two-carbon unit that enters the tricarboxylic acid (TCA) cycle[7]. The TCA cycle, which occurs in the mitochondria, completes the oxidation of acetyl-CoA into carbon dioxide (CO_2) while producing NADH and $FADH_2$ [8]. These reduced cofactors feed into the electron transport chain, which drives ATP production through oxidative phosphorylation. This process is highly efficient, generating the majority of ATP under aerobic conditions[9].

Alternatively, in settings where oxidative metabolism is limited, such as during rapid energy demands or low oxygen availability, pyruvate is converted to lactate through lactic acid fermentation[10,11]. This regenerates NAD^+ from NADH, which is critical for maintaining the flow of glycolysis by ensuring a continuous supply of NAD^+ [12]. However, this process results in a lower net ATP yield, limited to the two ATP produced during glycolysis, without further energy extraction from the complete oxidation of glucose to CO_2 .

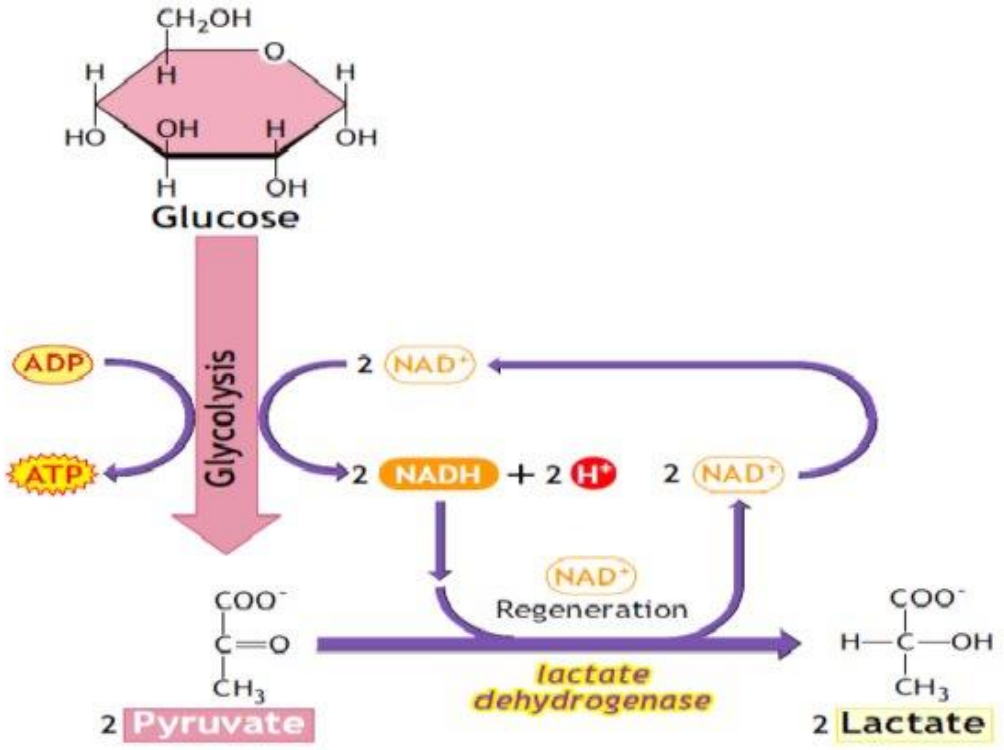

Figure 1.1. Glycolysis and lactic acid fermentation.

Glucose undergoes glycolysis, producing two molecules of pyruvate along with a net yield of two ATP and two NADH molecules. In aerobic glycolysis, pyruvate enters the tricarboxylic acid (TCA) cycle for further oxidation, generating large amounts of ATP. In anaerobic glycolysis, pyruvate is reduced to lactate by lactate dehydrogenase, regenerating NAD^+ from NADH and sustaining the glycolytic pathway.

Source: Adapted from McArdle et al., 2015[13]

1.1.2 Beta-oxidation

Beta-oxidation is a critical metabolic pathway responsible for the oxidation of fatty acids to generate ATP. This process primarily occurs in the mitochondria but can also take place in peroxisomes[14,15]. It provides a substantial source of energy,

contributing to approximately 80% of the body's energy production during periods of fasting[16]. Long-chain fatty acids (LCFAs), with chain lengths of 12 to 18 carbons, cannot directly cross the mitochondrial membranes and thus require the carnitine shuttle system for transport. Carnitine acts as a cofactor, facilitating the transport of LCFAs into the mitochondrial matrix, where β-oxidation occurs[17]. This system is mediated by two key enzymes: carnitine palmitoyltransferase 1 (CPT1), located in the outer mitochondrial membrane, and carnitine palmitoyltransferase 2 (CPT2), situated in the inner mitochondrial membrane. In contrast, short- and medium-chain fatty acids (SCFAs and MCFAs) with chain lengths of at least up to 8 carbons can cross the mitochondrial membrane in their nonesterified form and are activated inside the matrix, bypassing the carnitine shuttle[18–20].

Once inside the mitochondrial matrix, fatty acids undergo a multistep process of repeated oxidations at the β-carbon, transferring reducing equivalents in the form of NADH and FADH2 to the electron transport chain (ETC) to drive ATP synthesis. Each cycle of β-oxidation also generates acetyl-CoA, which enters the tricarboxylic acid (TCA) cycle to further contribute to ATP production[21].

Each round of β-oxidation involves four enzymatic steps, resulting in the shortening of the fatty acid chain by two carbons. The steps, along with their corresponding enzymes and cofactors, are as follows[21]:

1. Dehydrogenation of acyl-CoA to trans-Δ^2-enoyl-CoA, catalyzed by acyl-CoA dehydrogenase. This step introduces a double bond between the α and β

carbons and reduces FAD to FADH2. The enzyme transfers electrons from FADH2 to the electron-transferring flavoprotein (ETF), feeding into the respiratory chain.

2. Hydration of trans-Δ^2-enoyl-CoA to L-β-hydroxyacyl-CoA, catalyzed by enoyl-CoA hydratase, where a hydroxyl group is added to the β-carbon.
3. Dehydrogenation of L-β-hydroxyacyl-CoA (containing a hydroxyl group on the β-carbon) to β-ketoacyl-CoA, catalyzed by β-hydroxyacyl-CoA dehydrogenase. This step uses NAD+ as a cofactor, reducing it to NADH.
4. Thiolysis, in which β-ketoacyl-CoA is cleaved by β-ketothiolase, releasing acetyl-CoA and generating a shortened acyl-CoA for subsequent β-oxidation cycles.

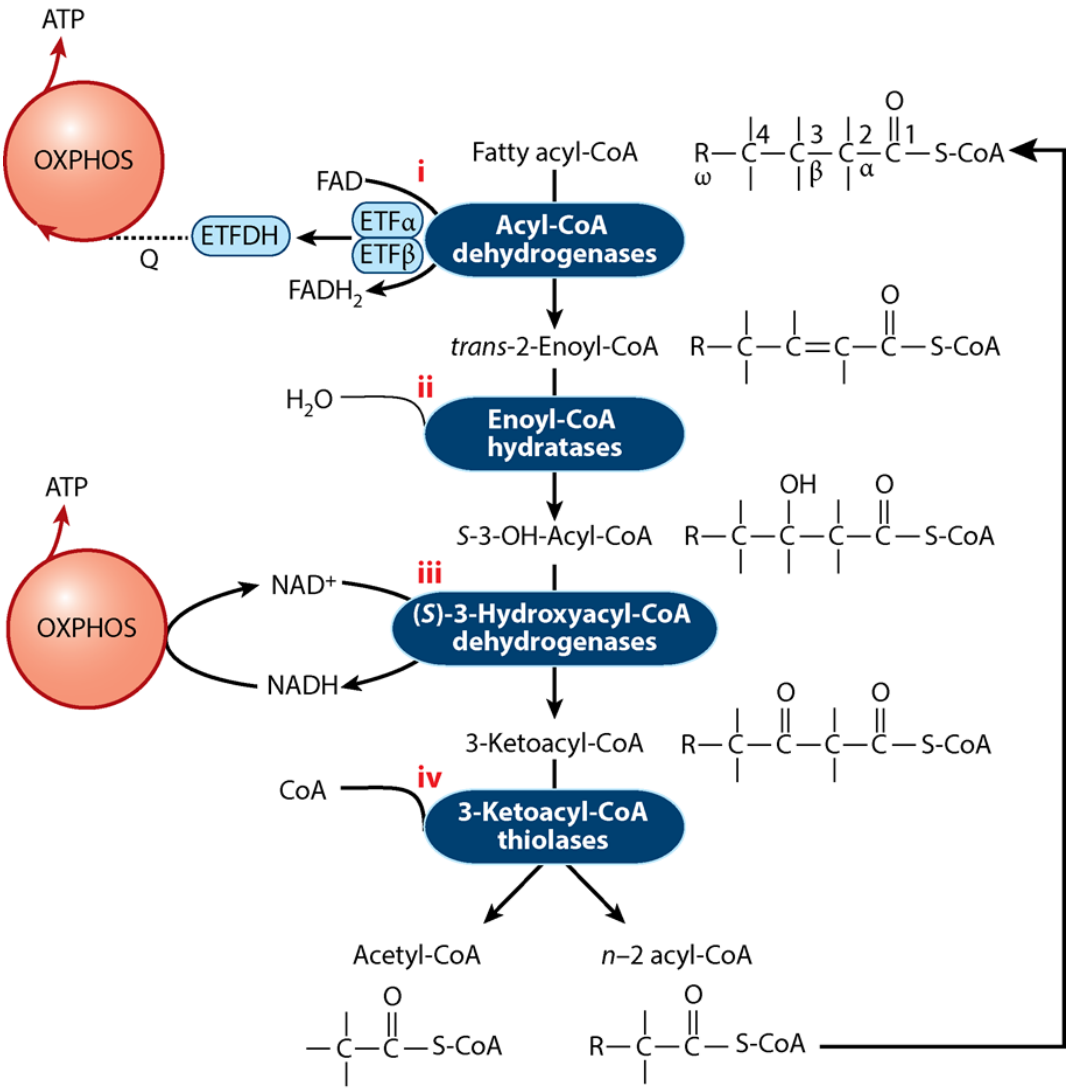

Figure 1.2. Fatty acid β-oxidation pathway

Fatty acid β-oxidation involves four enzymatic reactions that progressively shorten fatty acyl-CoAs by two carbon atoms per cycle, generating acetyl-CoA and reducing equivalents for ATP production. (i) Acyl-CoA dehydrogenases catalyze the initial dehydrogenation of fatty acyl-CoA to trans-Δ²-enoyl-CoA, using FAD as a cofactor. Electrons from $FADH_2$ are transferred via electron transfer flavoprotein (ETF) to the respiratory chain. (ii) Enoyl-CoA hydratases add water across the double bond, converting trans-Δ²-enoyl-CoA to (S)-3-hydroxyacyl-CoA, also known as β-hydroxyacyl-CoA. (iii) (S)-3-Hydroxyacyl-CoA dehydrogenases, requiring NAD^+, oxidize β-hydroxyacyl-CoA to 3-ketoacyl-CoA, producing NADH. (iv) 3-Ketoacyl-CoA thiolases cleave 3-ketoacyl-CoA, releasing acetyl-CoA and a shortened acyl-CoA, which reenters the β-oxidation cycle for further processing.

Source: Adapted from Houten et al., 2016[22]

Long-chain fatty acids (LCFAs) undergo initial oxidation by very-long-chain acyl-CoA dehydrogenase (VLCAD), which, like medium-chain acyl-CoA dehydrogenase (MCAD), uses FAD as a cofactor[21]. The remaining three steps of LCFA β-oxidation—hydration, dehydrogenation, and thiolysis—are carried out by the mitochondrial trifunctional protein (MTP), a multi-enzyme complex located in the inner mitochondrial membrane. MTP contains the enzymatic activities for enoyl-CoA hydratase, β-hydroxyacyl-CoA dehydrogenase, and β-ketothiolase, enabling efficient processing of LCFAs[23]. In contrast, the oxidation of medium-chain and short-chain fatty acids (MCFAs and SCFAs) likely occurs entirely in the mitochondrial matrix. These fatty acids do not appear to rely on membrane-bound complexes like MTP, but instead are processed by matrix-localized enzymes such as MCAD, crotonase, and β-ketothiolase[24]. However, there is a suggestion that MTP may catalyze the dehydrogenation of L-β-hydroxyacyl-CoA during MCFA oxidation[25].

In summary, β-oxidation is a highly efficient metabolic pathway that generates ATP through the sequential oxidation of fatty acids. Transport mechanisms and enzymatic processing differ depending on the chain length of the fatty acid substrate: LCFAs require the carnitine shuttle and are processed by membrane-bound complexes like MTP, while some MCFAs can bypass the carnitine shuttle and are processed by enzymes within the mitochondrial matrix. Importantly, for LCFAs, the

production of FADH2 and NADH occurs closer to the electron transport chain, as β-oxidation is carried out by enzymes located at the inner mitochondrial membrane. This proximity likely allows for more efficient transfer of reducing equivalents to the ETC compared to MCFAs, which are oxidized further away in the mitochondrial matrix.

1.1.3 ω-oxidation

ω-oxidation is an alternative fatty acid metabolism pathway that occurs in the endoplasmic reticulum (ER) microsomes[26,27]. Unlike β-oxidation, which shortens the fatty acid chain via thiolysis, ω-oxidation involves a three-step process where oxidation occurs at the ω-carbon—the carbon farthest from the carboxyl group[28]. This pathway produces dicarboxylic acids, which can subsequently enter the β-oxidation pathway for further breakdown[24,29,30]. ω-Oxidation primarily takes place in the liver and kidney and acts as a complementary pathway to β-oxidation, playing a relatively minor role under normal physiological conditions but becoming more significant during metabolic stress, such as prolonged fasting or starvation, when fatty acid oxidation is elevated[24,31].

1.1.4 TCA cycle

The tricarboxylic acid (TCA) cycle, also known as the citric acid cycle or Krebs cycle, is a central metabolic pathway that takes place in the mitochondrial matrix[8]. Comprising eight enzyme-driven reactions, the TCA cycle facilitates not only energy production, but also the generation of key intermediates for various biosynthetic pathways. Acetyl-CoA, derived from both glycolysis and β-oxidation, enters the cycle by combining with the four-carbon molecule oxaloacetate to form the six-carbon citrate. This step marks the beginning of the cycle, which produces the reducing equivalents 3 NADH and 1 $FADH_2$, critical for transferring electrons to the electron transport chain (ETC) to drive ATP synthesis[32]. Additionally, each cycle generates one molecule of GTP (or ATP, depending on the cell type) and releases two carbon atoms as CO_2 [33]. Thus, the TCA cycle acts as a key metabolic link, channeling acetyl-CoA from glycolysis and β-oxidation into the electron transport chain for efficient ATP generation.

1.1.5 Electron Transport Chain

The electron transport chain (ETC) is a central driver of cellular respiration, enabling highly efficient energy production by harnessing electrons from NADH and $FADH_2$. It consists of enzyme complexes embedded in the inner mitochondrial membrane, where the transfer of electrons ultimately drives ATP synthesis. As electrons flow

through these complexes, they facilitate the pumping of protons from the mitochondrial matrix into the intermembrane space, establishing a proton gradient[34]. This gradient powers Complex V (ATP synthase), which functions as a molecular motor to convert ADP into ATP[35]. At the final step of the chain, Complex IV (cytochrome c oxidase), the last proton pump, transfers electrons to oxygen, the terminal electron acceptor, which is reduced to form water.

NADH primarily donates its electrons to Complex I (NADH:oxidoreductase), initiating electron transport. Additionally, in certain tissues, such as muscle and brain, the glycerol-3-phosphate shuttle allows cytosolic NADH from glycolysis to transfer its electrons directly to ubiquinone (coenzyme Q), bypassing Complex I[36]. $FADH_2$ introduces electrons into the electron transport chain through multiple pathways, all of which converge at ubiquinone (coenzyme Q)[37]. First, during β-oxidation, $FADH_2$ donates electrons via the electron transfer flavoprotein (ETF) pathway, which then transfers them to electron transfer flavoprotein dehydrogenase (ETFDH), ultimately reducing ubiquinone. Second, in the TCA cycle, $FADH_2$ is generated during the conversion of succinate to fumarate, and these electrons are directly transferred to ubiquinone through Complex II (succinate dehydrogenase). Additionally, electrons from the glycerol-3-phosphate dehydrogenase shuttle and other $FADH_2$ -linked dehydrogenases also converge at ubiquinone. This convergence at ubiquinone, which serves as an electron shuttle between complexes, ensures the integration of various electron inputs, including those from NADH via Complex I, into the electron transport chain[37].

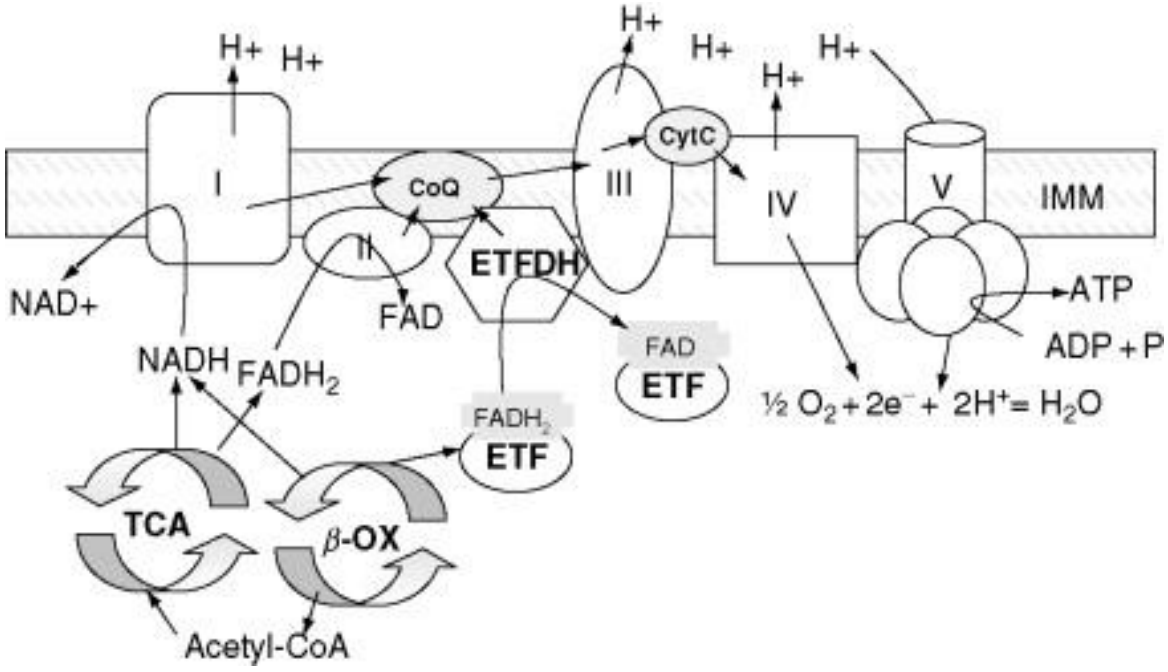

Figure 1.3 Electron transport chain (ETC) oxidizing NADH and $FADH_2$ in mitochondrial respiration.

The electron transport chain (ETC) oxidizes reducing equivalents from NADH and $FADH_2$ to drive ATP production. NADH donates electrons to Complex I, initiating electron flow through the ETC. $FADH_2$, generated from both β-oxidation and the tricarboxylic acid (TCA) cycle, contributes electrons through distinct pathways that converge at ubiquinone (coenzyme Q). During β-oxidation, $FADH_2$ transfers electrons via the electron transfer flavoprotein (ETF) to ETF dehydrogenase (ETFDH), ultimately reducing ubiquinone. In the TCA cycle, $FADH_2$ is produced during the conversion of succinate to fumarate and directly donates electrons to ubiquinone through Complex II (succinate dehydrogenase). These electrons, along with those from Complex I, are transferred sequentially through Complexes III and IV, creating a proton gradient across the inner mitochondrial membrane. This gradient powers ATP synthase (Complex V) to generate ATP. At the final step, electrons reduce oxygen to form water, completing the electron transport process

Source: Adapted from Goetzman, 2011[38]

The ETC complexes are large, multi-protein assemblies, typically encoded by both nuclear and mitochondrial genomes[39]. However, the complexes responsible for $FADH_2$ entry, such as Complex II and ETFDH, are entirely encoded by the nuclear genome[37,40,41]. Mutations in either nuclear or mitochondrial genes that directly or indirectly affect the ETC can lead to mitochondrial diseases, such as MELAS (Mitochondrial Encephalopathy, Lactic Acidosis, and Stroke-like episodes), resulting in defective energy production and associated metabolic dysfunction. Common symptoms of such disorders include muscle weakness, neurological deficits, and lactic acidosis[42].

1.2 Overview of Type 2 Diabetes

Type 2 diabetes (T2D) represents a major global health crisis, affecting hundreds of millions of individuals worldwide[43]. This metabolic disorder arises primarily from insulin resistance and pancreatic β-cell dysfunction, resulting in a chronic inability to maintain normal blood glucose levels. The condition is closely associated with obesity, a key risk factor[44,45], and its prevalence continues to rise in parallel with increasing rates of obesity[46]. The consequences of T2D extend far beyond poor glycemic control, significantly diminishing the quality of life for affected individuals and heightening the risk of severe complications, including cardiovascular disease, neuropathy, nephropathy, and retinopathy[47–50]. These complications not only lead to considerable morbidity and mortality but also place a heavy financial burden on healthcare systems globally[51]. In the European Union, for instance, diabetes management accounts for approximately 9% of total healthcare expenditures[52]. Effective interventions for both preventing and managing T2D are thus critical, given the enormous social, economic, and individual impact of the disease.

1.3 Metformin: A Widely Used Drug for Type 2 Diabetes

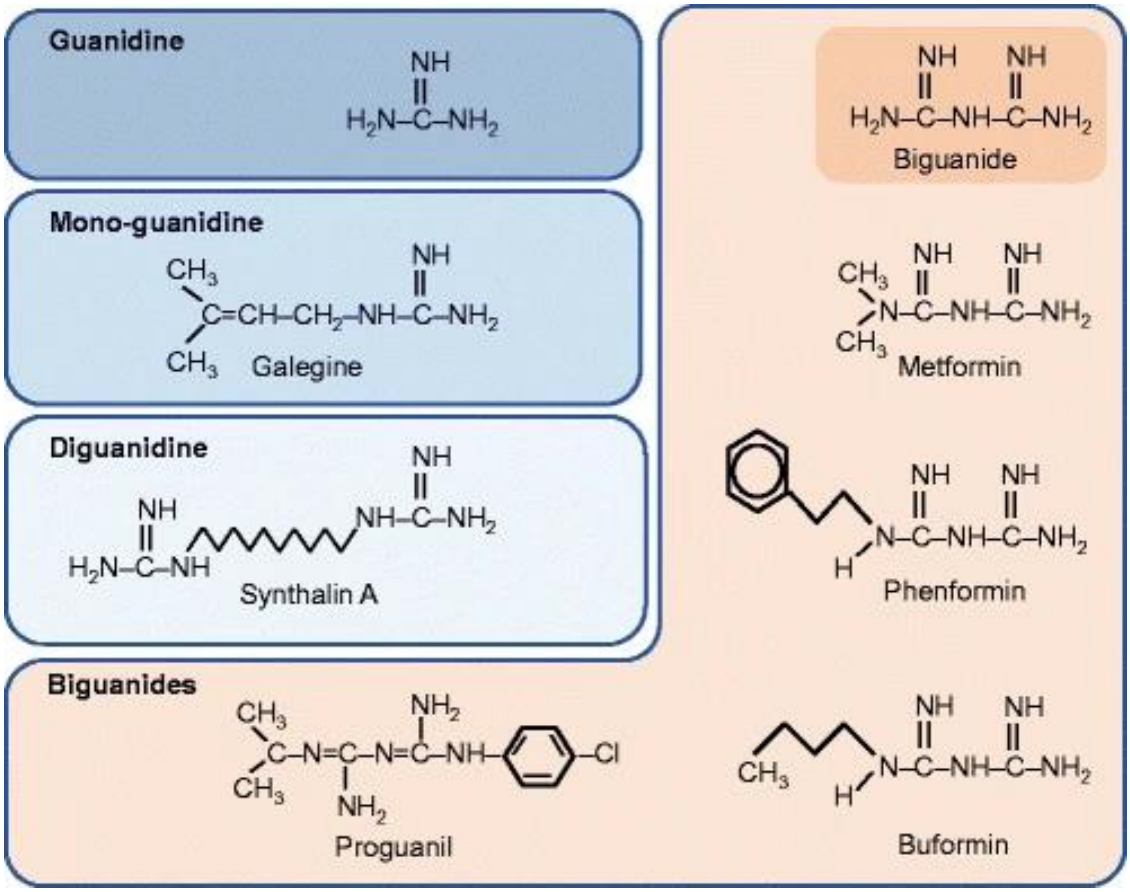

Figure 1.4. Structure of Guanidine and Biguanides, including Metformin.

Guanidine, a compound found in Galega officinalis, was historically noted for its ability to lower blood glucose levels in animals. Biguanides, formed by the fusion of two guanidine molecules, include clinically significant compounds like metformin, phenformin, and buformin. Although phenformin and buformin were discontinued due to their association with an increased risk of lactic acidosis, metformin remains widely approved for the treatment of Type 2 diabetes due to its favorable safety profile and glucose-lowering efficacy.

1.3.1 History and Development of Metformin

Metformin, a cornerstone in the management of Type 2 diabetes, belongs to the biguanide class of molecules, which also includes phenformin and buformin[53]. Its origins can be traced back to Galega officinalis, commonly known as French lilac, a plant historically used to treat excessive thirst and urination[54]. The active compound, guanidine, was first documented in the 1800's[55] and in 1918 was shown to lower blood glucose in rabbits[56]. However, it wasn't until 1922 that the biguanide metformin was synthesized[57], and in 1929, its blood glucose-lowering effects were demonstrated in animal studies, notably in rabbits[58,59].

The rediscovery and clinical development of metformin occurred in the mid-20th century, led by French physician Jean Sterne in 1957[60]. Metformin was initially overshadowed by phenformin, another biguanide that offered stronger glycemic control but carried a significantly higher risk of lactic acidosis[61,62], a potentially fatal complication[63]. The withdrawal of phenformin due to these safety concerns also impacted metformin's reputation[64]. However, metformin regained attention due to its much lower risk of lactic acidosis[62]. Its use expanded significantly after the U.S. Food and Drug Administration (FDA) approved it in 1995[65], supported by strong clinical evidence, including the landmark United Kingdom Prospective Diabetes Study (UKPDS) in 1998[66].

Metformin is typically the first-line treatment for Type 2 diabetes due to its ability to lower fasting blood glucose levels with minimal risk of hypoglycemia[67]. Additionally, it can be used in combination with other antidiabetic agents, such as sulfonylureas, DPP-4 inhibitors, SGLT-2 inhibitors, and insulin, offering a flexible approach to diabetes management[68]. Its appetite-suppressing properties also make it particularly beneficial in obese individuals, further enhancing its therapeutic value[69–71].

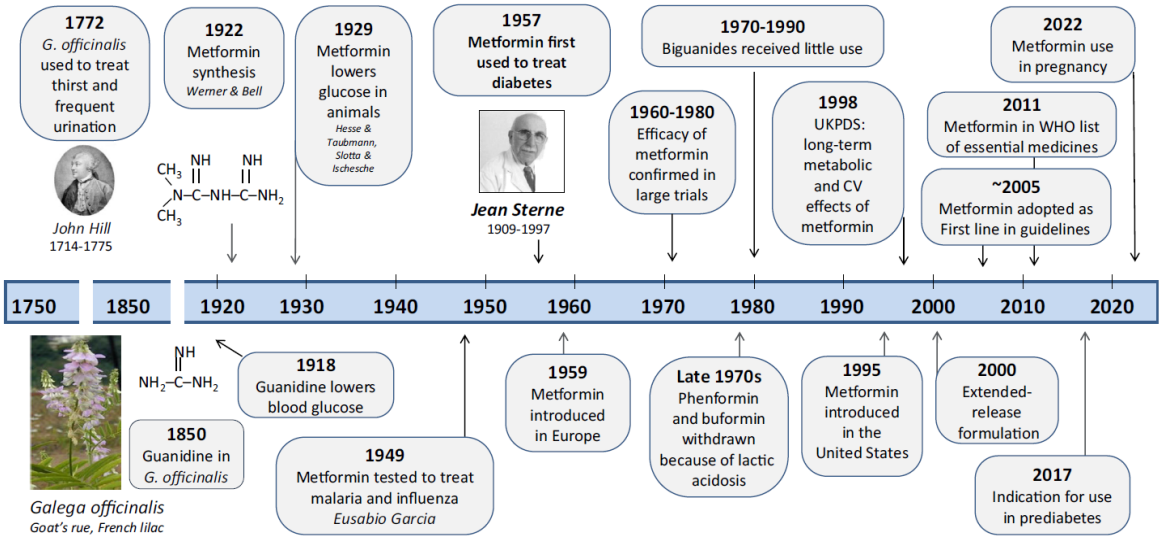

Figure 1.5. Timeline of metformin's development and clinical use.

Tracing metformin's discovery from the historical use of Galega officinalis in 1772, to its synthesis in 1922, and eventual approval for diabetes treatment in 1957. The timeline highlights key milestones, including the withdrawal of phenformin and buformin, and the widespread adoption of metformin following the UKPDS study in 1998.

Source: Adapted from Bailey, 2024[72]

1.3.2 Metformin and Glycemic Control

While the primary focus of this thesis is metformin's appetite-suppressing effects, it is essential to acknowledge its well-established role in glycemic control, which remains a central area of research and clinical use[73]. Metformin's glucose-lowering effects are attributed to multiple mechanisms across various tissues, with strong evidence supporting its reduction of hepatic gluconeogenesis, particularly in cases of poorly controlled blood glucose[74–76]. Additionally, there is growing evidence that the intestines may play a role as a glucose sink, contributing to blood glucose regulation[77].

The molecular mechanisms through which metformin exerts its glycemic control are still under investigation, with several pathways proposed. One commonly cited mechanism is the activation of AMP-activated protein kinase (AMPK), a key regulator of energy balance[78]. Metformin is also believed to inhibit mitochondrial complex I, potentially altering cellular energy states by increasing AMP levels and modifying the NADH/NAD+ ratio[79]. Additional mechanisms, such as the inhibition of mitochondrial glycerol-3-phosphate dehydrogenase and complex IV, have been suggested[80,81]. Recent studies have also pointed to the involvement of the microbiome and lysosomal pathways, suggesting metformin's effects may be more complex and multifaceted than previously thought[82,83].

1.3.3 Metformin and Appetite Suppression

Metformin's effect on body weight, particularly its ability to induce weight loss[70], is primarily attributed to its appetite-suppressing properties[84]. This reduction in appetite has been observed in patients with Type 2 diabetes, though the exact mechanisms underlying this effect remain an area of ongoing investigation[85]. Metformin-induced increases in the hormone GDF15 have been proposed to mediate appetite suppression[86,87]. GDF15 is a stress-responsive cytokine that is upregulated by cellular stressors such as mitochondrial dysfunction and hypoxia[88]. In response to metformin, GDF15 production has been shown to increase primarily in the intestines and kidneys[89,90]. However, recent findings have challenged whether GDF15 is the only or, indeed, the most important mechanism involved in metformin's appetite suppression[85].

Beyond GDF15, metformin has been linked to other gut-derived appetite-suppressing molecules[91]. Delayed glucose absorption in the gastrointestinal tract stimulates the secretion of glucagon-like peptide-1 (GLP-1) from L-cells, which, along with peptide YY (PYY), promotes satiety[91–94]. Further research is needed to clarify the mechanisms underlying metformin's effects on appetite.

1.3.4 Metformin Pharmacokinetics and Tissue Distribution

Metformin accumulates in certain tissues, with concentrations in the intestines reported to be 30 to 300 times higher than in the bloodstream[95]. In one human study, 3 hours post-metformin administration, intestinal concentrations reached approximately 4 mmol/kg, while blood levels were measured at 8–24 μmol/L. Elevated concentrations are also observed in the liver and kidneys, with levels in the portal vein reportedly 1.5 to 3 times higher than in the systemic circulation[80,96]. Additionally, metformin accumulates in mitochondria[97,98]. Pharmacokinetically, metformin is absorbed in the intestines with relatively poor bioavailability (50-60%) and follows flip-flop dynamics, where absorption in the intestines is slower than elimination by the kidneys[99]. As a positively charged molecule, it relies on organic cation transporters such as OCT1, OCT2, and OCT3, as well as other transporters including MATE1, PMAT, and SERT, for its cellular uptake and distribution[100]. Metformin is excreted unmetabolized through the kidneys[101]. Impaired kidney function is a contraindication for metformin use, as reduced renal clearance can increase the risk of lactic acidosis, a rare but serious complication[102].

1.3.5 Metformin and Intestinal Glucose Metabolism

Metformin has been shown to significantly impact glucose metabolism in the intestines, where concentrations are 30 to 300 times higher than in systemic circulation[95]. By reducing dietary glucose absorption, metformin allows more

glucose to reach the lower parts of the intestines[92]. It also enhances glucose uptake from the circulation, as demonstrated by PET scans using the glucose analog fluorodeoxyglucose (FDG), which reveal increased basolateral transport[103,104]. PET-MRI studies further indicate that some of this absorbed glucose enters the intestinal lumen, contributing to improved blood sugar regulation[77].

1.3.6 Metformin, Mitochondrial Function, and Lactate Production

At the high concentrations observed in the intestines (approximately 4 mmol/kg in the jejunum), metformin can inhibit complex I of the electron transport chain (ETC)[95]. Normally, complex I facilitates the oxidation of NADH to NAD+, a critical step in maintaining the cellular redox state. In the absence of sufficient NAD+ regeneration by complex I, cells rely on glycolysis to regenerate NAD+ by converting pyruvate into lactate[105]. Lactate levels have been shown to increase systemically in Type 2 diabetes (T2D) cohorts with metformin use, although this effect is not universal (see ref[106] for a review). Importantly, metformin leads to an increase in lactate levels in the portal vein, driven by both enhanced glucose uptake and complex I inhibition in the intestines[98,107,108].

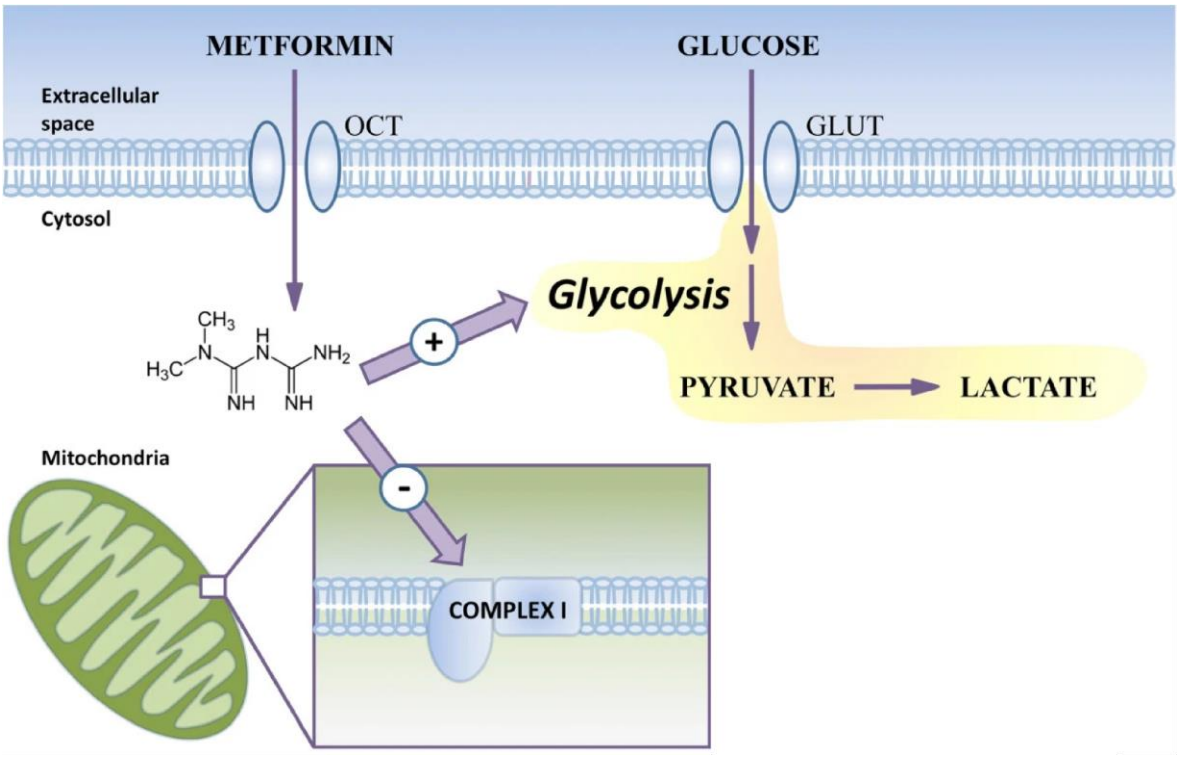

Figure 1.6 Metformin Inhibits Complex I Resulting in Lactate Production

Metformin is taken up into cells through transporters, including organic cation transporters (OCT), where it can inhibit complex I of the mitochondrial electron transport chain (ETC). This inhibition shifts energy production toward glycolysis, as cells rely on glycolysis to regenerate NAD+ by converting pyruvate to lactate in the absence of sufficient complex I activity. As a result, lactate accumulation occurs, most notably in the portal vein.

Source: Adapted from Andrzejewski et al., 2014[109]

1.3.7 Other Areas of Metformin Influence

Beyond glucose control and appetite suppression, metformin also influences inflammation, the gut microbiome, and the gastrointestinal system[110–113]. For

example, metformin has been shown to improve T cell function by increasing autophagy and enhancing mitochondrial bioenergetics[114]. Metformin also modulates the gut microbiome, promoting the growth of beneficial bacteria such as Akkermansia muciniphila[113]. This shift in the microbiome may play a role in its glucose-lowering and anti-inflammatory effects[115]. However, gastrointestinal side effects are common, with symptoms like nausea, vomiting, diarrhea, and bloating affecting about 20% of patients[116]. In some cases, changes in the microbiota may exacerbate these symptoms[116].

1.3.8 Metformin and the Regulation of Metabolites

Metformin's effects on metabolism extend beyond glucose regulation, influencing specific metabolites[117]. For instance, it increases the abundance of short-chain fatty acid-producing gut microbiota and reduces plasma levels of citrulline as well as certain acyl-alkyl phosphatidylcholines, highlighting its broad impact on metabolic processes[118–120].

1.3.9 Metformin and the Liver in Glucose Regulation

The liver plays a central role in glucose homeostasis, primarily through endogenous glucose production during fasting[121]. Metformin achieves higher concentrations in the hepatic portal vein compared to systemic circulation and accumulates notably in organs including the liver in addition to the intestines and kidneys[73,122]. The high

hepatic concentration of metformin is largely due to the abundant expression of organic cation transporter 1 and 3 (OCT1 & OCT3) in hepatocytes, facilitating its efficient uptake[100].

A principal mechanism by which metformin lowers blood glucose levels is by suppressing hepatic gluconeogenesis, particularly in patients with poorly controlled diabetes[75]. This effect, however, appears reduced in individuals whose diabetes is well-managed, indicating the glucose-lowering action of metformin may be dependent on the diabetic context[123].

Metformin's inhibitory effect on gluconeogenesis is notably substrate-specific and closely linked to the cellular redox state. It preferentially reduces gluconeogenesis from NAD+-dependent substrates, such as lactate and glycerol, making its inhibition distinct and less pronounced when substrates not requiring NAD+ are involved[124].

At higher concentrations, metformin inhibits mitochondrial complex I, disrupting the oxidation of NADH to NAD+. However, whether therapeutic hepatic concentrations of metformin are sufficient to significantly impact complex I activity remains uncertain[73]. Studies using mouse models, wherein mitochondrial complex I has been replaced with an alternative NADH-oxidizing enzyme insensitive to metformin, indicate a partial reduction in metformin's ability to lower glucose. These findings suggest complex I inhibition might partially mediate metformin's hepatic actions, but further research is required to determine whether its effects on glucose levels occur directly in the liver or indirectly, for example via intestinal-derived modulators[125].

Additionally, the involvement of AMP-activated protein kinase (AMPK) activation in metformin's hepatic glucose-lowering effects remains debated[126]. Both AMP-dependent and AMP-independent mechanisms of AMPK activation have been suggested; however, the precise role and importance of AMPK signaling in the hepatic actions of metformin remain unresolved[127].

Recent studies emphasize the importance of intestinal-liver crosstalk mediated by metabolites, including lactate, delivered to the liver via the portal vein[128]. Elevated intestinal lactate production, induced by metformin's intestinal effects, has been proposed to indirectly influence hepatic gluconeogenesis. Thus, lactate derived from the intestine might signal the liver to adjust gluconeogenic activity, presenting an integrated mechanism through which metformin modulates hepatic glucose production.

1.4 Lactate

As described in the glycolysis section, lactate is formed when pyruvate is converted by lactate dehydrogenase, regenerating NAD^+ in the process[129]. This reaction occurs in the cytosol and is essential for sustaining glycolytic flux under anaerobic conditions[105]. Systemic lactate levels rise in various physiological contexts, such as during intense exercise and postprandially[130,131]. Elevated lactate is also observed in pathological states, including sepsis and mitochondrial diseases[132,133]. Beyond metabolism, lactate acts as a signaling molecule, inhibiting lipolysis through

interaction with the G-protein-coupled receptor GPR81[134,135]. Additionally, recent evidence suggests lactate may suppress appetite, contributing to energy balance[136].

Lactate shuttle

Lactate is not merely a byproduct of anaerobic metabolism; it can also be produced and utilized in the presence of oxygen[130,137]. For example, activated immune cells engage in glycolysis and produce lactate despite sufficient oxygen availability, a process known as aerobic glycolysis[137]. Furthermore, lactate can be shuttled between organs or even between cells within the same tissue for oxidation, effectively decoupling glycolysis from oxidative phosphorylation. This lactate shuttle hypothesis is supported by tracer studies, which reveal high lactate turnover in the blood, indicating that some cells actively generate lactate while others actively utilize it[138]. Lactate is highly abundant in the bloodstream, typically present at concentrations around 1 mM, making it the second most abundant carbon metabolite after glucose[139]. Its transport into and out of cells is mediated by monocarboxylate transporters (MCTs), which enable its movement across cell membranes to support both its metabolic and signaling functions[140].

1.5 N-lactoyl Amino Acids

N-lactoyl amino acids are a class of metabolites synthesized through the condensation of lactate and amino acids via an amide bond[141]. These metabolites

are ubiquitous, having been detected in the serum of both humans and mice, indicating their broad presence across species[142]. N-lactoyl amino acids can be synthesized endogenously through enzymatic processes. For example, CNDP2 (Carnosine Dipeptidase 2), a cytosolic dipeptidase, catalyzes both the formation and degradation of N-lactoyl amino acids[141].

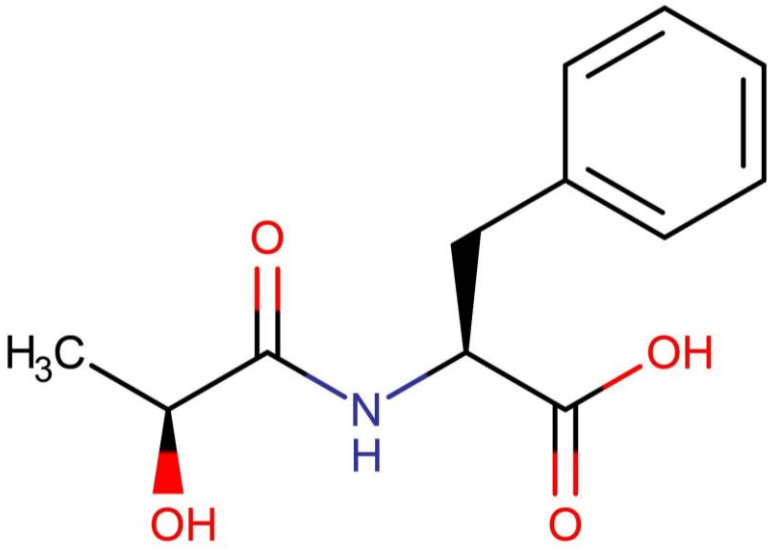

Figure 1.7 Structure of Lac-Phe (N-lactoyl phenylalanine)

Chemical structure of Lac-Phe (N-lactoyl phenylalanine), an N-lactoyl amino acid formed through the condensation of lactate and phenylalanine via an amide bond. Lac-Phe can be synthesized endogenously by the enzyme CNDP2 (Carnosine Dipeptidase 2)

CNDP2 - Carnosine Dipeptidase 2

CNDP2 is highly expressed in several tissues and cells, including macrophages, kidneys, and intestines, where it contributes to peptide bond metabolism[142]. CNDP2 acts on a range of substrates that contain amide bonds, beyond N-lactoyl amino acids[143]. As its name suggests, Carnosine Dipeptidase 1 (CNDP1) cleaves carnosine, a dipeptide composed of β-alanine and L-histidine. In contrast, despite its name, Carnosine Dipeptidase 2 (CNDP2) does not cleave carnosine but instead acts on dipeptides such as threonyl-threonine[143]. Recent studies show that CNDP2 can also catalyze the conjugation of the ketone body 3-hydroxybutyrate with amino acids via an amide bond, mirroring its role in N-lactoyl amino acid synthesis[144]. Furthermore, CNDP2, through its role in the cleavage of dipeptides, has been implicated in the regeneration of the tripeptide glutathione, a key antioxidant involved in cellular redox balance[145]. While CNDP2 is crucial for N-lactoyl amino acid formation, it is not the only mechanism responsible for their biosynthesis. CNDP2 knockout mice exhibit reduced levels of N-lactoyl amino acids, including N-lactoyl-phenylalanine (Lac-Phe), but their persistence at lower concentrations suggests alternative biosynthetic mechanisms for N-lactoyl amino acids exist[142].

Phenotypes Associated with Elevated N-lactoyl Amino Acids

The levels of N-lactoyl amino acids, particularly Lac-Phe, are influenced by various physiological and pathological conditions. Intense or anaerobic exercise is a potent stimulator of systemic lactate, driving the formation of these metabolites[141,142]. For example, Lac-Phe levels rise significantly following intense physical activity. In

mitochondrial disease MELAS (mitochondrial myopathy, encephalopathy, lactic acidosis, and stroke-like episodes), elevated systemic lactate is accompanied by corresponding increases in N-lactoyl amino acids[133]. Similarly, in sepsis, which is marked by increased systemic glycolysis, elevated lactate levels coincide with higher concentrations of N-lactoyl amino acids. Furthermore, the elevation of N-lactoyl amino acids in sepsis has been associated with higher mortality rates[133]. Phenylketonuria (PKU), a genetic disorder that impairs phenylalanine metabolism, also leads to the accumulation of N-lactoyl phenylalanine due to excess phenylalanine[141,146].

N-lactoyl Phenylalanine (Lac-Phe)

Lac-Phe, the most studied N-lactoyl amino acid, has been shown to suppress appetite in mice, and its levels correlate with reduced adiposity in humans[142,147]. In experimental models, exogenous administration of Lac-Phe reduces food intake and body weight in mice when administered via intraperitoneal injection. However, oral administration is ineffective, likely due to Lac-Phe hydrolysis in the gastrointestinal tract[142]. In wild-type and CNDP2 knockout mice, baseline food intake does not differ significantly, but after exercise, wild-types have higher Lac-Phe levels and reduced food intake[142]. This suggests that while Lac-Phe levels may have limited effects on appetite under basal conditions, it can modulate food intake in specific physiological contexts, such as exercise.

Transport and Export of N-lactoyl Amino Acids

Once synthesized, N-lactoyl amino acids are exported from cells, with higher concentrations found in cell culture media than within cells, suggesting active transport[142]. Although the primary transporter regulating serum N-lactoyl amino acid levels remains unidentified, solute carriers such as SLC17A1 and SLC17A3, involved in renal excretion, have been shown to modestly influence urinary Lac-Phe levels[148]. Knockout studies of the ABCC5 transporter, which has been implicated in Lac-Phe transport, did not significantly alter serum Lac-Phe levels[142]. This strongly suggests that other, yet unidentified, transporters are involved in the movement of N-lactoyl amino acids.

N-lactoyl Amino Acids as Signaling Molecules

In addition to their endogenous production, N-lactoyl amino acids have been identified in certain foods, such as Parmigiano-Reggiano cheese[149], and contribute to the "kokumi" flavor, which enhances richness in taste[150]. Molecular docking studies suggest that N-lactoyl amino acids, including Lac-Phe, may interact with taste receptors, reinforcing the hypothesis that they function as signaling molecules[151]. While Lac-Phe's appetite-suppressing role has been demonstrated, its mechanism of action remains unclear. It is hypothesized that Lac-Phe may act on the hypothalamus to regulate feeding behavior, potentially via G-protein coupled receptors (GPCRs)[142,152]. Further research is needed to clarify the pathways through which Lac-Phe mediates appetite suppression.

1.6 β-Hydroxy Fatty Acids

β-Hydroxy fatty acids are metabolites characterized by the presence of a hydroxyl group at the β-carbon, the third position in the fatty acid chain. Although sometimes referred to as 3-hydroxy fatty acids, we will consistently use the term β-hydroxy fatty acids in this thesis. Our focus will be on straight-chain β-hydroxy fatty acids, which vary in length and include short-chain (up to six carbons), medium-chain (seven to twelve carbons), and long-chain (thirteen or more carbons) variants.

β-Hydroxy fatty acids can also exist as conjugates with carnitine, forming β-hydroxy carnitines[153]. These conjugates generally have lower concentrations in the plasma; for instance, one study reported a mean concentration of just 0.01 μM for β-OH-C6:0 carnitine in healthy subjects[154]. Carnitine conjugation can facilitate the transport of β-hydroxy fatty acids produced in the mitochondria to the cytosol[155]. To standardize nomenclature, we employed a consistent naming convention throughout this thesis to easily distinguish β-hydroxy fatty acids of different chain lengths. For example, β-hydroxydecanoate, also known chemically as 3-hydroxydecanoate, which has 10 carbons and zero unsaturated bonds, is referred to as β-OH-C10:0 (Figure 1.8A).

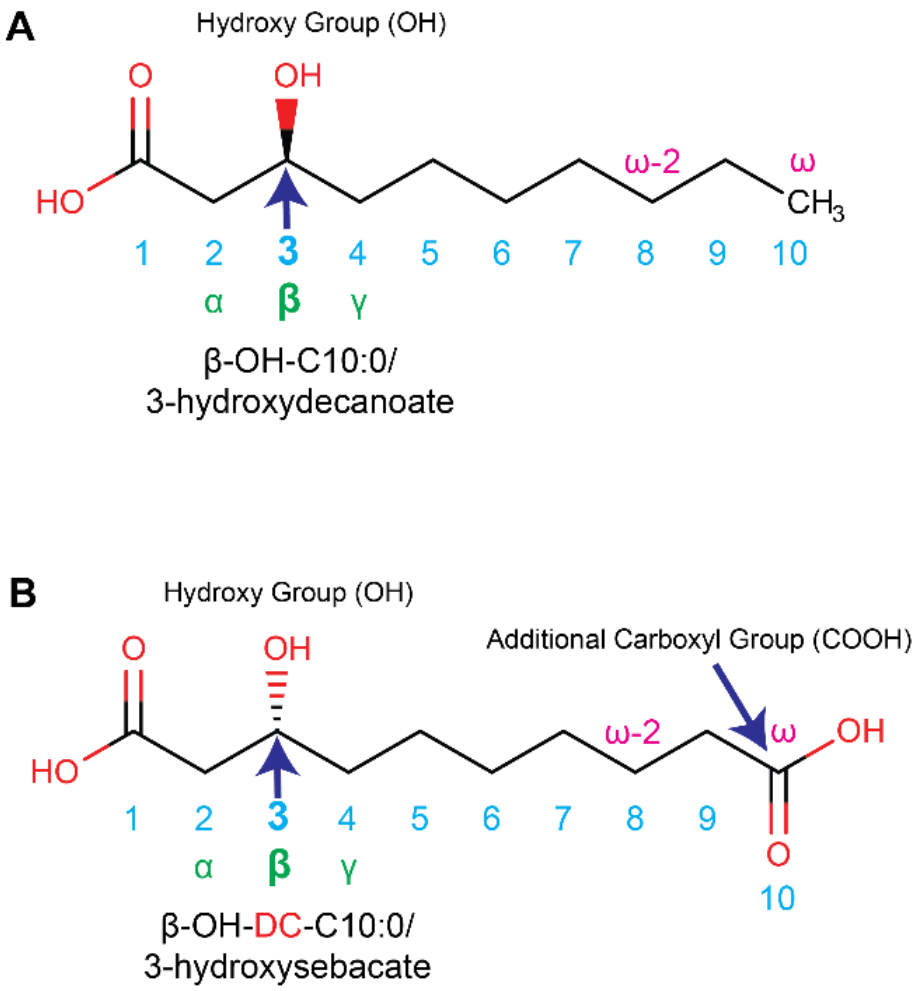

Figure 1.8: Structural Comparison of β-Hydroxy Fatty Acids

(A) Chemical structure of β-OH-C10:0 (3-hydroxydecanoate), a monocarboxylic β-hydroxy fatty acid. The hydroxy group (OH) is located at the β-position on the third carbon atom, as indicated by the arrow. The structure is annotated with carbon numbering (1-10), Greek letter designations (α, β, γ), and omega (ω) positions, highlighting the methyl terminus at the omega (ω) position.

(B) Chemical structure of β-OH-DC-C10:0 (3-hydroxysebacate), a dicarboxylic β-hydroxy fatty acid. Similar to (A), the hydroxy group (OH) is located at the β-position on the third carbon atom. However, this structure features an additional carboxyl group (COOH) at the omega (ω) position, making it a dicarboxylic acid. The structure is also annotated with carbon numbering (1-10), Greek letter designations (α, β, γ), and omega (ω) positions to emphasize the differences between monocarboxylic and dicarboxylic fatty acids.

Role in β-Oxidation

β-Hydroxy fatty acids function as intermediates in the β-oxidation pathway, a critical catabolic process for fatty acid metabolism (refer to the previous section on β-oxidation for detailed pathway mechanisms)[156]. $FADH_2$ is generated in the first step of this cycle. In the second step, β-hydroxy fatty acids are formed when the hydroxyl group is introduced at the β-carbon via the addition of water. This intermediate is further oxidized to a ketone in the third step, catalyzed by an NAD^+ -dependent enzyme[157]. An inadequate supply of NAD^+ can result in the accumulation of β-hydroxy fatty acids[153,158].

Regulation of β-Hydroxy Fatty Acid Levels

The plasma levels of β-hydroxy fatty acids are low, typically below 0.6 μM for species such as β-OH-C10:0, but can increase under specific physiological and pathological conditions[159–161]. Prolonged fasting and ketogenic diets, which enhance fatty acid oxidation, lead to elevated β-hydroxy fatty acid concentrations[162]. Metabolic disorders specifically affecting enzymes involved in β-oxidation, such as long-chain 3-hydroxyacyl-CoA dehydrogenase (LCHAD) deficiency and multiple acyl-CoA dehydrogenase deficiency (MADD), are associated with increased plasma levels of these metabolites[163]. Similarly, other mitochondrial diseases, including MELAS (mitochondrial encephalopathy, lactic acidosis, and stroke-like episodes) and MERRF (myoclonic epilepsy with ragged-red fibers), can elevate β-hydroxy fatty

acid levels due to their detrimental effects on mitochondrial function and energy metabolism[133,164].

A study of rat liver mitochondria revealed that β-hydroxy fatty acids are produced as racemic mixtures, containing both D- and L-isomers in roughly equal proportions[165]. This observation suggests that under certain conditions, the atypical D-isomer may be present in the circulation at higher-than-expected levels, warranting further investigation. These enantiomers are not typically measured separately in LC-MS metabolomics studies, which could lead to an underestimation of their distinct biological roles. In rat liver mitochondria, treatment with rotenone, a complex I inhibitor, has been shown to increase the production of medium- and long-chain β-hydroxy fatty acids, likely due to an altered $NADH/NAD^+$ ratio[165,166].

Signaling Roles of Medium-Chain β-Hydroxy Fatty Acids

Medium-chain β-hydroxy fatty acids, including β-hydroxyoctanoate (β-OH-C8:0) and β-hydroxydecanoate (β-OH-C10:0), act as signaling molecules. They activate the hydroxycarboxylic acid receptor 3 (HCA3), also known as GPR109B, encoded by the HCAR3 gene[167–170]. This receptor is expressed in higher primates, including humans, but not in rodents, making it more challenging to study[169]. HCA3 activation in human adipocytes mediates anti-lipolytic effects, underscoring its potential role in metabolic regulation. These metabolites exhibit biased agonism at HCA3, with β-OH-C8:0 and β-OH-C10:0 eliciting distinct cellular signaling responses[167]. Additionally, β-OH-C10:0 has been demonstrated to activate GPR84[171].

Medium-Chain β-Hydroxy Fatty Acids and Immune Regulation

Medium-chain β-hydroxy fatty acids can modulate immune responses through their interactions with HCA3 and GPR84[167,171]. HCA3 activation is generally associated with anti-inflammatory outcomes. For example, β-OH-C8:0 stimulation in macrophages induces an anti-inflammatory phenotype, characterized by reduced glycolytic activity and increased IL-10 production[172]. In contrast, activation of GPR84 promotes pro-inflammatory pathways[171]. Specifically, β-OH-C10:0 stimulation in macrophages results in a pro-inflammatory phenotype, as evidenced by increased TNFα and reactive oxygen species (ROS) production[172]. Moreover, medium-chain β-hydroxy fatty acids can be produced by bacteria and are frequently conjugated to bacterial lipopolysaccharides (LPS), which are widely used as immunostimulatory agents in research[172–174]. Nonetheless, the precise role of medium-chain β-hydroxy fatty acids in the immune system remains incompletely understood, necessitating further research to elucidate their functions and therapeutic potential.

Dicarboxylic β-Hydroxy Fatty Acids

β-hydroxy fatty acids also include a subclass characterized by the presence of carboxyl groups at both ends of the molecule, distinguishing them structurally and functionally from their monocarboxylic counterparts. As previously discussed, dicarboxylic acids are primarily generated through ω-oxidation, a process that can occur in microsomes in the liver[24]. This pathway extends beyond conventional β-oxidation by introducing a second carboxyl group at the omega position of fatty

acids. An example of this subclass is β-hydroxysebacate (β-OH-DC-C10:0), which contains ten carbon atoms, with a hydroxyl group located at the β-position (third carbon atom) and carboxyl groups at both termini (Figure 1.8B).

To maintain consistency in nomenclature, a standardized naming convention is employed throughout this thesis to distinguish dicarboxylic β-hydroxy fatty acids from other monocarboxylic β-hydroxy fatty acids. The prefix “β-OH-DC-” denotes the presence of both a β-hydroxy group and two carboxyl groups, followed by the carbon chain length and the number of double bonds. For example, β-OH-DC-C10:0 specifically refers to β-hydroxysebacate, with "DC" indicating its dicarboxylic nature.

Under specific physiological and pathological conditions, such as prolonged fasting and metabolic disorders, concentrations of dicarboxylic β-hydroxy fatty acids can rise. Prolonged fasting, for example, increases their excretion in urine due to enhanced fatty acid oxidation[175,176]. Similarly, elevated levels are observed in inborn errors of metabolism like 3-hydroxyacyl-CoA dehydrogenasedeficiency[175,177,178]. In these disorders, it is proposed that dicarboxylic β-hydroxy fatty acids are formed directly from the ω-oxidation of monocarboxylic β-hydroxy fatty acids, rather than as a result of incomplete β-oxidation of dicarboxylic acids[177]. This conversion enhances solubility and is thought to facilitate renal excretion, thereby reducing the potential for toxic accumulation of β-hydroxy fatty acids[176,177].

Both gastric bypass and eating certain foods can also increase levels of dicarboxylic β-hydroxy fatty acids. Following Roux-en-Y gastric bypass surgery, the increased urinary excretion of these metabolites months later suggests a lasting alteration in

the metabolism of these compounds[179]. The levels of these metabolites can also be modulated by specific foods. For example, Royal Jelly, produced by honeybees, does not contain the dicarboxylic β-hydroxy fatty acid β-OH-DC-C10:0, yet their serum levels rise following its consumption, indicating that dicarboxylic β-hydroxy fatty acids are endogenously derived from the fats in Royal Jelly[172]. This is likely due to the presence of a unique fatty acid in Royal Jelly called queen bee acid (10-hydroxy-2-decenoic acid, or 10-HDA). Although 10-HDA lacks a carboxyl group at the omega position (the last carbon of the chain), it contains a hydroxyl group at this omega carbon. It also has a double bond between the alpha (carbon 2) and beta (carbon 3) positions. Oxidative metabolism at these omega and beta positions could yield β-OH-DC-C10:0, linking 10-HDA to the synthesis of dicarboxylic β-hydroxy fatty acids[181]. This suggests that dietary components can influence the endogenous production of these metabolites.

1.7 Metabolomics

Metabolomics is the study of small molecules, or metabolites, that reflect the biochemical activities within a biological system. Its use can provide critical insights into cellular processes, disease states, and drug effects[182]. The major techniques for metabolomics are nuclear magnetic resonance (NMR) spectroscopy, gas chromatography-mass spectrometry (GC-MS), and liquid chromatography-mass spectrometry (LC-MS)[183]. NMR provides quantitative data, is non-destructive to samples, and requires minimal preparation[184]. However, it is less sensitive compared to LC-MS and GC-MS[185,186]. GC-MS is particularly useful for analyzing volatile and thermally stable compounds, whereas LC-MS is more versatile, allowing for the detection of a broader range of metabolites, including non-volatile and thermally labile compounds. Due to its flexibility and broader coverage, LC-MS is the preferred method in many metabolomics studies[185].

In metabolomics, two main approaches are used: targeted and untargeted. Targeted metabolomics is quantitative, focusing on measuring the absolute concentrations of a predefined set of metabolites[187]. In contrast, untargeted metabolomics provides relative quantitation, measuring as many metabolites as possible without prior knowledge of their identities. This allows for the discovery of novel biomarkers, although it reports relative changes in metabolite levels rather than absolute concentrations[188]. In this thesis, untargeted LC-MS datasets form the basis of the analysis.

In LC-MS, liquid chromatography (LC) first separates metabolites based on their physical and chemical properties, such as polarity and hydrophobicity, using a chromatographic column[189]. This separation is achieved using different combinations of mobile and stationary phases. For example, reverse-phase LC employs a non-polar stationary phase and a polar mobile phase, which is ideal for separating hydrophobic compounds[190,191]. In contrast, hydrophilic interaction chromatography (HILIC) uses a polar stationary phase and is better suited for separating hydrophilic metabolites[192]. In untargeted analysis, often multiple columns are used to capture a broader range of metabolites, in many of our datasets four different columns were employed.

After chromatographic separation, metabolites are ionized, often through electrospray ionization (ESI), which converts them into charged particles[193,194]. These ions are then weighed by the mass spectrometer (MS). One commonly used mass analyzer in metabolomics is the Orbitrap, which measures the mass-to-charge ratio (m/z) of ions with high precision and resolution[195,196]. This allows for the detection of thousands of metabolites in complex biological samples with exceptional sensitivity and specificity. LC-MS/MS (tandem mass spectrometry) is frequently used in untargeted metabolomics to obtain additional structural information[197]. In MS/MS analysis, after the initial mass measurement, ions are fragmented, and their fragmentation patterns are analyzed, adding an additional dimension that allows for more accurate metabolite identification[198–200].

LC-MS and LC-MS/MS produce peaks/features that represent metabolites or molecular fragments in the dataset. These peaks form the raw data, from which a

subset of metabolites can be identified with varying degrees of confidence[201]. These patterns are compared against established databases or libraries of known metabolites. The identification of metabolites in LC-MS/MS is typically based on a combination of retention times (how long a metabolite takes to elute during chromatography), m/z values, and fragmentation patterns from MS/MS analysis. The confidence in metabolite identification is categorized into different levels of annotation confidence[201]. Level 1 (Confirmed structure) annotation offers the highest confidence, requiring a match between the m/z value, retention time, and fragmentation pattern with those of an authentic chemical standard analyzed under identical conditions. Other levels of identification, such as Level 2 (Probable Structure) and Level 3 (Tentative Structure), provide lower confidence, relying on database matches or literature without confirmation from a standard. At the lowest levels, Level 4 (Unequivocal Molecular Formula) and Level 5 (Exact Mass), the identification may only provide basic information, such as molecular formula or mass, without determining the exact structure of the metabolite[201].

1.8 Multiple Mechanisms and Circuits Control Appetite

Appetite regulation in humans involves an interplay of both homeostatic and non-homeostatic signals. Non-homeostatic influences include hedonic factors, such as reward-driven eating, as well as societal and environmental cues like social context and meal timing[202,203]. In contrast, homeostatic regulation can respond to physiological energy demands, integrating signals from various brain regions and peripheral tissues[204].

Central to homeostatic appetite regulation are the hypothalamus and the brainstem. Within the arceus nucleus of the hypothalamus, two first order neuron populations play critical roles: agouti-related peptide/neuropeptide Y (AGRP/NPY) neurons, which promote feeding (orexigenic), and pro-opiomelanocortin (POMC) neurons, which suppress feeding (anorexigenic)[205]. AGRP/NPY neurons, when activated by signaling molecules, promote feeding behaviors[206]. These first-order neurons project to secondary regions within the hypothalamus including lateral hypothalamic area (LHA)and the paraventricular hypothalamus (PVT), modulating the melanocortin system, a crucial regulator of energy balance[206]. Conversely, activation of POMC neurons also modulates the melanocortin system via receptors including MC4R to suppress appetite[207].

The brainstem provides another key pathway for appetite regulation. The Nucleus tractus solitarii(NTS) can integrate neuronal signals originating from the gastrointestinal (GI) tract through vagal afferent pathways[208].

Peripheral signaling molecules influencing appetite originate from various tissues, including adipose tissue, the pancreas, and the gastrointestinal tract[205]. For instance, leptin, produced by adipose tissue, signals satiety to the hypothalamus by activating POMC neurons and inhibiting AGRP/NPY neurons[209]. Insulin from the pancreas similarly modulates hypothalamic activity to negatively regulate feeding behavior[209].

Gastrointestinal-derived signals encompass several key hormones and peptides modulated in response to nutrient ingestion[202]. Ghrelin from the stomach, cholecystokinin (CCK) from enteroendocrine cells in the duodenum and ileum, and peptide YY (PYY) and glucagon-like peptide-1 (GLP-1) from L-cells in more distal intestinal regions all serve as critical appetite modulators[210–215]. These gastrointestinal hormones signal via direct neurons vagal efferent pathways to the brainstem, and signal via humoral signalling to the hypothalamus, thereby contributing to the overall integration of signals that determine feeding behavior and energy balance[202].

1.9 Thesis Aims

Metformin is a widely used anti-diabetic drug known primarily for its role in glucose regulation[73]. However, despite extensive research on its clinical benefits, the precise molecular mechanisms through which metformin exerts its therapeutic effects remain only partially understood[127]. The goal of this thesis is to expand our understanding of the broader metabolic effects of metformin. Recent advances in untargeted metabolomics have provided a more comprehensive view of metformin's

impact, revealing alterations in metabolites beyond glucose[117]. These findings suggest that metformin influences a diverse array of metabolic pathways that were previously unrecognized in this context. By identifying these novel metabolites, we can gain deeper insights into how metformin modulates these pathways, potentially uncovering new mechanisms underlying its therapeutic effects and furthering our understanding of its role in disease management.

Preliminary analysis of T2D patients treated with metformin led us to hypothesize that two classes of metabolites—N-lactoyl amino acids, including the appetite regulator Lac-Phe, and β-hydroxy fatty acids—are increased with metformin treatment. Furthermore, we hypothesize that N-lactoyl amino acids, such as Lac-Phe, rise following feeding.

1.9.1 Specific Aims

1. To analyze untargeted metabolomics data from our in-house Brigham cohort, including obese individuals with and without T2D, to identify metabolites most influenced by metformin treatment.
2. To source and analyze additional metabolomics datasets to validate and extend the metformin-associated metabolite patterns, specifically focusing on N-lactoyl amino acids and β-hydroxy fatty acids, across different populations and cohorts.
3. To investigate whether feeding increases Lac-Phe and related N-lactoyl amino acids, and to determine which specific meal compositions have the greatest impact on their levels.

Chapter 2 - Methods

2.1 Software and Tools

2.1.1 Software Used

The computational and statistical analyses in this research were primarily conducted using Python (version 3.8.12). I extensively utilized Python's Pandas library for data pre-processing and manipulation, and Matplotlib for generating visualizations. Both Visual Studio Code (version 1.91.1) and Jupyter Notebook (version 7.1.2) were employed as the primary development environments throughout the analysis.

GraphPad Prism (version 10.3.0) was used for statistical analyses and figure creation.

Microsoft Excel 2016 (version 16.0.4927.1000) was used as a calculator and for creating tables.

Adobe Illustrator (version 28.6) was employed to refine and finalize figures generated from the above software, ensuring they were publication-ready.

2.1.2 Python Package Library

The computational analyses for this research were conducted within a controlled conda environment, ensuring a consistent setup throughout the analysis. The following is a list of the Python packages included in this environment, specified with

their exact versions using the `package==version` notation to enable reproducibility.

```
absl-py==2.1.0, aiohttp==3.8.1, aiosignal==1.2.0,
alabaster==0.7.13, anndata2ri==1.3.1, anndata==0.8.0,
annoy==1.17.2, anyio==4.3.0, appdirs==1.4.4, argon2-cffi-
bindings==21.2.0, argon2-cffi==23.1.0, arrow==1.3.0,
asciitree==0.3.3, asttokens==2.4.1, async-lru==2.0.4, async-
timeout==4.0.2, attrs==23.2.0, babel==2.14.0, backcall==0.2.0,
backports.functools-lru-cache==2.0.0, backports.zoneinfo==0.2.1,
beautifulsoup4==4.12.3, biopython==1.81, bioservices==1.10.0,
biothings-client==0.3.0, bleach==6.1.0, branca==0.6.0,
brotli==1.0.9, brotlipy==0.7.0, build==1.1.1,
cachecontrol==0.14.0, cached-property==1.5.2, cachy==0.3.0,
celltypist==1.6.2, certifi==2024.2.2, cffi==1.16.0, charset-
normalizer==3.3.2, cleo==2.1.0, click-plugins==1.1.1,
click==8.1.7, cligj==0.7.2, clikit==0.6.2, cloudpickle==3.0.0,
cmappy==4.0.1, colorama==0.4.6, colorlog==6.8.2, comm==0.2.2,
commonmark==0.9.1, contourpy==1.1.1, crashtest==0.4.1,
cryptography==42.0.5, cycler==0.12.1, cytoolz==0.12.3, dask-
image==2021.12.0, dask==2023.5.0, dataclasses==0.8,
debugpy==1.8.1, decorator==4.4.2, decoupler==1.5.0,
defusedxml==0.7.1, deprecated==1.2.13, distlib==0.3.8,
dnspython==2.6.1, docopt==0.6.2, docrep==0.3.2, docutils==0.20.1,
dulwich==0.21.7, easydev==0.12.0, entrypoints==0.4, et-
xmlfile==1.1.0, exceptiongroup==1.2.0, executing==2.0.1,
fasteners==0.17.3, fastjsonschema==2.19.1, filelock==3.13.1,
fiona==1.9.5, flatbuffers==1.12, flit-core==3.9.0, folium==0.14.0,
fonttools==4.50.0, fqdn==1.5.1, frozenlist==1.3.0,
fsspec==2024.3.1, future==1.0.0, geopandas==0.13.2,
gevent==23.9.0.post1, goatools==1.3.9, graphtools==1.5.2,
greenlet==3.0.3, grequests==0.6.0, grpcio==1.62.1, gseapy==0.12.0,
h11==0.14.0, h2==4.1.0, h5py==3.10.0, harmonypy==0.0.5,
hpack==4.0.0, html5lib==1.1, httpcore==1.0.4, httpx==0.27.0,
hyperframe==6.0.1, hyperopt==0.2.7, idna==3.6, igraph==0.11.4,
imagecodecs-lite==2019.12.3, imagecodecs==2023.1.23, imageio-
ffmpeg==0.4.9, imageio==2.34.0, imagesize==1.4.1, importlib-
metadata==7.1.0, importlib-resources==6.4.0, inflect==5.6.0,
installer==0.7.0, ipykernel==6.29.3, ipython-genutils==0.2.0,
ipython==8.12.2, ipywidgets==8.1.2, isoduration==20.11.0,
jaraco.classes==3.3.1, jedi==0.19.1, jinja2==3.1.3, joblib==1.3.2,
json5==0.9.24, jsonpointer==2.4, jsonschema-
```

specifications==2023.12.1, jsonschema==4.21.1, jupyter-client==8.6.1, jupyter-core==5.7.2, jupyter-events==0.10.0, jupyter-lsp==2.2.4, jupyter-server-terminals==0.5.3, jupyter-server==2.13.0, jupyterlab-pygments==0.3.0, jupyterlab-server==2.25.4, jupyterlab-widgets==3.0.10, jupyterlab==4.1.5, kaleido==0.2.1, keras==2.9.0, keyring==24.3.1, kiwisolver==1.4.5, lazy-loader==0.3, leidenalg==0.10.2, libclang==14.0.1, lightning-utilities==0.11.0, llvmlite==0.41.1, locket==1.0.0, lockfile==0.12.2, lxml==5.1.0, magic-impute==3.0.0, markdown-it-py==3.0.0, markdown==3.6, markupsafe==2.1.5, matplotlib-inline==0.1.6, matplotlib-scalebar==0.8.1, matplotlib==3.7.3, mdurl==0.1.2, mistune==3.0.2, mkl-service==2.4.1, mofapy2==0.7.0, more-itertools==10.2.0, moviepy==1.0.3, mpmath==1.3.0, msgpack==1.0.7, multidict==6.0.2, munkres==1.1.4, mygene==3.2.2, natsort==8.4.0, nbclassic==1.0.0, nbclient==0.10.0, nbconvert==7.16.3, nbformat==5.10.3, nest-asyncio==1.6.0, networkx==3.1, notebook-shim==0.2.4, notebook==7.1.2, numba==0.58.1, numcodecs==0.9.1, numpy==1.24.4, omnipath==1.0.5, openai==0.27.6, openpyxl==3.1.2, opt-einsum==3.3.0, outcome==1.3.0.post0, overrides==7.7.0, packaging==24.0, pandas-stubs==2.1.1.230928, pandas==2.0.3, pandocfilters==1.5.0, parso==0.8.3, partd==1.4.1, pastel==0.2.1, patsy==0.5.6, pexpect==4.9.0, pickleshare==0.7.5, pillow==10.2.0, pims==0.6.0, pip==24.0, pkginfo==1.10.0, pkgutil-resolve-name==1.3.10, platformdirs==4.2.0, plotly==5.19.0, ply==3.11, poetry-core==1.9.0, poetry-plugin-export==1.7.1, poetry==1.8.2, pooch==1.8.1, proglog==0.1.10, prometheus-client==0.20.0, prompt-toolkit==3.0.42, protobuf==4.25.3, psutil==5.9.8, ptyprocess==0.7.0, pure-eval==0.2.2, py4j==0.10.9.7, pyasn1==0.4.8, pycparser==2.21, pydeprecate==0.3.0, pydot==1.4.2, pygments==2.17.2, pygsp==0.5.1, pylev==1.4.0, pymongo==4.6.2, pynndescent==0.5.11, pyopenssl==24.0.0, pyparsing==3.1.2, pyproj==3.5.0, pyproject-hooks==1.0.0, pyqt5-sip==12.12.2, pyqt5==5.15.9, pyreadr==0.4.7, pyro-api==0.1.2, pyro-ppl==1.9.0+f02dfb9, pyrsistent==0.20.0, pysocks==1.7.1, python-dateutil==2.9.0, python-json-logger==2.0.7, python-pptx==0.6.23, pytorch-lightning==1.3.8, pytz==2024.1, pywavelets==1.4.1, pywin32-ctypes==0.2.2, pywin32==306, pywinpty==2.0.13, pyyaml==5.4.1, pyzmq==25.1.2, rapidfuzz==3.6.2, referencing==0.34.0, requests-cache==0.4.13, requests-toolbelt==1.0.0, requests==2.31.0, rfc3339-validator==0.1.4, rfc3986-validator==0.1.1, rich==13.7.1, rpds-py==0.18.0, rpy2==3.5.14, rsa==4.8, scanpy==1.9.1, scikit-image==0.21.0, scikit-learn==1.3.2, scikit-misc==0.1.4, scipy==1.10.1, scprep==1.1.0, scrublet==0.2.3, scvi-tools==0.14.5,

```
seaborn==0.13.2, selenium==4.15.2, send2trash==1.8.2, session-
info==1.0.0, setuptools==58.5.3, shap==0.37.0, shapely==2.0.2,
shellingham==1.5.4, sip==6.7.12, six==1.16.0, slicer==0.0.8,
slicerator==1.1.0, sniffio==1.3.1, snowballstemmer==2.2.0,
sortedcontainers==2.4.0, soupsieve==2.5, sphinx==7.1.2,
sphinxcontrib-applehelp==1.0.4, sphinxcontrib-devhelp==1.0.2,
sphinxcontrib-htmlhelp==2.0.1, sphinxcontrib-jsmath==1.0.1,
sphinxcontrib-qthelp==1.0.3, sphinxcontrib-serializinghtml==1.1.5,
squidpy==1.2.2, stack-data==0.6.2, statannot==0.2.3,
statannotations==0.4.4, statsmodels==0.14.1, stdlib-list==0.10.0,
suds-community==1.1.2, sympy==1.12, tasklogger==1.1.2,
tenacity==8.2.3, tensorboard-data-server==0.7.0, tensorboard-
plugin-wit==1.8.1, tensorboard==2.16.2, tensorflow-
estimator==2.9.0, tensorflow-io-gcs-filesystem==0.26.0,
termcolor==1.1.0, terminado==0.18.1, texttable==1.7.0,
threadpoolctl==3.4.0, tifffile==2023.7.10, tinycss2==1.2.1,
toml==0.10.2, tomli==2.0.1, tomlkit==0.12.4, toolz==0.12.1,
torch==2.2.0, torchmetrics==1.3.2, tornado==6.4, tqdm==4.66.2,
traitlets==5.14.2, trio-websocket==0.11.1, trio==0.23.1, trove-
classifiers==2024.3.3, types-python-dateutil==2.9.0.20240316,
types-pytz==2024.1.0.20240203, typing-extensions==4.10.0, typing-
utils==0.1.0, tzdata==2024.1, tzlocal==5.0.1, umap-learn==0.5.5,
unicodedata2==15.1.0, uri-template==1.3.0, urllib3==2.2.1,
validators==0.19.0, virtualenv==20.25.1, wcwidth==0.2.13,
webcolors==1.13, webencodings==0.5.1, websocket-client==1.7.0,
werkzeug==3.0.1, wheel==0.43.0, widgetsnbextension==4.0.10, win-
inet-pton==1.1.0, wrapt==1.16.0, wsproto==1.2.0, xarray==2022.3.0,
xgboost==2.0.3, xlsxwriter==3.1.9, xmltodict==0.13.0, yarl==1.7.2,
zarr==2.11.3, zipp==3.17.0, zope.event==5.0, zope.interface==6.2
```

2.2 Cohort Description

This research relied on data from two distinct sources: one cohort was recruited directly by the Lynch lab, of which I am a member, while several other cohorts were sourced from previously published studies.

2.2.1 In-House Cohort

The Brigham and Women's Hospital Cohort was the only cohort recruited and managed directly by the research team at the Lynch Lab.

Brigham and Women's Hospital Cohort

The study was conducted at Brigham and Women's Hospital, Boston, from August 2019 to December 2019. The participants were categorized into five groups: Obese with Type 2 Diabetes (T2D), Obese Pre-Diabetic, Obese Non-T2D, Lean Pre-Diabetic, and Lean Non-T2D.

All patient procedures took place at Brigham and Women's Hospital. In total, 33 volunteers were recruited for the study. The breakdown of the groups was as follows: Obese T2D: 8 participants (3 women, 5 men) with a BMI range of 30-45 and Hemoglobin A1c (HbA1c) levels between 5.7-9%. It is important to note that one participant was not adhering to their prescribed metformin regimen. Another individual had a BMI marginally below the initial target (29.8). Obese Pre-Diabetic: 3 participants (2 men, 1 woman), including one individual with a BMI slightly below the initial target (BMI 28.3). Obese Non-T2D: 11 participants (3 men, 8 women), with BMI ranges primarily within 30-45, including one individual with a BMI slightly below the initial target (29). Lean Pre-Diabetic: 1 participant (man) with a BMI of 19.6.

Lean Non-T2D: 10 participants (2 men, 8 women), all within the targeted BMI range for lean controls.

Ethics declarations

Patients attending the Diabetes clinic at Brigham and Women's Hospital were recruited prospectively. All patients provided written informed consent. This study was reviewed and approved by the Brigham and Women's Hospital Institutional Review Board (IRB 2020P002554 and 2019P001128).

Recruitment Methodology

Volunteers for the study were recruited from the diabetes clinic and/or the weight management clinics at Brigham and Women's Hospital for the obese groups with or without Type 2 Diabetes (T2D). In addition, flyers placed in clinical and nonclinical areas within the hospital were used to recruit lean control subjects.

The study included men and women aged 18 to 75 years. For lean controls, Caucasian and African American individuals were required to have a Body Mass Index (BMI) of 18.5 to 24.9, while Asian adults needed a BMI of 18.5 to 23.0. The obese cohorts, whether with or without prediabetes or diabetes, had inclusion criteria specifying a BMI of 30 to 45 and HbA1c levels between 5.7% and 9.5%. Individuals diagnosed with diabetes were primarily managed with metformin, with some also receiving insulin. However, the study excluded current smokers; those pregnant or planning pregnancy during the study; individuals with serious uncontrolled cardiovascular, nervous system, pulmonary, renal, or gastrointestinal diseases;

those with serologic evidence of HIV, Hepatitis B, or Hepatitis C; a history of tuberculosis; liver disease characterized by elevated hepatic enzymes; or any hematologic abnormalities within the last 12 months, including a white blood count outside the range of 3,000 to 14,000/μL, lymphocyte count below 500/μL, platelet count under 150,000 /μL, hemoglobin levels less than 10 g/dL, or neutrophil count below 2,000 cells/μL. Additional exclusion criteria were poor glycemic control (HbA1c over 9.5% for those in the diabetes group), major psychiatric illness, or ongoing alcohol or drug abuse.

2.2.2 Cohorts from Previously Published Studies

The study also incorporated data from several cohorts that were part of previously published studies, detailed below.

TwinsUK Cohort Overview

The TwinsUK study involved 2,069 participants, predominantly of European ancestry, from the TwinsUK registry[216]. The cohort was primarily female (96.6%), with participants aged between 32 to 73 years at the first of three visits, which spanned 8 to 18 years. Throughout the study, a total of 6,196 samples were collected. We excluded 8 of these samples due to missing data on more than 175 metabolites. Among these, 86 volunteers were identified as having Type 2 Diabetes (T2D) in at least one blood draw, resulting in 162 T2D samples. Notably, metformin was detected in 71 of these T2D samples. Detailed methodologies and further

insights for this dataset have been previously discussed[217]. The samples were processed by Metabolon. Stored samples were collected between 1997 and 2012

Danish Metformin Intervention Study Overview

The 2019 Danish study at Aarhus University Hospital involved a 12-week treatment of metformin for recent-onset Type 2 Diabetes (T2D) patients and age-BMI matched non-diabetic controls. This intervention included 24 individuals with T2D and 12 non-diabetic controls, all receiving 2000 mg of metformin daily. For a comprehensive understanding of the study design, participant demographics, and methodologies, please refer to the original publication[123]. The samples were processed by Metabolon. Samples were collected between 2013 and 2016.

Jordanian/Saudi Acute Metformin Study Overview

Conducted at the Jordan Center for Pharmaceutical Research in Amman, Jordan, the 2021 study involved 26 healthy young male subjects from Jordan. Each participant, aged 18–50 years, received a single oral dose of 500 mg metformin hydrochloride. Blood samples were collected at five specific time points: pre-drug administration, 1.5 hours before the maximum serum concentration of metformin (Cmax), at Cmax, 2 hours after Cmax, and 36 hours post-administration, amounting to a total of 130 samples for metabolomic analysis.

The participants were not fasted during the study. The evening before metformin administration, all subjects consumed a standard dinner at least 10 hours before

taking the drug. A standard breakfast was provided 30 minutes before drug administration, with standard meals served at 6 and 12 hours post-administration. For detailed methodologies please refer to the original study[218]. This was the only metabolomics dataset in our study not produced by Metabolon, but rather by an inhouse lab.

One-Hour Post-Mixed Meal Metabolic Response Study

In the 2020 study conducted at Nuvisan GmbH in Neu-Ulm, Germany, 30 participants were divided into three groups: Type 2 Diabetes (T2D), Pre-Diabetic, and Metabolically Healthy, each comprising 10 individuals. The research centred around a standardised mixed meal test (MMT), performed on three separate days, resulting in a total of 90 instances where metabolite levels were assessed before and after meal consumption. Serum samples were collected 30 minutes before and 1 hour after the meal. Recruitment criteria included HbA1c, fasting and OGTT-challenged glucose, C-peptide, and intact proinsulin measurements. For T2D participants on metformin, the medication was paused the evening prior to the MMT. Detailed methodology of the study can be found in the original publication[219]. The samples were processed by Metabolon.

Date Fruit and Oral Glucose Tolerance Test Study

Conducted at the Medical Laboratories Clinic in Doha, Qatar, the 2018 nutritional challenge study assessed the plasma metabolome in 21 healthy volunteers—comprising 13 females and 8 males- following the consumption of Khlas and Deglet

Nour date fruits compared to an oral glucose tolerance test. Volunteers participated in three separate challenges with a week's interval between each, consuming either a glucose drink or ten fruits from the specified date varieties. Blood samples were taken at baseline and at 30, 60, 90, and 120 minutes after intake. The study identified 1089 blood circulating metabolites. Detailed methodology of the study can be found in the original publication[220]. The samples were processed by Metabolon.

High Fat Diet Intervention Study Cohort Overview

Conducted at the Australian Catholic University in 2018, a cohort study was conducted involving 24 overweight/obese sedentary men. Assessments were conducted on three separate days: initially under volunteers' habitual diets, after a 5-day high-fat diet, and following an additional 5 days of the high-fat diet with an exercise intervention. Participants were randomised into three groups to compare the effects of morning and evening exercise against no exercise. On the days of metabolomic sampling, participants refrained from exercise. Serum for metabolomics was drawn pre-breakfast at approximately 7:15 am and again at 7:15 pm, following a 6:30 pm dinner. Further details are available in the study's publication[221]. The samples were processed by Metabolon. Samples were collected between March 2017 and August 2017.

ADDITION-Denmark Cohort Overview

The 2015–2016 study at Aarhus University Hospital, Denmark, involved 97 participants who were part of the original ADDITION-Denmark cohort. This cohort included individuals with screen-detected Type 2 Diabetes (T2D), with or without diabetic polyneuropathy (DPN), and age- and sex-matched healthy, lean controls.

The original ADDITION-Denmark study was a screening study that identified volunteers with Type 2 Diabetes (T2D). In the context of this metabolomics study, participants had been living with T2D for an average of 13 years. During the follow-up examination, fasting blood samples were collected, vital signs were assessed, anthropometric measurements were taken, and diabetic polyneuropathy (DPN) was evaluated—all within the same visit.

Healthy control participants were carefully evaluated to ensure they had not developed diabetes or any other neurological disease since the initial screening, and they also underwent normal nerve conduction studies.

Based on the detection of metformin in serum, 70 of the 97 T2D volunteers had metformin detected, while 27 did not. Further details are available in the study's publication[222].

The samples were processed by Metabolon. Samples were collected between October 2015 and June 2016

Weill Cornell EDRN Prostate Cancer Cohort Overview

Conducted at Weill Cornell Medicine in New York City between 2008 and 2017, the Early Detection Research Network (EDRN) Prostate Cancer Cohort involved the recruitment of 1,144 adult male participants. For metabolomics profiling, a subset of 580 participants with comprehensive 12- and 24-month follow-up data was selected. Within the subset of 580 participants, 267 were diagnosed with prostate cancer and 313 were controls. Fasting blood samples were drawn from all participants prior to the biopsy. Among these, 61 participants had diabetes, with metformin detected in the plasma of 35 individuals, while 26 did not have metformin detected. Detailed clinical parameters were recorded for each participant, including biopsy results, prostate cancer diagnosis, and follow-up clinical information up to two years.

Eligibility for the study required that participants had no prior history of prostate cancer or prostate biopsies and were scheduled for a prostate biopsy based on clinical suspicion of prostate cancer. This suspicion was primarily triggered by elevated prostate-specific antigen (PSA) levels, abnormal digital rectal exam (DRE) findings, or suspicious imaging results.

The collected biological specimens, including biopsy tissue, urine, and blood, were processed and biobanked at Weill Cornell Medicine.

A comprehensive explanation of the study's methodology is available in the dedicated data descriptor published by the authors[223].

The samples were processed by Metabolon. Samples were collected between 2008 to 2017

Qatari Continuous Glucose Infusion Study Cohort Overview

The 2020 interventional cohort study conducted in Qatar involved 47 clinically healthy Arab male participants who received a continuous glucose infusion. These participants were selected based on criteria ensuring they had no known diseases or pathologies, with recruitment criteria including normal blood counts, liver function tests, and metabolic markers such as HbA1c and fasting glucose levels.

The participants were aged between 18 and 60 years, with a BMI ranging from 16 to 28. Participants underwent a hyperinsulinemic-euglycemic clamp (HIEC) procedure. Blood samples were collected at two time points: after an overnight fast and 120 minutes post-insulin infusion during the clamp, for untargeted metabolomics analysis.

For detailed methodologies and a comprehensive description of the study's design, please refer to the original publication[224].

The samples were processed by Metabolon.

BARIA Study Cohort Overview

In a 2022 study involving Dutch patients[225], the BARIA study cohort[226] was utilized to investigate the metabolic responses to a liquid mixed meal. This cohort comprised 106 individuals with morbid obesity who were scheduled for bariatric surgery.

Participants were categorized based on their diabetic status into three groups: individuals with normal glucose tolerance (NGT, n = 27), pre-diabetes (Pre-D, n = 57), and Type 2 Diabetes (T2D, n = 22). Classification was determined using fasting blood glucose and HbA1c levels, following the criteria established by the American Diabetes Association.

A standardized 2-hour Mixed Meal Test (MMT) was administered within three months prior to surgery. The MMT consisted of two 125 ml servings of a nutritional drink (Nutridrink compact, Nutricia®), with glucose syrup as the exclusive carbohydrate source. This meal was consumed after a minimum of nine hours of fasting. Untargeted metabolomic analysis was performed on EDTA plasma samples collected both at baseline (fasting) and two hours post-MMT.

This study and its findings were described in a preprint published on BioRxiv[225] and have not yet undergone peer review.
The samples were processed by Metabolon.

2.3 Determination and Classification of Metabolic Status

Determination and Classification of Type 2 Diabetes Status Across Cohorts

In most studies that relied on diabetic status, the Type 2 Diabetes (T2D) classification of volunteers was directly noted in the available metadata. However, there were two notable exceptions. In the "Weill Cornell EDRN Prostate Cancer Cohort," the metadata simply recorded general diabetic status without specifying the type. For the purposes of this study, these cases were included as T2D.

The second exception was the Twins UK cohort, where T2D status was not explicitly recorded in the metadata but was instead derived from a series of questionnaires that volunteers had completed over many years. These questionnaires, stored in Excel sheets, contained various types of data: binary indicators of whether a volunteer was diabetic at specific points in time, as well as recall data where volunteers reported the age at which they were diagnosed with diabetes.

Due to the nature of the Twins UK cohort data, where volunteers only completed a subset of available surveys, a comprehensive approach was needed to infer the T2D status. By collating and analyzing the responses, it was possible to estimate a range of dates during which a volunteer likely transitioned to a diabetic state. For example, a volunteer might not have been diabetic in December 2005 but was classified as diabetic by March 2007. This allowed us to categorize each of the three samples collected from each volunteer as "Not T2D" (n=5,876), "T2D" (n=162), or "Status

Unknown" (n=150) when there was insufficient information to make a definitive classification.

To ensure the accuracy of our classifications, we excluded any volunteers who indicated in their questionnaires that they had Type 1 diabetes or gestational diabetes. Additionally, responses that were clearly inconsistent, such as a volunteer reporting being diabetic in one year but not in subsequent years without plausible explanation, were filtered out. This approach ensured that the classification of T2D status was as accurate as possible given the available data.

Metformin Status Determination

In intervention studies, the metformin status of volunteers was known. For observational studies, metformin status was inferred from untargeted metabolomics data, assuming volunteers were on the drug if it was detected in their blood. Questionnaire data from the Twins UK cohort was also considered but deemed less accurate, though it correlated with the metabolomics-based method.

Fasting Status Determination

Fasting status was known for all studies except the Brigham study. In the Twins UK cohort, fasting status was collated from survey data, though this information was sometimes missing. Volunteers were categorized as Fasted (n=4,474), Non-Fasted (eaten within hours, n=129), or Unknown (n=1,585).

2.4 Statistical Methods

2.4.1 General Statistical Methods

Metabolomics Data Handling and Normalization

Metabolon untargeted metabolomics data were obtained either by reading from Excel spreadsheets or by ingesting data via Python from the Metabolomics Workbench resource. The Python package **`pandas`** was used to organize and manipulate the data.

These datasets had been pre-processed by Metabolon using their standard procedure, which includes median normalization on a per-compound basis for each batch of samples to ensure consistency and comparability across batches. For more details on this process, see [227].

However, for two of the cohorts—Weill Cornell EDRN Prostate Cancer Cohort and Jordanian/Saudi Acute Metformin Study Cohort —raw area counts were used instead of normalized values. In the case of the Weill Cornell EDRN Prostate Cancer cohort, only the raw values were provided, and the batch information was not available in the Metabolomics Workbench resource, making it impossible to recreate normalized values. Similarly, the **Jordanian/Saudi Acute Metformin Study Cohort** also utilized raw area counts, it was the only non-Metabolon dataset.

Volcano Plot Analysis

For most volcano plots across the studies, statistical significance was typically determined using a two-tailed Student's t-test for independent samples, which compares the means of two independent groups to assess statistically significant differences. This was implemented using the **`ttest_ind`** function from the **`scipy.stats`** module in Python, and the test was performed independently for each metabolite.

In the One-Hour Post-Mixed Meal Metabolic Response Study, where paired samples (e.g., pre- and post-prandial states of the same individuals) were analyzed, a paired two-tailed Student's t-test was used instead. This test, implemented with the **`ttest_rel`** function from **`scipy.stats`** in Python, was also performed independently for each metabolite to assess changes within the same subjects over time.

For visualization purposes, p-values and fold changes were log-transformed to -Log10 and Log2, respectively.

ROC Curve Analysis

Receiver operating characteristic (ROC) curve analysis was conducted using the **`roc_curve`** and **`roc_auc_score`** functions from the **`scikit-learn`** package in Python. ROC curves were generated independently for each metabolite, with the area under the curve (AUC) calculated to assess their predictive accuracy.

Time Course Normalization

For both time course analyses in the Jordanian/Saudi Acute Metformin Study and the Date Fruit and Oral Glucose Tolerance Test Study, Lac-Phe levels were normalized to individual baseline measurements to ensure consistent assessment of changes over time.

Correlation Analysis

Spearman's rank correlation coefficients were applied to evaluate correlations between different factors, unless otherwise specified, using pandas in Python

Calculation of Lac-Phe Increase Across Metformin and Feeding Cohorts

The quoted size increase in Lac-Phe for the 4 metformin cohorts is calculated as follows: for the Brigham cohort, by dividing the average Lac-Phe levels in obese T2D by the average levels in obese non-T2D; in TwinsUK cohort, by dividing the average Lac-Phe levels of T2D on metformin by the average levels of T2D not on metformin; for the Danish study (NCT01729156), by comparing average levels post a 12-week intervention vs. pre-intervention for healthy controls and T2D's. The quoted size increase in Lac-Phe for the feeding cohort is calculated by dividing the average post-meal Lac-Phe values by the pre-meal values; notably, mixed meal values were not normalized to baseline, unlike the other cohorts where baseline-normalized values were used.

2.4.2 Cohort-Specific Statistical Analyses

Brigham Cohort

In the Brigham Cohort, Lac-Phe levels were analyzed using an ordinary one-way ANOVA with with Sidák's multiple comparisons test to identify significant differences (Prism). Relationships between metformin levels and Lac-Phe were assessed using simple linear regression, with the goodness of fit expressed as an R-squared value (Prism).

TwinsUK Cohort

The effect of T2D diagnosis and metformin initiation was analyzed using a two-way ANOVA, with multiple comparisons adjusted using Fisher's LSD test (Prism). To examine the effect of the fasted state on T2D in the TwinsUK cohort, unpaired t-tests were used (Prism). Correlations between various parameters were evaluated using Spearman's rank correlation coefficients unless otherwise stated (Python).

Jordanian/Saudi Acute Metformin Study

In the Jordanian/Saudi acute metformin study, one-sample t-tests were used to independently compare normalized Lac-Phe levels at each time point against the pre-metformin baseline (Prism).

Danish Metformin Intervention Study

In the Danish Metformin Intervention Study (NCT01729156), statistical significance from baseline to post-12-week samples was assessed using Welch's two-sample t-test on log-transformed data. These statistics, along with fold changes, were provided in the supplemental data of the original publication[123] and were originally calculated by Metabolon.

One-Hour Post-Mixed Meal Metabolic Response

In the One-Hour Post-Mixed Meal Metabolic Response cohort, a mixed-effects model with Sidák's multiple comparisons test was applied to assess significance versus baseline (Prism).

High Fat Diet Intervention Study

For the High Fat Diet Intervention Study, one-sample t-tests were employed to assess significance against baseline levels (Prism).

Date Fruit and Oral Glucose Tolerance Test Study

To compare the effects of date fruit interventions with an oral glucose tolerance test, the area under the curve (AUC) was calculated using Prism.

ADDITION-Denmark Study

In the ADDITION-Denmark Cohort, β-Hydroxy Fatty Acids levels were analyzed using an ordinary one-way ANOVA with with Sidák's multiple comparisons test to identify significant differences (Prism).

Fold changes and p-values for tables were calculated in the same manner as in the volcano analysis, using the ttest_rel function from the scipy.stats module in Python.

Weill Cornell EDRN Prostate Cancer Study

In the Weill Cornell EDRN Prostate Cancer Cohort, β-Hydroxy Fatty Acids levels were analyzed using an ordinary one-way ANOVA with with Sidák's multiple comparisons test to identify significant differences (Prism).

Fold changes and p-values for tables were calculated in the same manner as in the volcano analysis, using the ttest_rel function from the scipy.stats module in Python.

Qatari Continuous Glucose Infusion Study

In the Qatari Continuous Glucose Infusion Study, Lac-Val levels were analyzed using a paired two-sided t-test to assess significance between pre- and post-clamp samples (Prism).

2.5 Untargeted Global Metabolite Profiling

Metabolon, Inc. performed untargeted metabolite profiling for seven out of the eight cohorts involved in our comprehensive analysis. The Jordanian/Saudi Acute Metformin Study is the only cohort for which Metabolon did not conduct the metabolomics analysis[218]. Detailed methodologies for all cohorts can be found in their respective original publications.

Example Metabolomics Methods for Brigham and Women's Hospital Cohort

Sample preparation and data generation were performed as described previously by Metabolon, Inc[227]. In brief, sample preparation involved protein precipitation and removal with methanol, shaking and centrifugation. The resulting extracts were profiled on an accurate mass global metabolomics platform consisting of multiple arms differing by chromatography methods and mass spectrometry ionization modes to achieve broad coverage of compounds differing by physiochemical properties such as mass, charge, chromatographic separation, and ionization behavior. The details of this platform have been described previously[228] Metabolites were identified by automated comparison of the ion features in the experimental samples to a reference library of chemical standard entries that included retention time, molecular weight (m/z), preferred adducts, and in-source fragments as well as associated MS spectra, and were curated by visual inspection for quality control using proprietary software developed at Metabolon[227,229].

2.6 Metabolite Identification and Mapping

N-lactoyl amino acid identification

N-lactoyl amino acids have been labeled as unknown and mislabeled in existing metabolomic datasets. Upon querying Metabolon, they provided us with an update on the specific metabolite identifications. This allowed us to systematically identify and correct these mislabelings throughout the cohorts included in our analysis, using our updated mapping table to ensure the accurate representation of N-lactoyl amino acids in our study.

Clarification regarding previous misannotation of N-lactoyl amino acids

The misidentification issue arose because both 1-carboxyethylphenylalanine and N-lactoyl phenylalanine primary peaks share identical mass-to-charge ratios (e.g., m/z = 236.0928). Although our primary focus here is on N-lactoyl phenylalanine (Lac-Phe), similar misannotation issues apply to other N-lactoyl derivatives. The misannotation originated when Metabolon mistakenly produced N-lactoyl amino acids as unintended reaction byproducts during the synthesis of chemical standards for 1-carboxyethyl amino acids. Consequently, when N-lactoyl amino acids were detected in biofluids, they were incorrectly mapped to the contaminated 1-carboxyethyl amino acid standards. An independent research group collaborating with Metabolon has since provided further structural elucidation, clearly differentiating Lac-Phe from 1-carboxyethylphenylalanine through tandem mass spectrometry (MS/MS)[148]. Specifically, the absence of a characteristic daughter ion (m/z = 192), exclusively observed in 1-carboxyethylphenylalanine, distinguished

Lac-Phe. Additionally, liquid chromatography-mass spectrometry (LC-MS) experiments demonstrated distinct retention times for Lac-Phe (~12 min) compared to 1-carboxyethylphenylalanine (~17 min).

Mapping and Selection of β-Hydroxy Fatty Acids

To identify relevant β-hydroxy fatty acids, we selected all fatty acids that contained a β-hydroxy group and had a straight-chain structure, excluding branched compounds like 3-hydroxy-3-methylglutarate. Both saturated and unsaturated fatty acids were included in the analysis. In the Metabolon datasets, metabolites were listed with names such as 3-hydroxyoctanoate and 3-hydroxysebacate. To facilitate easy comparison, we mapped these to our β-hydroxy naming convention, which includes the chain length, the number of double bonds (":0"), and the designation "DC" for dicarboxylic acids. For example, 3-hydroxyoctanoate was mapped to β-OH-C8:0, and 3-hydroxysebacate was mapped to β-OH-DC-C10:0.

2.7 Data Availability

Metabolomic data for the Brigham cohort are provided in the supplementary materials of our recent publication: Metformin and feeding increase levels of the appetite-suppressing metabolite Lac-Phe in humans[230]

Upon Access to the TwinsUK metabolomics dataset can be applied for through the TwinsUK Resource Executive Committee.

We used data posted with the original manuscripts, from the following 3 studies:

1. Short-term variability of the human serum metabolome depending on nutritional and metabolic health status[219].
2. Metabolic changes of the blood metabolome after a date fruit challenge[220].
3. Metformin increases endogenous glucose production in non-diabetic individuals and individuals with recent-onset type 2 diabetes[123].

Data from the following 2 articles can be requested from the corresponding authors:

1. A Metabolic Pattern in Healthy Subjects Given a Single Dose of Metformin: A Metabolomics Approach[218].
2. The effect of morning vs evening exercise training on glycaemic control and serum metabolites in overweight/obese men: a randomised trial[221].

We downloaded data from two studies available on the Metabolomics Workbench resource:

1. **Study ID: ST001411** - Plasma lipid metabolites associate with diabetic polyneuropathy in a cohort with type 2 diabetes[222]

2. **Study ID: ST002498** - Plasma metabolomics profiling of 580 patients from an Early Detection Research Network prostate cancer cohort[223]

2.8 Code Availability

Scripts for analyzing data from the three publicly available cohorts are posted on GitHub at https://github.com/barryfscott/Metformin-Feeding-Lac-Phe-Analysis.

2.9 Funding and Data Sharing Contributions

This work was supported by NIH 5R01AI134861 and R01AI134861-04S1 and Science Foundation Ireland under the SFI Centre for Research Training in Genomics Data Science grant 18/CRT/6214. We wish to thank the patients and their families for participating in this research project. TwinsUK is funded by the Wellcome Trust, Medical Research Council, Versus Arthritis, European Union Horizon 2020, Chronic Disease Research Foundation (CDRF), Zoe Ltd, the National Institute for Health and Care Research (NIHR) Clinical Research Network (CRN) and Biomedical Research Centre based at Guy's and St Thomas' NHS Foundation Trust in partnership with King's College London. We extend our sincere thanks to Trine Moholdt[221] and Anas M Abdel Rahman[218] for providing valuable metabolomics data from their cohorts and for their insightful responses to our queries.

Chapter 3 - Metformin Drives an Increase of the Appetite-Suppressing Metabolite Lac-Phe

Introduction

Metformin is prescribed to over 150 million people worldwide and acts to reduce blood glucose [127,231] and weight[70,84] in T2D patients. Despite its widespread use, the exact mechanisms underlying its therapeutic effects remain incompletely understood[127]. While other biguanide class drugs like phenformin raised concerns over lactic acidosis[232] metformin's association with this condition is exceptionally rare. Lactate levels have been shown to increase in T2D cohorts with metformin use, but the effect is not universal (see [106]for review). Metformin's impact on weight loss is attributed to its appetite-suppressing properties, though the mechanisms involved are still unclear. While metformin-induced increases in the hormone GDF15 were proposed to mediate appetite suppression[86,87] recent findings have challenged whether this is the only or indeed most important mechanism involved[233].

N-Lactoyl phenylalanine (Lac-Phe) is a metabolite generated by the peptidase Carnosine Dipeptidase 2 (CNDP2)[141], which enzymatically fuses lactate and phenylalanine. Lac-Phe has been recently shown to be an appetite suppressor when administered to obese mice and has been correlated to weight loss in humans engaged in regular exercise[142,147]. In humans, Lac-Phe has also been reported to increase with intense exercise[141,142], in phenylketonuria[141], and in mitochondrial disease (MELAS)[133]. However, whether lactate derived metabolites such as Lac-Phe might contribute to the appetite-suppressing activities of metformin treatment has not been previously investigated.

Both Type 2 Diabetes (T2D) and metformin significantly alter the serum metabolome, impacting a wide array of metabolites beyond glucose[117,234]. Metabolomic studies often focus on a narrow set of predefined molecules, potentially overlooking key metabolites that play crucial roles in disease pathophysiology or therapeutic responses. However, advances in untargeted metabolomics now provide an opportunity to capture a more comprehensive metabolite profile, allowing for the discovery of novel biomarkers and pathways associated with T2D and its treatments[185,235]. To harness this capability, the Lynch Lab recruited a cohort from Brigham and Women's Hospital, including obese T2D volunteers treated with metformin and obese non-T2D volunteers. In this chapter, we initially examine the metabolic alterations associated with T2D before focusing on the changes induced by one of its treatments—metformin.

3.1 Serum Metabolite Profiling Reveals Increased Lac-Phe in T2D Volunteers

In the present study, serum samples were collected from 33 volunteers at Brigham and Women's Hospital, comprising lean non-T2D, lean pre-T2D, obese non-T2D, obese pre-T2D, and obese T2D volunteers (Table 3.1). Untargeted metabolomic profiling was performed using ultra-high-performance liquid chromatography–tandem mass spectroscopy (UPLC–MS/MS), quantifying 1,168 serum metabolites. Comparing the serum metabolomes of T2D (n=21) and non-T2D (n=8) volunteers in the Brigham cohort revealed trends consistent with previous T2D metabolomic studies[234]. As expected, metabolites such as glucose, leucine, mannose, and lactate were significantly elevated in the T2D group, while 1,5-anhydroglucitol (1,5-AG), which typically decreases in T2D, was significantly lower[234] (Figure 3.1).

The data show a marked increase in all measured N-lactoyl amino acids in T2D volunteers, a finding that had not been previously reported in the context of T2D. Given that our cohort included several lean non-T2D volunteers, but not lean T2D volunteers, we narrowed our analysis to only the obese volunteers (BMI primarily between 30–45) to reduce potential confounding effects of obesity. This approach allowed us to isolate the impact of T2D on N-lactoyl amino acid levels. The observed increases in N-lactoyl amino acids are likely related to T2D itself, rather than any potential effect of obesity (Figure 3.2).

Historically, N-lactoyl amino acids were not commonly reported in metabolomic datasets; in fact, as of February 2024, only three studies out of 2,621 in the online repository “Metabolomics Workbench” included Lac-Phe measurements. It transpires that N-lactoyl amino acids were mislabelled in metabolomic studies. For instance, a recent study detected increases in N-lactoyl amino acids in a subgroup of T2D volunteers, but N-lactoyl amino acids were erroneously reported as 1-carboxyethyl amino acids. Other studies simply report Lac-Phe as unknown compound X-15497 (Table 3.2). Given the interesting properties of Lac-Phe as an appetite suppressor[142], we focused on this particular N-lactoyl amino acid. These data show that Lac-Phe levels were 5.7-fold higher in obese T2D individuals compared to obese non-T2D control volunteers (Figure 3.3). A significant increase was also observed between obese T2D and pre-diabetic individuals (Figure 3.3).

To support these findings, the serum metabolomic data from the extensive TwinsUK cohort were investigated. This dataset, consisting predominantly of middle-aged female participants, provided over 2,000 individual metabolic profiles with over 6,000 serum samples collected from 1997 to 2012. The cohort included 162 T2D samples out of 6,034 total samples (Figure 3.4). In this larger cohort, only two N-lactoyl amino acids were measured, Lac-Phe (N-lactoyl phenylalanine) and N-lactoyl valine, both of which were again observed to be significantly increased in T2D individuals, and were among the most significantly elevated metabolites (Figure 3.5 and Figure 3.6).

Brigham Cohort

Patient Description	Number of patients
Lean, Non-T2D	10
Lean, Pre-T2D	1
Obese, Non-T2D	11
Obese, Pre-T2D	3
Obese, T2D	8

Table 3.1: Brigham cohort: Including Lean Non-T2D's, Obese Non-T2D's and Obese T2D's volunteers

Distribution of 33 participants in the Brigham cohort, categorised by their Type 2 diabetes (T2D) status and body mass index (BMI). For lean controls, Caucasian and African American individuals were required to have a BMI of 18.5–24.9 kg/m², whereas Asian adults needed a BMI of 18.5–23.0 kg/m². The obese cohorts, whether with or without pre-diabetes or diabetes, had inclusion criteria specifying a BMI of 30–45 kg/m². Some participants were slightly outside their target BMI ranges. Detailed inclusion criteria and participant information can be found in the Methods section

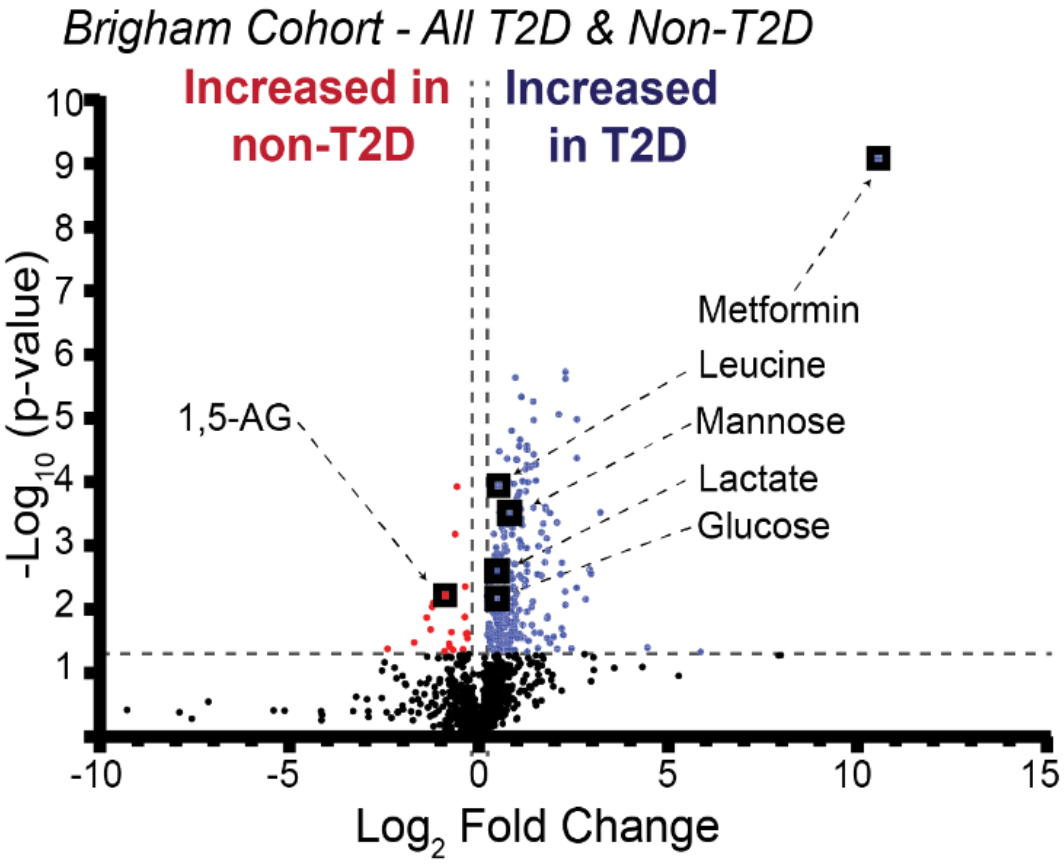

Figure 3.1: Brigham Cohort: Metabolite Comparison Between T2D and Non-T2D

Volcano plot comparing the serum metabolomes of all T2D (n=21) and non-T2D (n=8) individuals in the Brigham cohort. Metabolites significantly (p=0.05) upregulated (blue) and downregulated (red) in T2D compared to non-T2D individuals are shown. Each metabolite was independently analysed using two-tailed Student's t-test

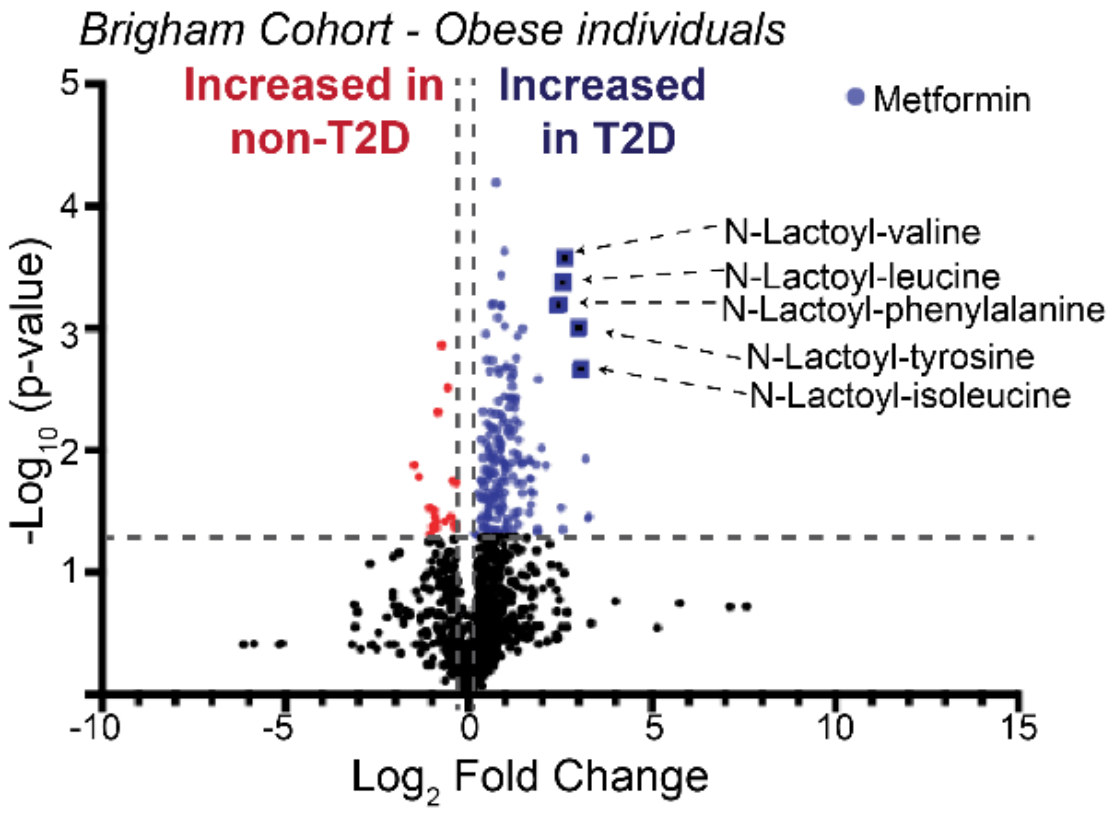

Figure 3.2: N-lactoyl Amino Acids: Markedly Increased Metabolites in Type 2 Diabetes

Volcano plot comparing the serum metabolomes of obese T2D (n = 8) and obese non-T2D (n = 11) individuals from the Brigham cohort. This analysis focuses solely on the obese subset of the cohort. Metabolites significantly ($P < 0.05$) upregulated (blue) and downregulated (red) in T2D compared to non-T2D individuals are shown, with N-lactoyl amino acids highlighted. Each metabolite was independently analysed using a two-tailed Student's t-test.

Unknown	Incorrect ID	Correct ID
X-13529	1-carboxyethylvaline	N-lactoyl valine
X-15497	1-carboxyethylphenylalanine	N-lactoyl phenylalanine
X-18889	1-carboxyethylleucine	N-lactoyl leucine
X-22102	1-carboxyethylisoleucine	N-lactoyl isoleucine
X-19561	1-carboxyethyltyrosine	N-lactoyl tyrosine
X-25607	1-carboxyethylhistidine	N-lactoyl histidine

Table 3.2: Correction of metabolite mislabelings

This table delineates the original unknown labels assigned to N-lactoyl amino acids (Unknown column), their previous misidentifications (Incorrect ID column) and their verified correct identifications (Correct ID column). These mappings were used to accurately identify metabolites reported in our cohorts.

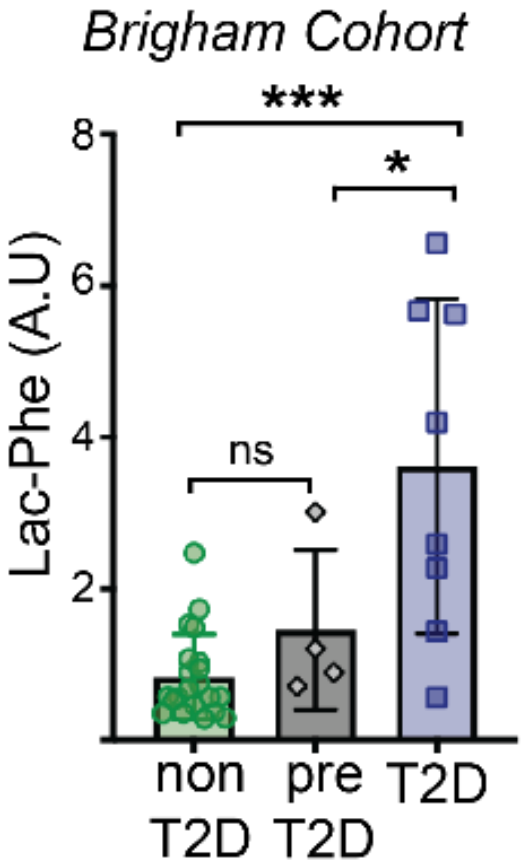

Figure 3.3: Lac-Phe is significantly increased in T2D in Brigham cohort

Lac-Phe levels in non-T2D (n = 21), pre-T2D (n = 4), and T2D (n = 8) individuals from the Brigham cohort. Data are represented as mean ± s.d. Statistical significance is indicated (*P = 0.0198 and ****P < 0.0001; NS, non-significant), and comparisons were made using one-way ANOVA with Šídák's post test.

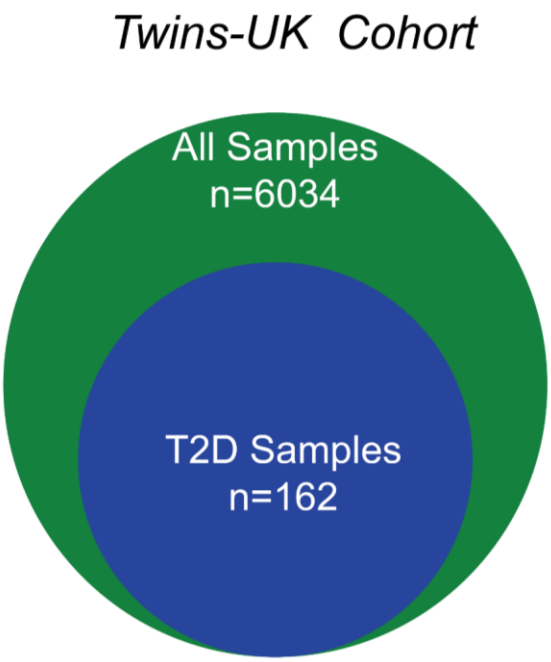

Figure 3.4: TwinsUK Cohort: Distribution of T2D Serum Samples

The nested circle diagram shows the distribution of T2D samples within the TwinsUK cohort. The largest circle represents all samples (n = 6,034) and the inner circle represents T2D samples (n = 162).

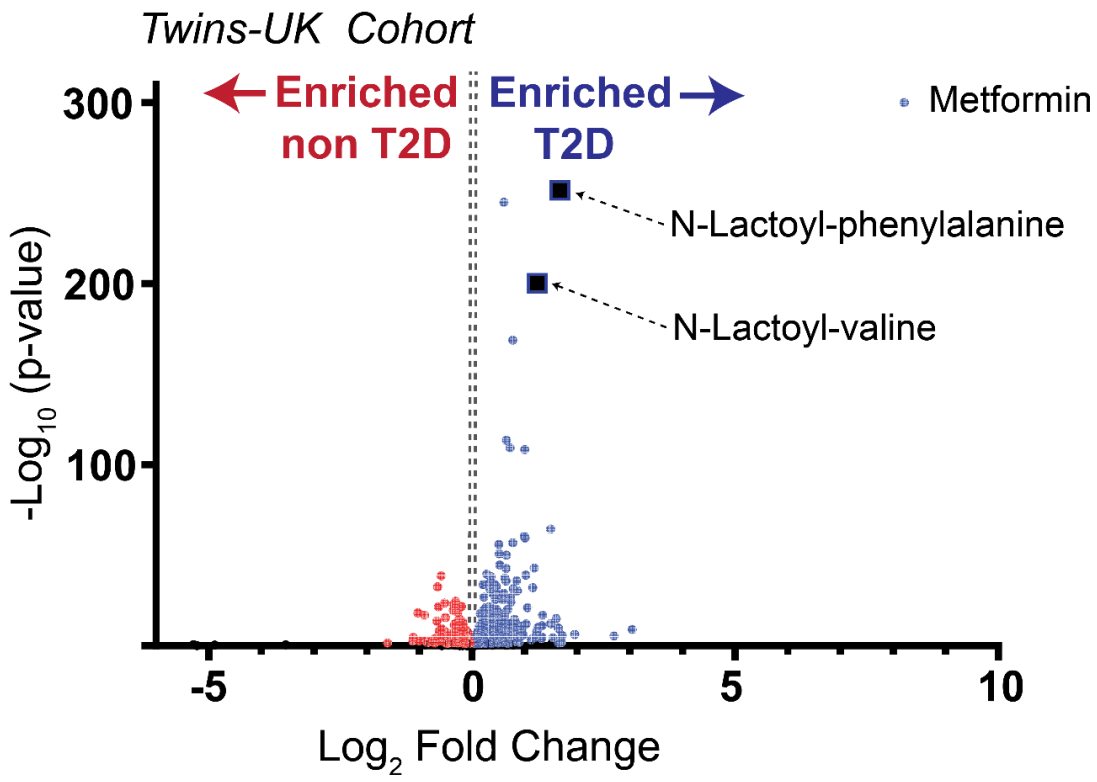

Figure 3.5: N-lactoyl amino acids are increased in T2D in TwinsUK cohort

Volcano plot comparing the serum metabolomes of non-T2D (n = 5,876) and T2D (n = 162) individuals from the TwinsUK cohort. Metabolites significantly ($P < 0.05$) upregulated (blue) and downregulated (red) in T2D compared to non-T2D individuals are shown, with N-lactoyl amino acids highlighted. Each metabolite was independently analyzed using a two-tailed Student's t-test.

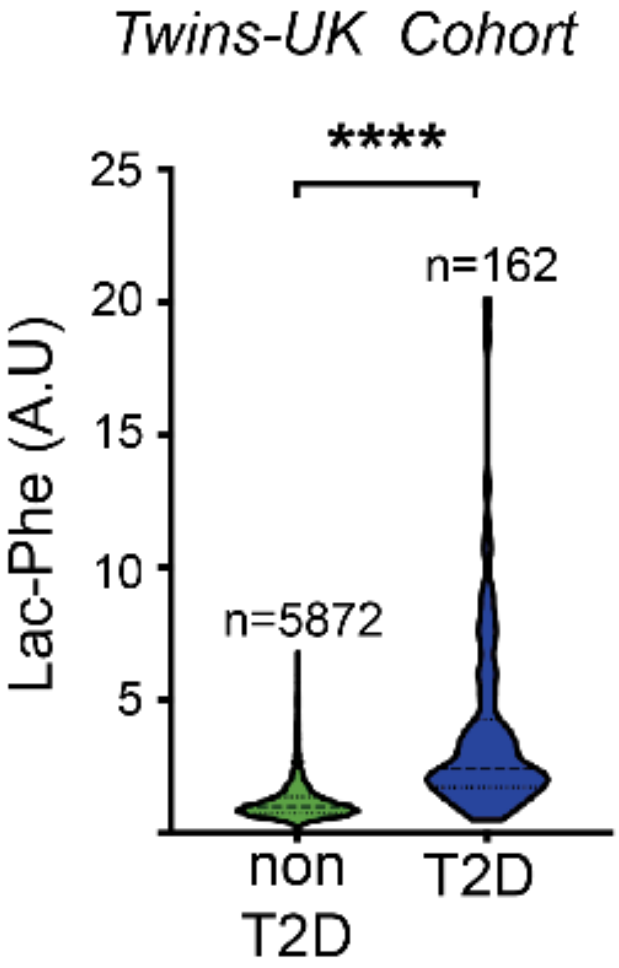

Figure 3.6: Significant Increase in Lac-Phe in T2D: TwinsUK Cohort

Lac-Phe levels in non-T2D (n = 5,872) and T2D (n = 162) individuals from the TwinsUK cohort. Data are shown as a violin plot with median (dashed line) plus maximum and minimum quartiles (dotted line). Statistical significance is indicated (****P < 0.0001), and comparisons were made using a two-tailed Student's t-test.

3.2 Lac-Phe Elevation Primarily Linked to Metformin Use in T2D Volunteers

Lac-Phe concentrations strongly correlated with levels of other N-lactoyl amino acids, such as N-lactoyl tyrosine, within the Brigham cohort (Figure 3.7). We also noticed that N-lactoyl amino acids were also highly correlated with metformin levels (Figure 3.8), and considering the widespread use of metformin in individuals with T2D, we explored whether serum Lac-Phe levels might be influenced by metformin treatment. Specifically, a strong correlation was observed between Lac-Phe and metformin concentrations (Spearman ρ=0.76) among individuals with T2D, in the Brigham and Women's Hospital (Figure 3.9b). Although metformin use was an inclusion criterion for the T2D volunteers in this particular study, in one volunteer's sample metformin was not detected, and this coincided with the lowest observed Lac-Phe measurement (Figure 3.9 a, b). It emerged that this volunteer had actually discontinued taking metformin. This data led us to hypothesize that the increased Lac-Phe in the serum of individuals with T2D might be driven by metformin rather than T2D itself.

The hypothesis that metformin, rather than T2D itself, drives the increase in serum Lac-Phe levels was further tested using the TwinsUK dataset. This dataset spans samples collected from 1997 to 2012, a period marked by the expanded use of

metformin in T2D management. The TwinsUK dataset includes a total of 6,034 serum samples, with 162 from volunteers with T2D. Of these, 91 samples were from volunteers treated with metformin (Figure 3.10), allowing for a direct comparison between those on metformin and those who were not. Lac-Phe levels were considerably higher in T2D volunteers treated with metformin, not only compared to non-T2D volunteers but, more importantly, compared to T2D individuals who were not receiving metformin (Figure 3.11). Analysis of these T2D samples revealed that the two N-lactoyl amino acids measured in this study, Lac-Phe (N-lactoyl phenylalanine) and N-lactoyl valine, were among the most significantly elevated metabolites in the metformin-treated group (Figure 3.12).

When the metadata of T2D volunteers were analysed to see what factors best correlated to Lac-Phe levels, we discovered that metformin treatment was the most significant factor, ahead of ‘years since T2D diagnosis’ and ‘BMI score’ (Table 3.3). This provided further evidence that metformin treatment leads to higher serum Lac-Phe levels.

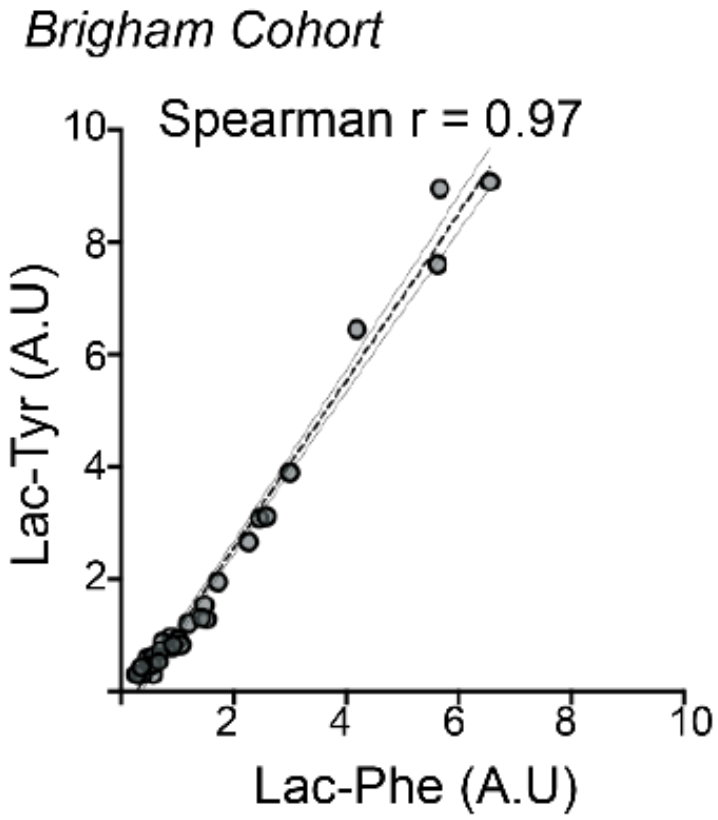

Figure 3.7: High Correlation Among N-lactoyl Amino Acids
Spearman's rank correlation between Lac-Phe and N-lactoyl-tyrosine (Lac-Tyr) among all volunteers in the Brigham cohort (n = 33). The graph shows mean linear regression with 95% confidence intervals, demonstrating a strong correlation (Spearman's r = 0.97).

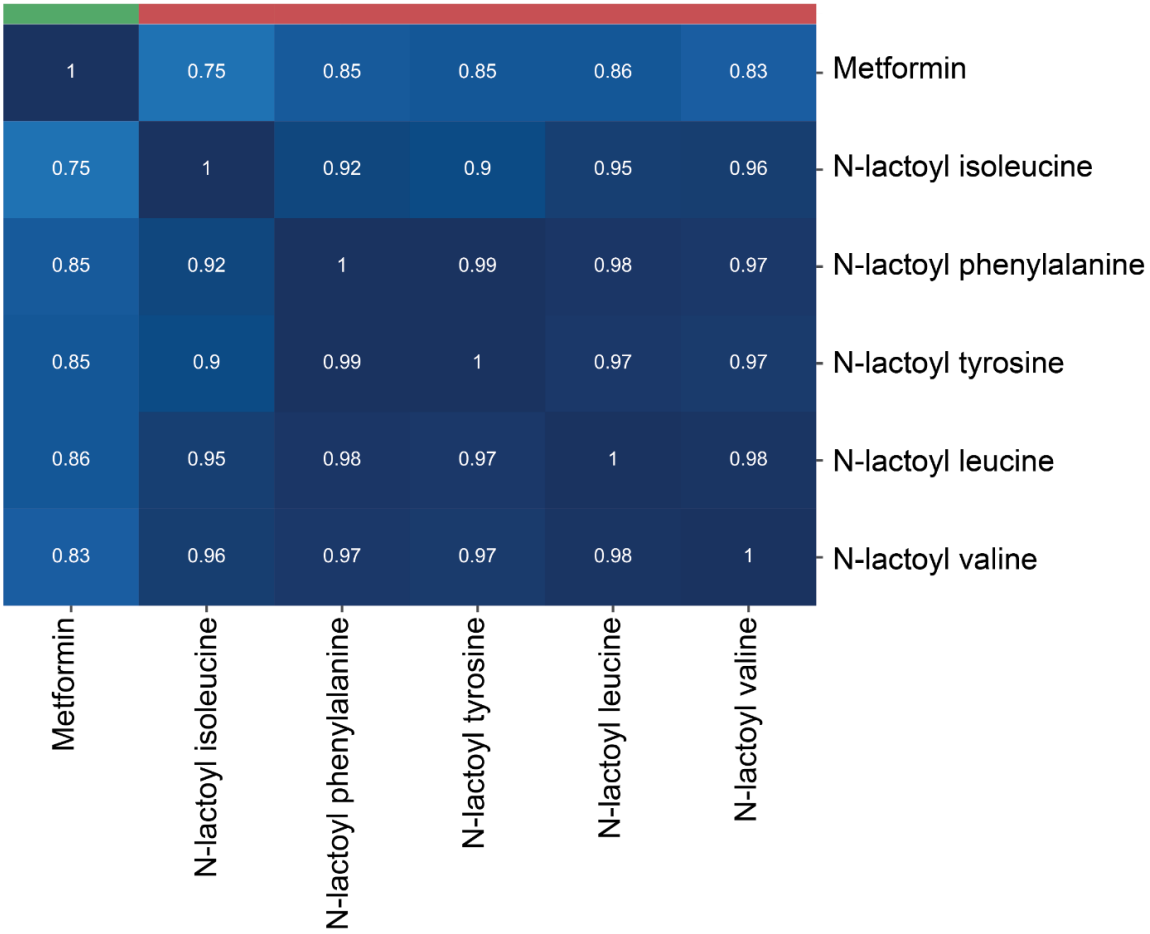

Figure 3.8: N-lactoyl amino acids are highly correlated with metformin
Correlation heatmap showing the relationships between metformin and N-lactoyl amino acids (N-lactoyl isoleucine, N-lactoyl phenylalanine, N-lactoyl tyrosine, N-lactoyl leucine, and N-lactoyl valine) in samples from all 33 volunteers in the Brigham cohort. The columns are color-coded: green for metformin, red for N-lactoyl amino acids. The heatmap is annotated with Pearson correlation coefficients.

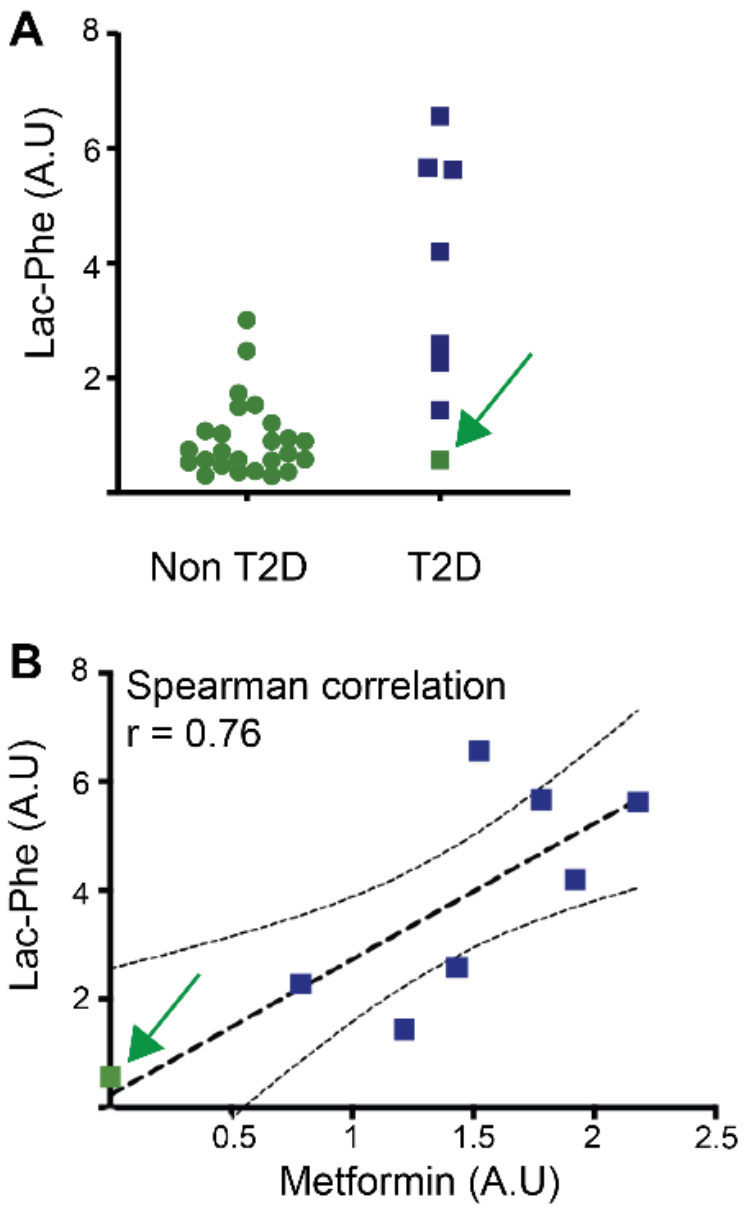

Figure 3.9: In T2D patients metformin levels positively correlate with Lac-Phe.

a, Serum Lac-Phe levels in non-T2D (n=25) and T2D (n=8) individuals from the Brigham cohort. The data points are presented as individual values for each participant. Blue points represent volunteers taking metformin, green points are volunteers not taking metformin. The green arrow indicates a volunteer with T2D who had stopped taking their metformin medication, showing lower Lac-Phe levels similar to those of non-T2D individuals.

b, Spearman's rank correlation between metformin and Lac-Phe levels in T2D individuals (n=8) from the same cohort. The graph depicts the linear regression with 95% confidence intervals. The green arrow highlights the same volunteer as in panel

A who had lower levels of Lac-Phe and was not taking their prescribed metformin treatment. The correlation coefficient (r) is 0.76, suggesting a strong positive relationship between metformin intake and Lac-Phe levels.

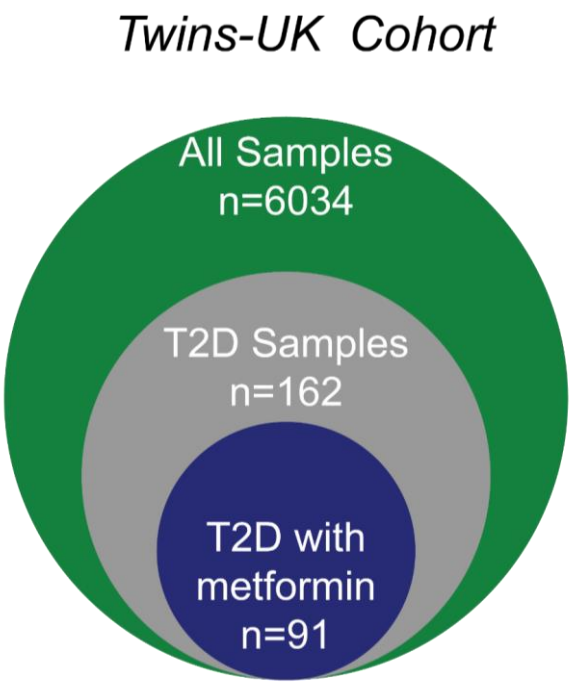

Figure 3.10: TwinsUK Cohort: Includes T2D Serum Samples with and without Metformin

The nested circle diagram illustrates the distribution of samples in the TwinsUK cohort. The largest circle represents all samples (n = 6,038), the middle circle represents T2D samples (n = 162), and the smallest circle represents T2D samples treated with metformin (n = 91).

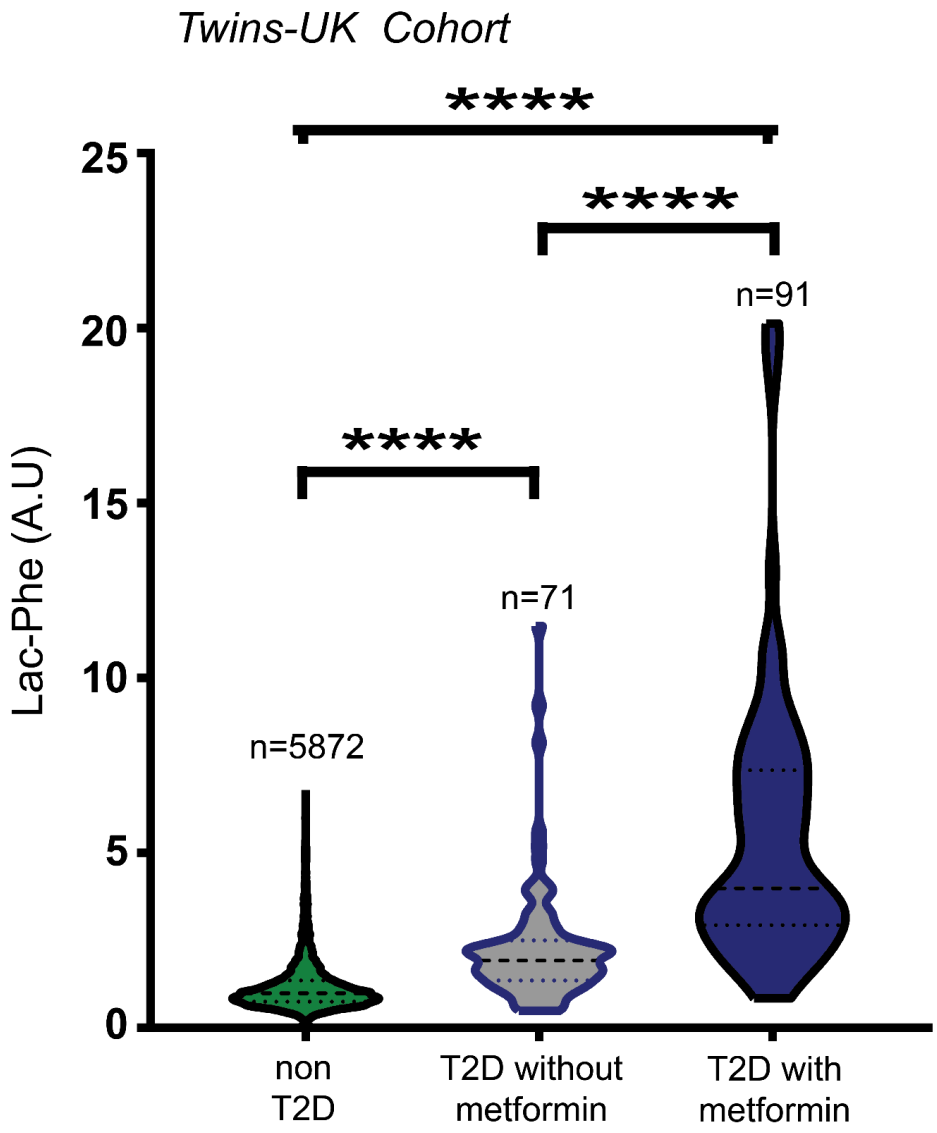

Figure 3.11: Lac-Phe is Increased in T2D's Treated with Metformin

Lac-Phe levels in non-T2D (n = 5,872) volunteers, T2D volunteers without metformin treatment (n = 91), and T2D volunteers with metformin treatment (n = 71) from the TwinsUK cohort. Data are shown as violin plots with median (dashed line) and maximum and minimum quartiles (dotted lines). Statistical significance is indicated (****P < 0.0001), and comparisons were made using one-way ANOVA with Šídák's post test.

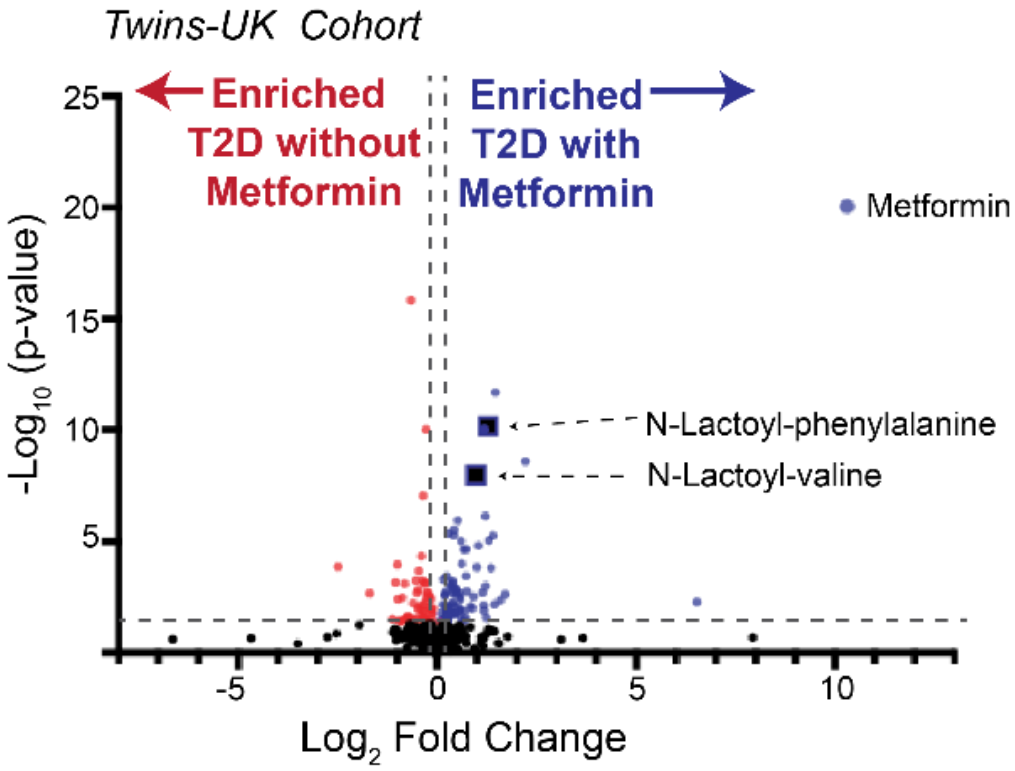

Figure 3.12: N-lactoyl Amino Acids: Markedly Increased Metabolites in Type 2 Diabetes Taking Metformin

Volcano plot comparing the serum metabolomes of T2D individuals with (n = 71) and without (n = 91) metformin treatment from the TwinsUK cohort. Metabolites significantly ($P < 0.05$) upregulated (blue) and downregulated (red) with metformin treatment are shown, with N-lactoyl amino acids highlighted. Each metabolite was independently analysed using a two-tailed Student's t-test.

Twins-UK Cohort

Metadata column	Spearman Correlation
Metformin in serum	58%
Years T2D	38%
Non Fasted	33%
>5yr T2D	29%
BMI>30	22%
BMI	20%
Age >70	13%
Age	12%
VitC in serum	2%
Age at diagnosis	-13%

Table 3.3: Correlation of Metformin and Fasting Status with Lac-Phe Levels in TwinsUK Volunteers

Spearman's rank correlation in T2D samples (n = 162) versus non-metabolite metadata: Metformin in serum, Years T2D (years since T2D diagnosis), Non-Fasted (volunteer had eaten within 6 hours of sample collection), >5yr T2D (more than 5 years since T2D diagnosis), BMI >30, BMI, Age >70, Age, VitC in serum (ascorbate detected in metabolomics), and Age at diagnosis (age when volunteer received a T2D diagnosis). The data shows the correlation percentages, with positive correlations in blue and negative correlations in red.

3.3 Metformin Shows a Stronger Relationship with Lac-Phe Than Lactate

The increase in serum Lac-Phe with metformin is logical, given that Lac-Phe is a fusion of lactate and phenylalanine, and lactate has been reported to rise with metformin use. To explore this further, we also examined lactate levels across three groups in the TwinsUK cohort: non-T2D individuals, T2D patients **not** treated with metformin, and T2D patients treated with metformin—similar to our previous analysis of Lac-Phe (Figure 3.13). Our analysis revealed a statistically significant elevation in serum lactate levels among metformin-treated individuals compared to both non-T2D individuals and T2D patients not on metformin (Figure 3.13). However, the increase in lactate was less pronounced compared to the elevation of serum Lac-Phe (Figure 3.13). Serum Lac-Phe levels showed a much stronger response to metformin, as demonstrated by the ROC curve in Figure 3.14. The area under the curve (AUC) for serum Lac-Phe was 0.83, significantly higher than the AUC for lactate at 0.65. This indicates that serum Lac-Phe is not only more sensitive to metformin treatment but also serves as a more specific and reliable biomarker for identifying metformin use in T2D patients.

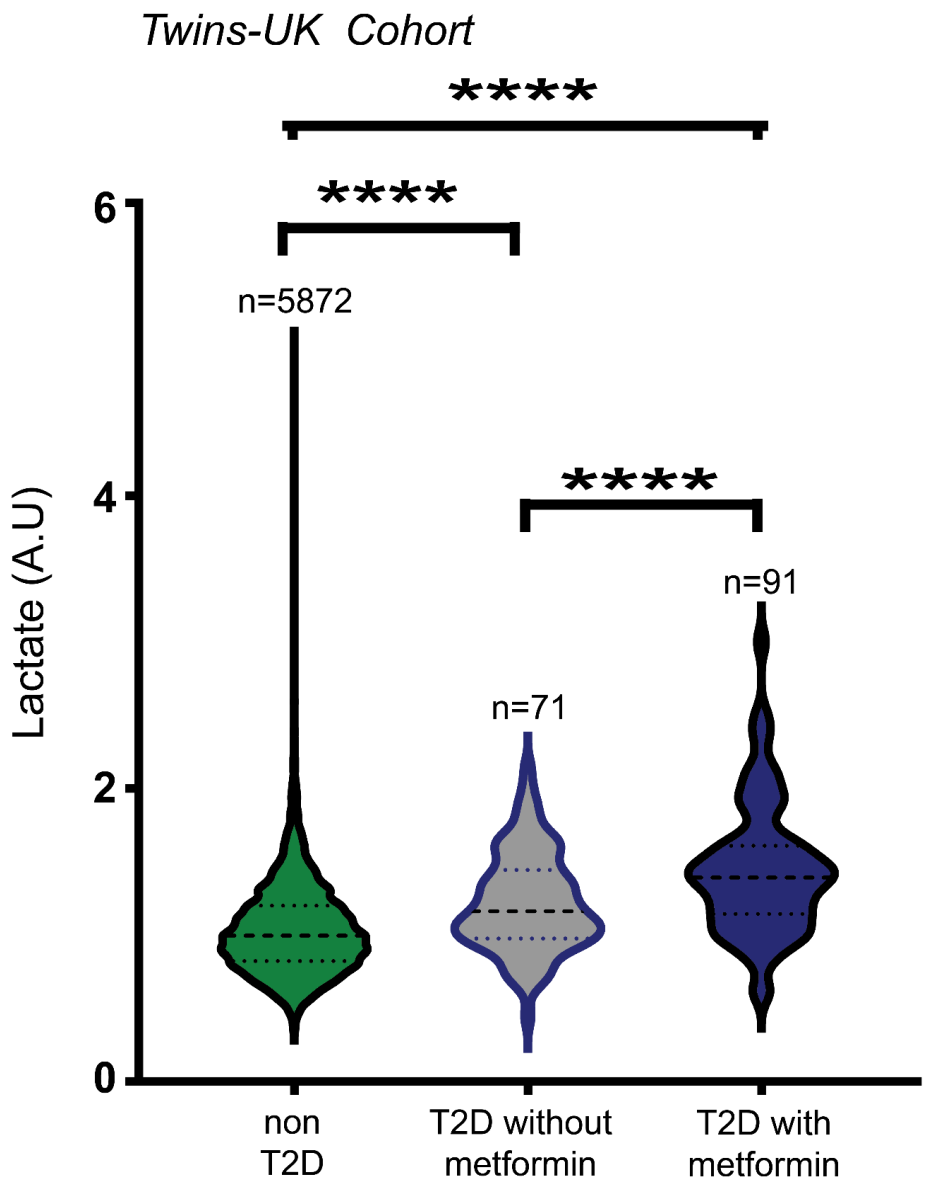

Figure 3.13: Metformin Correlates with Lactate Levels: TwinsUK Cohort
Lactate levels in non-T2D (n = 5,872) volunteers, T2D volunteers without metformin treatment (n = 91), and T2D volunteers with metformin treatment (n = 71) from the TwinsUK cohort. Data are shown as violin plots with median (dashed line) and maximum and minimum quartiles (dotted lines). Statistical significance is indicated (****P < 0.0001), and comparisons were made using one-way ANOVA with Šídák's post test.

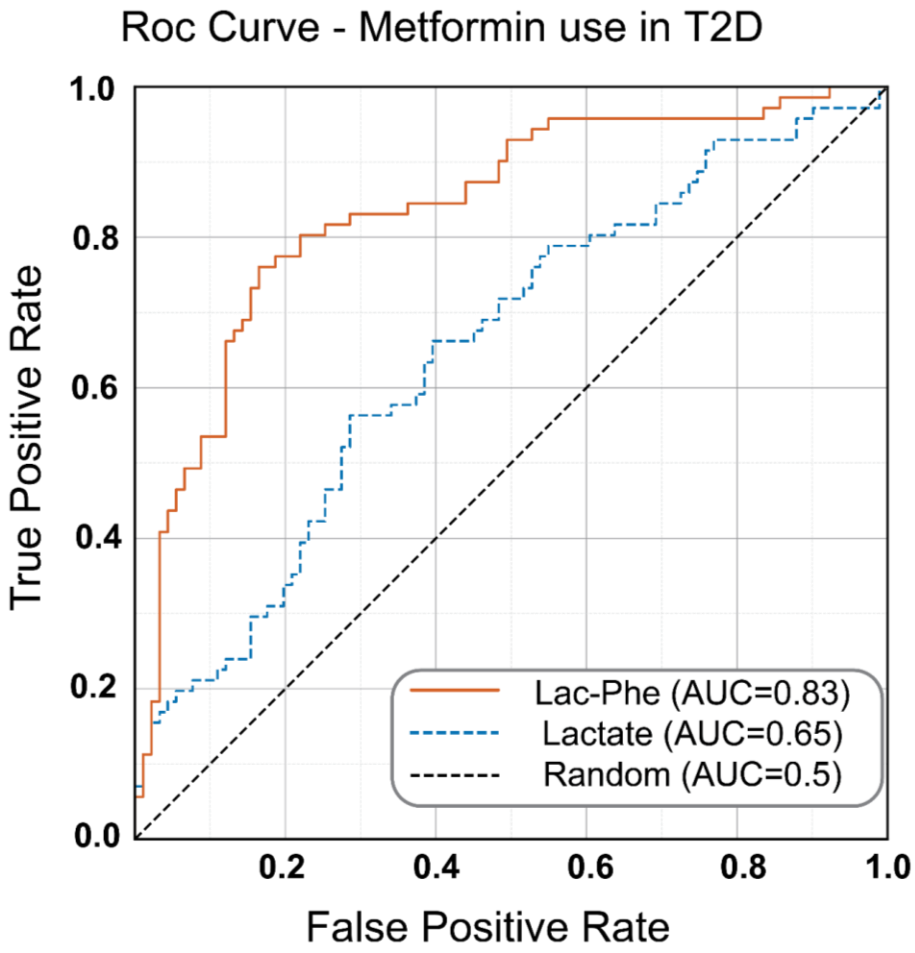

Figure 3.14: Lac-Phe is a Superior Predictor of Metformin Treatment Compared to Lactate

ROC curves comparing the ability of Lac-Phe and lactate to predict metformin treatment among T2D samples from the TwinsUK cohort. The analysis included T2D samples without metformin treatment (n = 71) and T2D samples with metformin treatment (n = 91). The area under the curve (AUC) for Lac-Phe is 0.83, indicating a superior predictive value compared to lactate, which has an AUC of 0.65. A random classifier is represented with an AUC of 0.5.

3.4 Initiation of Metformin Treatment in TwinsUK Cohort Leads to Increased Lac-Phe Levels

The TwinsUK dataset included three serum samples collected from each volunteer between 1997 and 2012. This period was crucial, as it coincided with a significant expansion in metformin's role in T2D management. With an average of 6.5 years between blood draws, the extended sampling period allowed for changes in volunteers' diabetic and medication status to occur. These data can be used to trace the trajectory of Lac-Phe levels in volunteers whose T2D and metformin status changed over time (Figure 3.15).

Volunteers newly diagnosed with T2D and starting metformin treatment exhibited a significant elevation in Lac-Phe levels. In contrast, those newly diagnosed with T2D but not initiating metformin therapy did not show a significant change in Lac-Phe levels (Figure 3.15). Similarly, among volunteers consistently diagnosed with T2D over successive blood draws, the introduction of metformin treatment led to a substantial rise in Lac-Phe levels. In contrast, volunteers who remained with T2D but did not initiate metformin therapy did not show a significant change in Lac-Phe levels (Figure 3.15). These findings pointed to a likely causal link between metformin use and elevated Lac-Phe levels.

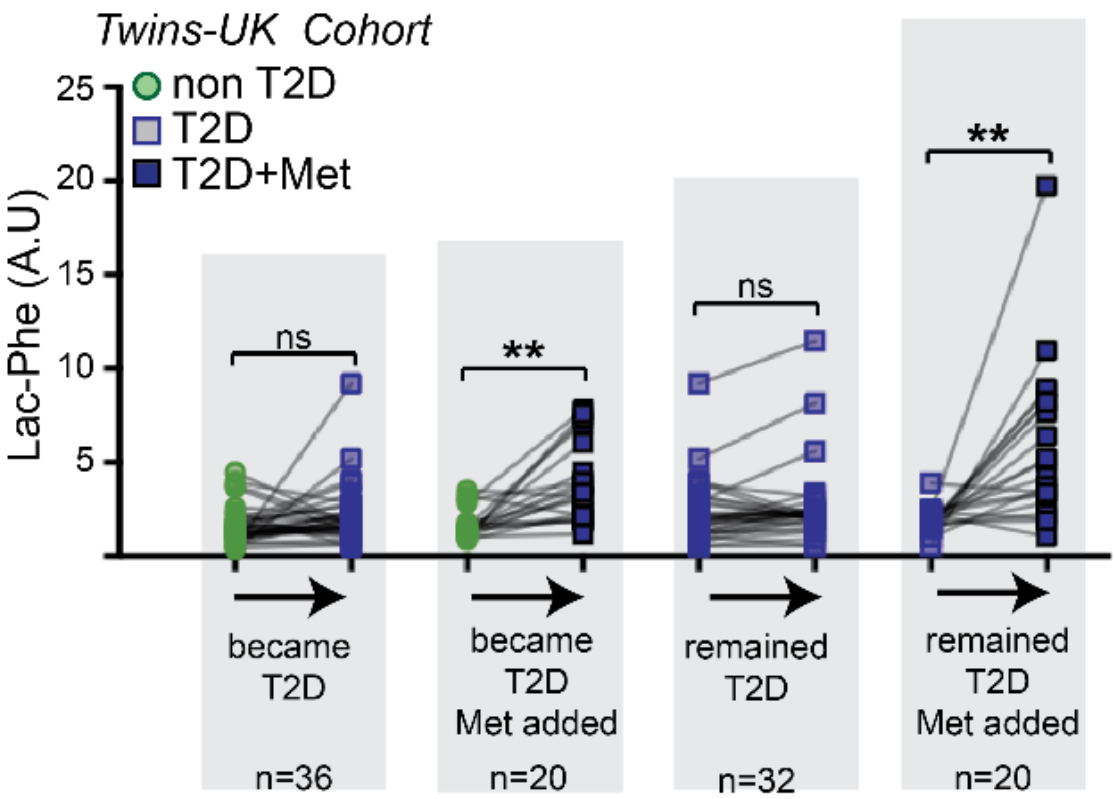

Figure 3.15: Lac-Phe Levels Rise After Metformin Treatment Initiation: TwinsUK Cohort

TwinsUK volunteers provided three serum samples, with an average of 6.5 years between samples. Paired data are shown for volunteers whose T2D status changed and/or who commenced metformin treatment between samples (**P < 0.01, ****P < 0.0001; NS, non-significant). Data were analysed using two-way ANOVA with Fisher's LSD post test.

3.5 Interventional Studies Confirm Metformin-Associated Increases in Lac-Phe

To establish a causal link between metformin treatment and elevated Lac-Phe levels, data from two previously published interventional studies were analysed. In a 2019 Danish study[123] (NCT01729156) patients with recent-onset T2D who were over 50 years of age and BMI-matched non-diabetic controls, with 12 volunteers in each group, underwent 12 weeks of metformin treatment. Serum metabolomics was performed before and after the 12-week intervention. Although no difference was observed in the levels of phenylalanine, tyrosine, valine, leucine and isoleucine in the serum of either T2D or non-T2D groups, there were clear and significant increases in the corresponding N-Lactoyl amino acids, including Lac-Phe (Figure 3.16). Post-treatment untargeted metabolomic analysis measured a more than 80% increase in Lac-Phe levels in both groups (Figure 3.16). Indeed, even acute metformin treatment leads to increased Lac-Phe levels. A Jordanian study[218] gave 26 young healthy men a single oral dose of metformin and performed non-targeted metabolomic analysis over the course of 36 h. Levels of Lac-Phe quickly increased alongside those of metformin with a peak in serum Lac-Phe observed corresponding to the maximum concentration observed (Cmax) of metformin (Figure 3.17). Taken together, these interventional studies that encompassed both long-term and acute metformin dosing provide compelling evidence that metformin treatment induces elevated serum Lac-Phe levels.

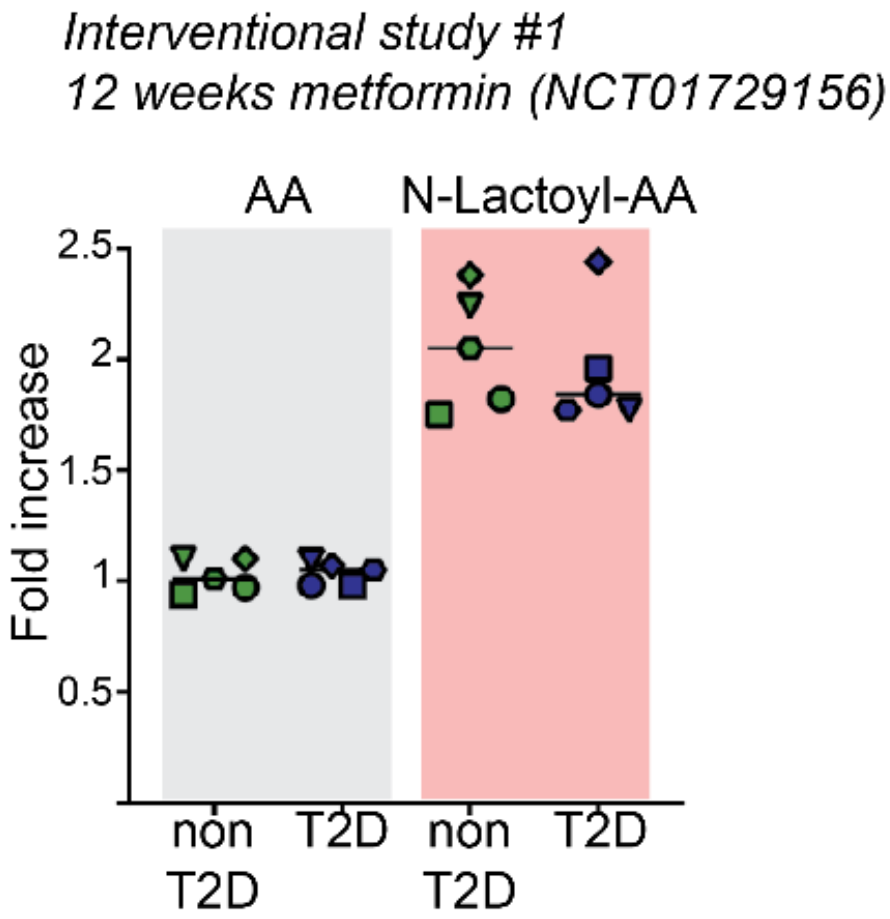

Figure 3.16: Significant Increase in N-lactoyl Amino Acids Following 12 Weeks of Metformin Treatment

Comparison of amino acid (AA) and N-lactoyl-amino acid (N-lactoyl-AA) levels after a 12-week metformin intervention, relative to pre-treatment levels, in a 2019 Danish study (NCT01729156). Fold increases for patients with recent-onset T2D and age/BMI-matched non-T2D controls (n = 12 per group) are shown for five separate AAs and the corresponding N-lactoyl-AA: phenylalanine (circle), tyrosine (square), valine (hexagon), leucine (triangle), and isoleucine (diamond). Statistical significance is indicated (*P < 0.05). Data are mean values. Data were analysed using Welch's two-sided Student's t-test.

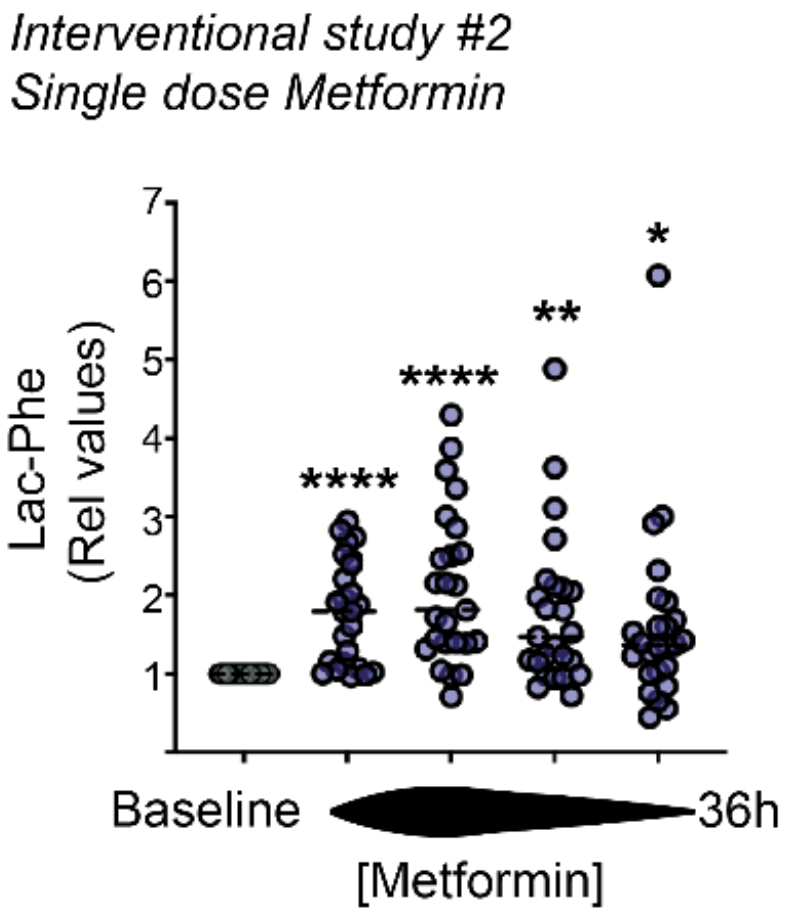

Figure 3.17: Significant Increase in Lac-Phe Following a Single Dose of Metformin

Lac-Phe levels (relative to baseline) over 36 hours after a single oral dose of metformin in a study involving 26 young healthy male volunteers. Lac-Phe values were measured before the maximum metformin concentration (Cmax) in the serum, at the Cmax, and after the Cmax. A final sample was taken 36 hours after dosing (**P = 0.0086, ***P = 0.0005, and ****P < 0.0001). Data are individual data points. Statistical significance was determined using a one-sample t-test against a theoretical value of 1.

3.6 Discussion

Type 2 Diabetes (T2D) significantly alters the serum metabolome[234], yet many affected metabolites remain underexplored. Metabolomic studies are often limited in scope, focusing on a narrow set of molecules, leaving gaps in our understanding of these metabolic changes. Advances in untargeted metabolomics have allowed for the detection and quantification of a broader array of metabolites, revealing new insights into how T2D and its treatments impact the metabolome. However, varying confidence levels in metabolite identification can sometimes lead to errors. Level 1 annotation offers the highest level of confidence in LC-MS-based metabolomics. It involves matching key properties, such as m/z value and retention time, of the metabolite of interest against an authentic standard of the same metabolite, analyzed using the same LC-MS system. Despite these advancements, misidentifications can still occasionally occur. For example, this study exploited the fact that N-lactoyl amino acids were initially misclassified as 1-carboxyethyl amino acids. In this study, we aimed to identify key metabolites influenced by T2D or its treatment that may play pivotal roles in the disease's pathophysiology or therapeutic responses. This led us to further investigate the metabolomic effects of metformin.

Our study conclusively demonstrates that metformin treatment significantly increases the levels of N-lactoyl amino acids, including the appetite-suppressing molecule N-lactoyl phenylalanine (Lac-Phe). This increase was consistently

observed across four diverse human cohorts, representing different sexes, age groups, and geographic regions, underscoring the robust relationship between metformin use and elevated Lac-Phe levels. Moreover, this effect was not confined to individuals with T2D but extended to non-diabetic individuals, indicating that metformin's influence on this metabolite is independent of diabetic status.

Complementary Insights from Related Study

While our study provides strong evidence that metformin treatment significantly increases levels of the appetite-suppressing metabolite N-lactoyl phenylalanine (Lac-Phe), several important considerations should be noted. First, although Lac-Phe has been identified as an appetite suppressor in the context of exercise[142], our study does not directly establish that the observed increase in Lac-Phe mediates metformin’s appetite-suppressing effects. Importantly, previous research has shown that Lac-Phe does not universally suppress appetite[142]. For example, intraperitoneal injection of Lac-Phe reduced food intake in obese mice but had no effect in lean mice, even at higher doses[142]. Additionally, CNDP2 knockout mice, which have reduced Lac-Phe biosynthesis, exhibited similar food intake to wild-type mice when fed a high-fat diet, with an exercise intervention required to reveal the appetite-suppressing effect of Lac-Phe[142]. Furthermore, while we have clearly demonstrated that metformin leads to elevated blood Lac-Phe levels, our study does not elucidate the mechanism by which metformin induces this elevation.

Lac-Phe mediates metformin's appetite suppression

It is important to highlight that our findings[230] were published in Nature Metabolism alongside a complementary study[236], which demonstrated that Lac-Phe likely mediates metformin's appetite-suppressing effects.The study used global CNDP2 knockout mice. CNDP2 is the enzyme primarily responsible for producing Lac-Phe. In these knockout mice, Lac-Phe levels were reduced by 50% at baseline and by 80% following metformin treatment. To investigate the role of Lac-Phe in appetite suppression, both wild-type and CNDP2 knockout mice were first placed on a high-fat diet to induce weight gain before being treated with metformin. Wild-type mice showed significant reductions in both cumulative food intake and body weight compared to saline-treated controls. However, CNDP2 knockout mice did not exhibit reductions in food intake or body weight, indicating that Lac-Phe is crucial for the appetite-suppressing and weight-reducing effects of metformin.

In addition to the mouse model findings, a mediation analysis in a human cohort suggested that Lac-Phe is a likely mediator of metformin's weight loss effects in humans. Together, these findings indicate that Lac-Phe plays a critical role in enabling metformin to suppress appetite, both in mice and likely in humans.

Mechanism of Increased Lac-Phe Production

This complementary study also provides mechanistic insight into how metformin induces the elevation of Lac-Phe. Metformin is known to inhibit mitochondrial

Complex I[237,238], a key component of the electron transport chain responsible for oxidizing NADH to NAD+ and driving ATP production. When Complex I is inhibited, cells require an alternative pathway to generate ATP and regenerate NAD+. In response, they increase their reliance on glycolysis, which serves two critical functions: it produces ATP independently of oxidative phosphorylation and restores NAD+ by oxidizing NADH to NAD+ during the conversion of pyruvate to lactate. Increased glycolysis can also lead to excess lactate production, which could serve as a substrate for Lac-Phe synthesis. The researchers demonstrated in cell lines that both metformin and rotenone, a Complex I inhibitor, increased Lac-Phe levels, which implicates Complex I inhibition as the primary driver of Lac-Phe production.

Metformin reaches its highest concentrations in the intestines[239–241]. The researchers used VIL1-cre floxed mice to knock out CNDP2 specifically in enterocytes. In this enterocyte-specific knockout, there was no Lac-Phe response to metformin, demonstrating that Lac-Phe is produced in the intestines in response to metformin. This is the first time the tissue responsible for Lac-Phe production has been definitively identified. In other contexts, such as exercise, sepsis, or phenylketonuria, the exact tissue driving increased Lac-Phe levels remains unclear. The finding that the gut is the primary tissue of Lac-Phe production in response to metformin raises the possibility that the intestines could generate the excess Lac-Phe during exercise, which has been shown to suppress appetite in this context. Future studies using these intestine-specific knockout mice could help determine

whether the gut contributes to exercise-induced Lac-Phe production and its effects on appetite regulation.

Additionally, the researchers used cell lines and tracing experiments to show that increased extracellular lactate was not required for Lac-Phe production. This suggests that lactate generated from glucose via glycolysis, either locally or within the same cell, can be used by CNDP2 to produce Lac-Phe. This finding is consistent with previous research that has shown increased lactate production in the intestines in response to metformin treatment[242,243]. This suggests that the Lac-Phe generated by enterocytes in response to metformin is likely driven by the excess lactate produced within these cells. However, it is also possible that lactate from other local cells in the gut could contribute to Lac-Phe production by being taken up by enterocytes. A recently developed mouse model, where the lactate transporter MCT1 is knocked out specifically in the intestines, could help clarify this[244]. If extracellular lactate is required for Lac-Phe production, then Lac-Phe levels would likely not rise in response to metformin in these mice. Additionally, metformin has been shown to impact the gut microbiome[111,245,246], raising the possibility that lactate produced by gut bacteria could also contribute to Lac-Phe synthesis. Studies using germ-free mice could help determine whether the microbiome plays a role in this process.

Furthermore, in this study, cell line experiments revealed a greater reduction in Lac-Phe levels following metformin treatment compared to baseline conditions in CNDP2

knockout cells. This suggests that CNDP2 is responsible for producing a substantial portion of the Lac-Phe in response to metformin. One possibility is that other Lac-Phe-producing mechanisms may be near saturation under normal conditions, with CNDP2 playing a key role in generating the additional Lac-Phe observed during metformin treatment. Another possibility is that metformin drives the increased expression or function of CNDP2, enhancing its capacity to produce Lac-Phe. This hypothesis could be tested experimentally by assessing CNDP2 expression and activity levels following metformin administration.

The researchers also investigated whether Lac-Phe mediates its appetite-suppressing effects through other known regulators of appetite, specifically PYY[247], GLP-1[248], and GDF15[86,87], which have previously been shown to be modulated by metformin. When they examined the CNDP2 knockout mice compared to wild-type mice, they found no significant changes in the levels of PYY, GLP-1, or GDF15, suggesting that Lac-Phe does not exert its appetite-suppressing effects through these pathways.

GDF15 is known to increase with metformin treatment and has previously been reported as the primary driver of metformin's appetite suppression[86,87], although this has been disputed[85]. To further investigate the role of GDF15, the researchers inhibited the GDF15 receptor in mice to observe whether this altered Lac-Phe's effects on appetite suppression. Interestingly, in CNDP2 knockout mice, appetite was still suppressed even when the GDF15 receptor was inhibited, indicating that

GDF15 is not the primary mediator of Lac-Phe's effects. However, the data suggested there may be a slight reduction in the overall appetite-suppressing effect when the GDF15 receptor was inhibited. This observation, though not entirely conclusive, raises the possibility that GDF15 could play a complementary role in Lac-Phe's regulation of appetite. Notably, GDF15 and Lac-Phe display similar regulatory patterns across various physiological contexts. For instance, both increase with exercise, metformin treatment, and in response to mitochondrial disease (MELAS), as well as obesity[86,87,133,142,249]. This overlap suggests the possibility that GDF15 and Lac-Phe may act synergistically in regulating appetite, potentially working together to exert more pronounced effects.

In summary, the complementary study provides a clearer understanding of how metformin stimulates Lac-Phe production. High concentrations of metformin in the intestines likely inhibit complex I in enterocytes, leading to increased lactate production, which drives Lac-Phe synthesis by CNDP2 in these cells.

Clinical Implications and Future Directions

This study also showed that Lac-Phe did not influence metformin's glycemic control, indicating that Lac-Phe's effects are independent of metformin's glucose-lowering action. However, another study reported a correlation between Lac-Phe—initially misidentified as 1-carboxyethylphenylalanine—and poorer glycemic control[250], as indicated by higher A1c levels. This raises questions for further investigation. One possibility is that individuals with higher A1c levels received higher doses of

metformin, leading to elevated Lac-Phe levels as a byproduct of more aggressive treatment. Alternatively, could metformin produce a higher Lac-Phe response in those with elevated glycemia? Baseline Lac-Phe levels appear higher in untreated Type 2 diabetes patients, as seen in both the TwinsUK and Danish cohorts (data not shown). Elevated Lac-Phe levels might indicate a strong physiological attempt to restore normoglycemia, with the intestines acting as a glucose sink. This raises the question of whether Lac-Phe could serve as a readout for intestinal glucose clearance, reflecting how much glucose is being processed in this way. Perhaps individuals with higher increases in Lac-Phe after metformin initiation might experience larger reductions in glycemia upon metformin treatment. Future metformin interventional studies that track both fasting and postprandial glucose changes alongside Lac-Phe could help clarify these relationships.

Metformin is known to cause gastrointestinal side effects in some patients, such as nausea, diarrhea, and abdominal discomfort[251,252]. These side effects can limit its tolerability. Given that Lac-Phe is produced in response to metformin concentrations that inhibit complex I in the intestines, Lac-Phe may serve as a proxy for metformin concentration in enterocytes. This presents a novel tool for personalized treatment approaches. Monitoring Lac-Phe levels might help predict gastrointestinal side effects or indicate whether Lac-Phe itself contributes to these symptoms.

While we observed a consistent and significant increase in Lac-Phe levels in response to metformin, the response was heterogeneous across individuals. Further studies are needed to identify factors that influence both baseline Lac-Phe levels and the variability in Lac-Phe response to metformin. Potential contributors could include differences in sex, gastrointestinal function, or kidney function. Although not explicitly highlighted in publications, supplementary data from several studies suggest that reduced kidney function, notably lower glomerular filtration rate, is associated with increased Lac-Phe levels[253,254]. This may be due to the kidney's high expression of CNDP2, the enzyme responsible for Lac-Phe synthesis[141]. However, CNDP2 could also be involved in Lac-Phe breakdown in the kidney, hydrolyzing it into lactate and phenylalanine, as the cleavage of the amide bond in Lac-Phe is chemically favorable. Additionally, Lac-Phe transporters have been identified in the kidney, further supporting a role in regulating Lac-Phe levels. A kidney-specific CNDP2 knockout model would be invaluable for understanding the kidney's role in Lac-Phe metabolism and the variability observed in Lac-Phe levels.

A recent study demonstrated that Lac-Phe levels are significantly elevated in sepsis and serve as a predictor of increased mortality[255]. Given the critical role of the immune system in sepsis[256], this suggests that Lac-Phe could play a role in immune regulation. Activated immune cells, such as macrophages, are known to upregulate glycolysis and produce excess lactate[137,257], and Lac-Phe has been shown to be produced by these cells[142], raising the possibility that it may be involved in broader immune processes. We have observed increased expression of CNDP2 in public

datasets following immune activation (data not shown). Additionally, recent Mendelian randomization studies suggest a causal relationship between Lac-Phe and the inflammatory skin condition rosacea[258]. However, the incidence of rosacea and T2D are possibly correlated[259], so this relationship may be confounded by metformin treatment.

Metformin is known for its anti-inflammatory properties[260,261], raising the question of whether Lac-Phe could act as a mediator of these effects? Further investigation into the role of Lac-Phe in immune cell populations could provide valuable insights into this potential immunomodulatory mechanism.

Unresolved Mechanisms of Lac-Phe in Appetite Regulation

One of the biggest unknowns remains how Lac-Phe exerts its appetite-suppressing effects. It has been suggested that Lac-Phe may act via GPCR receptors in the brain[142,152], such as those in the hypothalamus, a key region that regulates hunger and satiety. In food research, Lac-Phe has been shown to have taste properties, specifically enhancing the kokumi sensation[150]. Molecular docking studies suggest that Lac-Phe can interact with taste receptors[151]. However, it is still unclear whether Lac-Phe's appetite-suppressing effects are mediated locally within the gut or through signaling pathways that affect distant organs such as the hypothalamus. Further research is needed to explore these mechanisms and determine the precise pathways through which Lac-Phe affects appetite and energy balance, including identifying potential receptors or other pathways involved.

Targeting Lac-Phe Axis for Obesity Treatment

In conclusion, this chapter establishes a strong link between metformin and Lac-Phe, highlighting its potential role in appetite suppression. Metformin, a well-tolerated and widely prescribed drug, inadvertently exploits the Lac-Phe pathway to reduce appetite, which suggests that deliberately targeting this axis could lead to new treatments for obesity. By developing drugs that specifically harness Lac-Phe's effects, we could achieve stronger appetite-suppressing outcomes, potentially offering a new class of safe and effective therapies for metabolic diseases like obesity. Given the transformative success of GLP-1 receptor agonists in obesity treatment[262,263], Lac-Phe represents a similarly promising target for addressing the global obesity epidemic.

Chapter 4 - Feeding Drives an Increase of the Appetite-Suppressing Metabolite Lac-Phe

Introduction

Having demonstrated that Lac-Phe levels increase in response to metformin treatment, we sought to investigate whether similar fluctuations occur under other physiological conditions where Lac-Phe might also exert its appetite-suppressing effects. Previous studies have shown that Lac-Phe levels rise not only during intense exercise but also in conditions such as phenylketonuria and mitochondrial disease[133,141,142]. To extend our investigation, we analyzed metabolomics datasets from our existing cohorts and actively sought new cohorts to broaden our understanding of the factors that modulate Lac-Phe dynamics.

4.1 T2D Volunteers Who Didn't Fast Had Higher Lac-Phe Levels in the TwinsUK Cohort

When TwinsUK T2D volunteer metadata were analysed, we also noticed that there was a strong correlation between serum Lac-Phe levels and the fed/fasting status of the individual (Table 3.3 - first introduced in the previous chapter). It is well established that lactate levels increase after eating, and so we were intrigued to investigate whether the highly elevated Lac-Phe levels in metformin-treated T2D individuals were impacted by the feeding or fasting state. In the TwinsUK cohort, although most samples were collected under fasted condition, there was a subset of T2D samples from individuals who had eaten within 6 h of sample collection.

When the data for fed and fasted metformin-treated T2D individuals were interrogated, a trend toward increased Lac-Phe levels was observed in the fed volunteers (Figure 4.1). Although Lac-Phe levels were generally lower in T2D volunteers not treated with metformin, we observed a significant difference within this group based on their feeding status. Specifically, individuals who had eaten within 6 hours had significantly higher Lac-Phe levels compared to those who were fasted. These findings suggest that serum Lac-Phe levels are increased by feeding, independent of metformin treatment. (Figure 4.2).

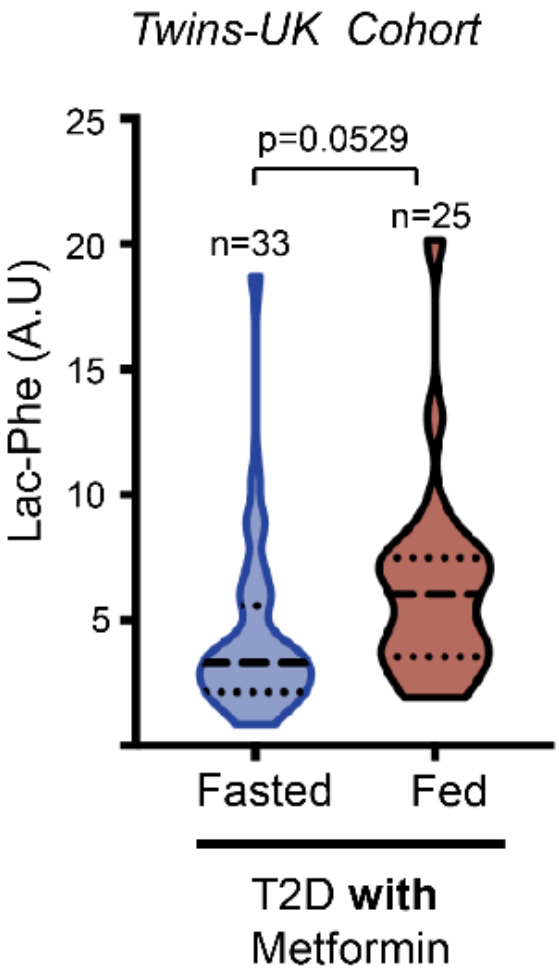

Figure 4.1: Among T2D with Metformin, Non-Fasted Individuals Have Higher Lac-Phe Levels

Lac-Phe levels in T2D volunteers with metformin treatment under fasted (blue, n = 33) and non-fasted (red, n = 25) conditions. Volunteers in the non-fasted group had eaten within 6 hours. The data are presented as violin plots with median (dashed line) and maximum and minimum quartiles (dotted line). The difference between groups approached statistical significance (p = 0.0529). Data were analyzed using two-sided Student's t-test.

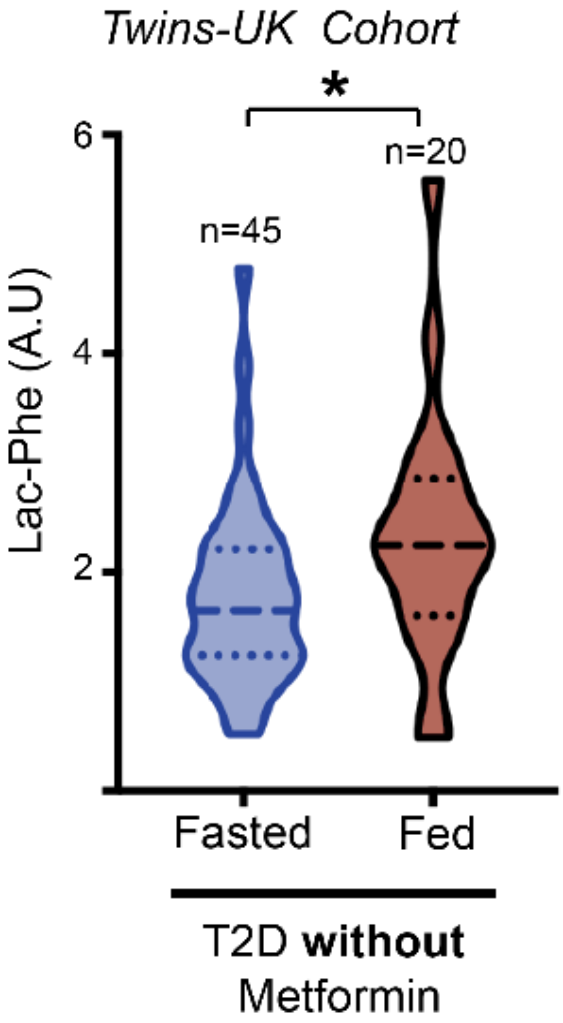

Figure 4.2: Among T2D Without Metformin, Non-Fasted Individuals Have Higher Lac-Phe Levels

Lac-Phe levels in T2D volunteers without metformin treatment under fasted (blue, n = 45) and non-fasted (red, n = 20) conditions. Volunteers in the non-fasted group had eaten within 6 hours. The data are presented as violin plots with median (dashed line) and maximum and minimum quartiles (dotted line). Statistical significance is indicated by *P = 0.034. Data were analyzed using two-sided Student's t-test.

4.2 Serum N-lactoyl Amino Acids Including Lac-Phe Increased 1 Hour Post-Mixed Meal in 100% of Healthy Controls, Pre-diabetic, and T2D Volunteers

Given Lac-Phe's appetite-suppressing properties, we speculated that its elevation post-meal could act as a feedback mechanism in appetite regulation. Analysis of data from a 2020 interventional study further substantiated these findings[219]. The study involved T2D, pre-diabetic and metabolically healthy volunteers, with ten individuals per group. For the T2D group participants who were on metformin, the medication was paused the night before each of the study days. On three separate days within a 1-month period, each group underwent a mixed-meal test—a liquid meal replacement shake plus a solid protein bar—resulting in 90 instances where metabolite levels were assessed before and after feeding. In all 90 cases, a postprandial increase in Lac-Phe levels was observed, with an average increase of 186% 1 h after meal consumption (Figure 4.3). Lac-Phe stood out as one of the metabolites with the most significant response to food intake (Figure 4.4). In addition to Lac-Phe, all other measured N-lactoyl amino acids - N-lactoyl leucine, N-lactoyl valine, and N-lactoyl isoleucine - also increased in all 90 cases and were amongst the most significant upregulated metabolites postprandially. (Figure 4.4).

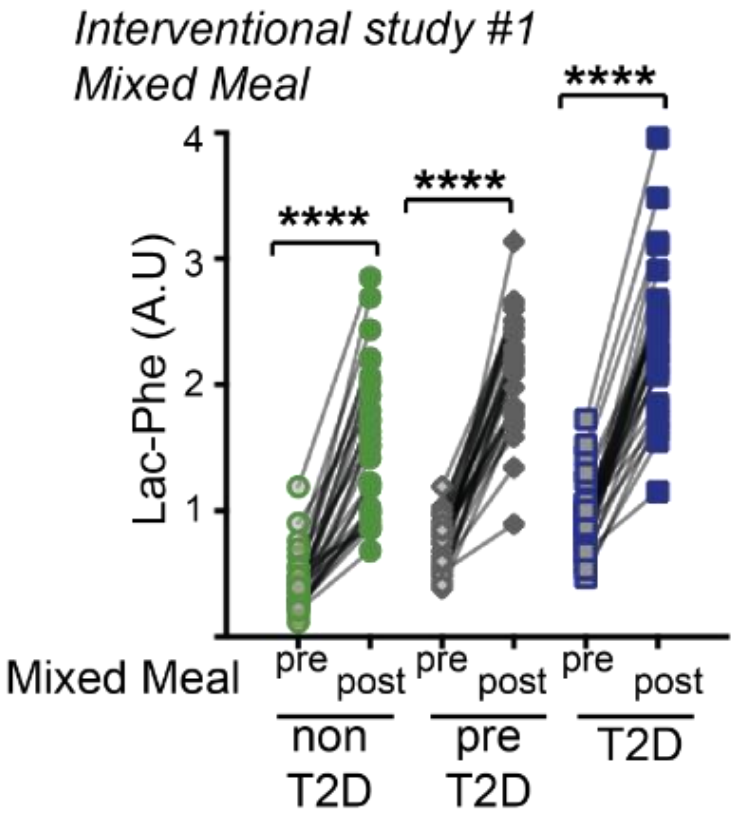

Figure 4.3: Post-Prandial Increase in Lac-Phe After Mixed Meal Across Metabolic Statuses

Lac-Phe levels 30 minutes before (pre) and 1 hour after (post) a standardized mixed meal test (MMT) involving non-T2D (green, n = 10), pre-T2D (gray, n = 10), and T2D (blue, n = 10) volunteers. Each volunteer completed the test on three separate days, resulting in a total of 90 paired samples (n = 30 for each group). The data are presented as individual paired data points. Statistical significance is indicated by ****P < 0.0001. Data were analyzed using two-way ANOVA with Sidak's post test.

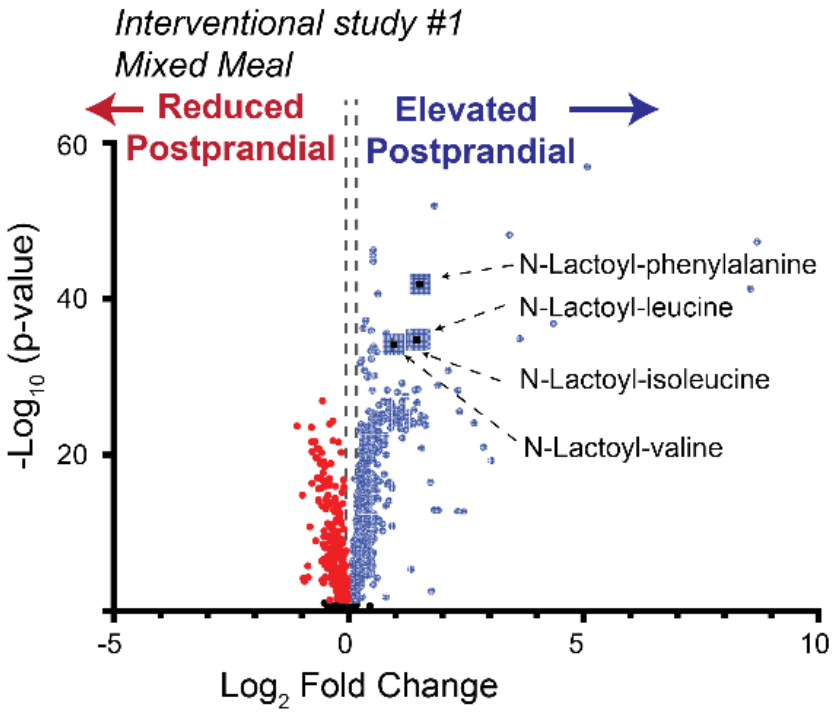

Figure 4.4: N-lactoyl Amino Acids - Among the Most Significantly Increased Metabolites Post-Prandial

Volcano plot comparing the serum metabolomes of 90 paired samples (pre and post) from 30 volunteers over three separate days. The volunteers were from three different groups (non-T2D, pre-T2D, and T2D; 10 each). Metabolites significantly upregulated (blue) and downregulated (red) post-prandially are shown, with N-lactoyl amino acids highlighted. Each metabolite was independently analysed using a paired two-tailed Student's t-test.

4.3 Consistent Lac-Phe Levels Across Visits Suggest Individual Setpoints

Given that volunteers were sampled on three separate occasions within a single month, this provided a unique opportunity to assess inter-individual differences in Lac-Phe levels. We examined the consistency of individual Lac-Phe levels across these three sampling points. Individuals had consistent baseline Lac-Phe and post-prandial Lac-Phe across these three visits (Fig. 4.5). The variation between the three visits by each individual accounted for only 0.08% of the total variation in the study (Figure. 4.5). Multiple factors could contribute to inter-individual differences in baseline Lac-Phe levels. Such observations suggest the existence of distinct Lac-Phe setpoints among individuals.

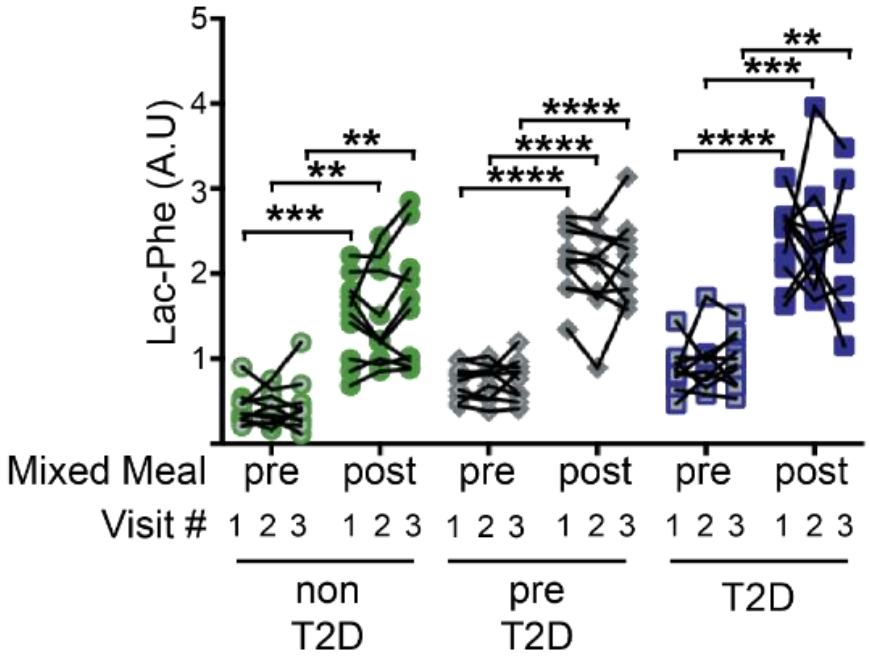

Figure 4.5: Stable Baseline Lac-Phe Levels in Non-T2D, Pre-T2D, and T2D Individuals

Lac-Phe levels 30 minutes before (pre) and 1 hour after (post) a standardized mixed meal test (MMT) involving non-T2D (green, n = 10), pre-T2D (gray, n = 10), and T2D (blue, n = 10) volunteers. Each volunteer completed the test on three separate days (labeled visit 1, 2, and 3). The data are presented as individual linked measurements for each volunteer across the three visits. Statistical significance is indicated by **P < 0.01, ***P < 0.001, and ****P < 0.0001. Data were analyzed using a two-way ANOVA with Tukey post-test comparing paired pre and post measurements for each group on each visit

4.4 Elevated Postprandial Lac-Phe Following Both Habitual and High-Fat Meals

A 2021 Australian interventional cohort study[221] provided additional evidence of Lac-Phe's response to varying dietary challenges. This study involved 24 overweight/obese sedentary men who underwent assessments on different days under distinct dietary regimes. Serum samples were collected for metabolomic analysis before breakfast and after dinner, where the dinner was either their standard habitual diet or a high-fat diet. The results were striking, showing a greater than 160% increase in Lac-Phe levels both in participants who consumed their standard meal and in those consuming high-fat meals (Figure 4.6). These data suggest that Lac-Phe levels increase with diverse types of diet. Notably, in all cases above, the volunteers consumed a solid component in their meal.

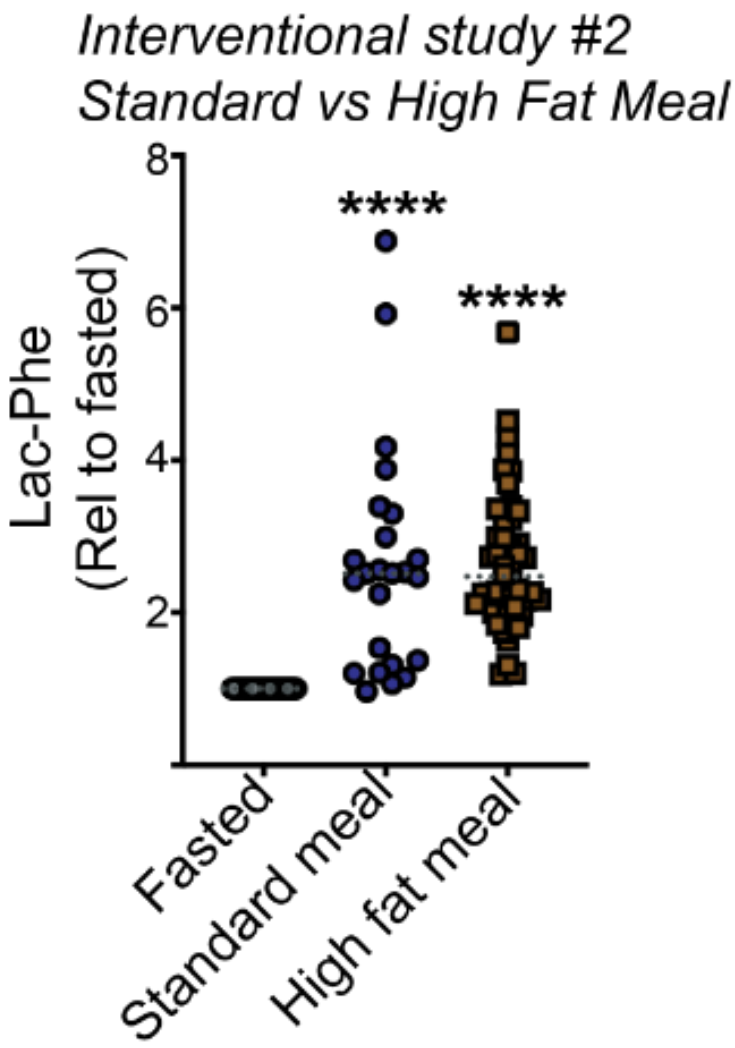

Figure 4.6: Elevated Lac-Phe Levels Post-Prandially Following Both Habitual and High-Fat Meals

Lac-Phe levels after a volunteer's habitual meal (n = 24) or high-fat meal (n = 48), relative to fasted levels, in 24 overweight/obese sedentary men. Serum samples were taken before breakfast (fasted), after a standard meal, and approximately 45 minutes after a high-fat meal. The data are presented as individual data points with mean values indicated. Statistical significance is indicated by ****P < 0.0001. Data were analyzed using a one-sample t-test against a theoretical value of 1.

4.5 Significant Increase in Lac-Phe with Sugary Dates Compared to Liquid Glucose

To test whether a liquid diet also induced Lac-Phe levels, the data were analysed from volunteers before and after consuming either liquid sugar (glucose) or sugar-rich date fruits. These data were from a 2018 nutritional challenge study conducted in Qatar[220]. In this study, 21 healthy volunteers underwent plasma metabolomic assessments after the consumption of either Khalas or Deglet Nour date fruits or, alternatively, oral glucose. Notably, the composition of dates is predominantly sugars with minimal protein content and a small amount of fibre (Figure 4.7). Each volunteer took part in three separate dietary challenges, spaced a week apart, involving the consumption of either ten date fruits or a glucose drink. Blood samples were collected at baseline and at intervals of 30 min, 60 min, 90 min and 120 min after intake. Lac-Phe levels increased over 220% in response to both date fruit varieties (Figure 4.8). A similar pattern was observed for other N-lactoyl amino acids including Lac-Val (N-lactoyl valine) (Figure 4.8). In contrast, the response to the liquid glucose challenge, although significant, was considerably lower, with only a 37% increase in Lac-Phe levels measured. This data suggests that the composition of a meal, rather than just its caloric content, can significantly influence the response of the appetite-suppressing metabolite Lac-Phe.

Contents%	Khalas dates
Moisture	16.1%
Crude fibre	2.5%
Fat	0.12%
Protein	1.2%
Fructose	32.4%
Glucose	36.5%
Sucrose	nd
Total Sugars	68.9%

Figure 4.7: Nutritional Composition of Dates: High Sugar Content
Nutritional information for Khalas dates. The table shows the percentage contents of moisture, crude fiber, fat, protein, fructose, glucose, sucrose (not detected), and total sugars in Khalas dates.

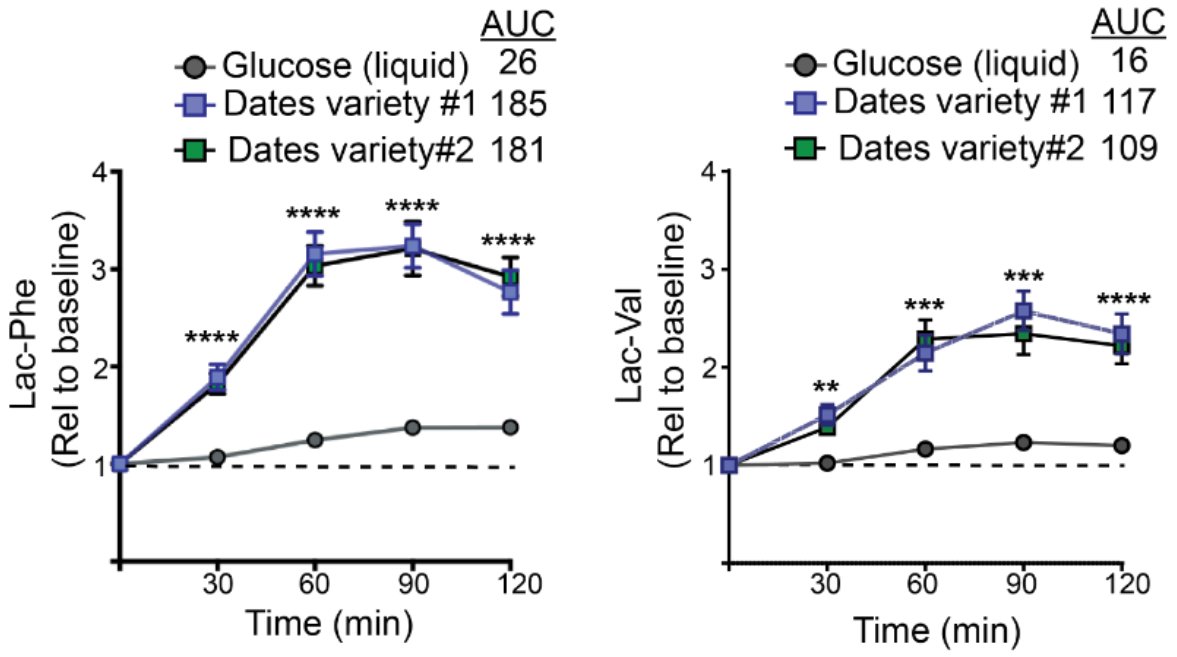

Figure 4.8: Significant Lac-Phe and Lac-Val Increase with Sugary Dates Compared to Liquid Glucose

Left panel: Lac-Phe levels relative to baseline after feeding with liquid glucose or dates.
Right panel: Lac-Val levels relative to baseline after feeding with liquid glucose or dates. Twenty-one participants undertook three separate dietary challenges, consuming either a glucose solution (OGTT, n = 21), ten fruits of Deglet Nour dates (n = 21), or ten fruits of Khalas dates (n = 20, one volunteer did not participate). Blood samples were collected before intake and at intervals up to 120 minutes afterward. The area under the curve (AUC) is shown for each dietary challenge. The data are presented as mean ± s.e.m. Statistical significance is indicated by **P < 0.01, ***P < 0.001, and ****P < 0.0001. Data were analysed using two-way ANOVA with Tukey's post test

4.6 Glucose-Based Interventions Do Not Drive a Large Increase in N-lactoyl Amino Acids

We've observed that liquid glucose leads to a lower N-lactoyl amino acid response compared to a more diverse set of meal types. Two studies allowed us to explore this further. Firstly, a 2021 Qatari interventional cohort study provided an opportunity to examine the effects of glucose infusion. In this study, N-lactoyl valine (Lac-Val) was the only N-lactoyl amino acid measured, though N-lactoyl amino acids are consistently correlated with each other in serum (Figure 3.8). The study involved 47 clinically healthy male subjects, where metabolites were measured before and after a hyperinsulinemic-euglycemic clamp—a technique designed to assess glucose metabolism (Figure 4.9). Despite the administration of glucose during the clamp, there was no significant rise in Lac-Val levels; in fact, Lac-Val levels decreased. This suggests that route of ingestion of glucose is an important factor influencing N-lactoyl amino acid levels. Secondly, a 2022 study involving 109 Dutch volunteers assessed the response to a liquid mixed meal in which glucose syrup served as the primary carbohydrate source (Table 4.1). Glucose syrup is composed of mono-, di-, and polysaccharide chains of glucose. Although the meal was more complex than liquid glucose alone—containing 36.6g of carbohydrates per 100ml—it produced only a modest increase of about 25% in N-lactoyl amino acids, including Lac-Phe. This response was observed in morbidly obese individuals across all metabolic statuses: non-T2D, pre-diabetic, and T2D (Figure 4.10).

Our analysis conclusively demonstrates that Lac-Phe levels consistently rise after meals, a finding evident in both observational and interventional studies. However, our data also shows that the method of nutrient intake—whether through eating or direct infusion—matters, and that the meal composition can have differential impacts on Lac-Phe levels, and therefore likely different effects on hunger signaling.

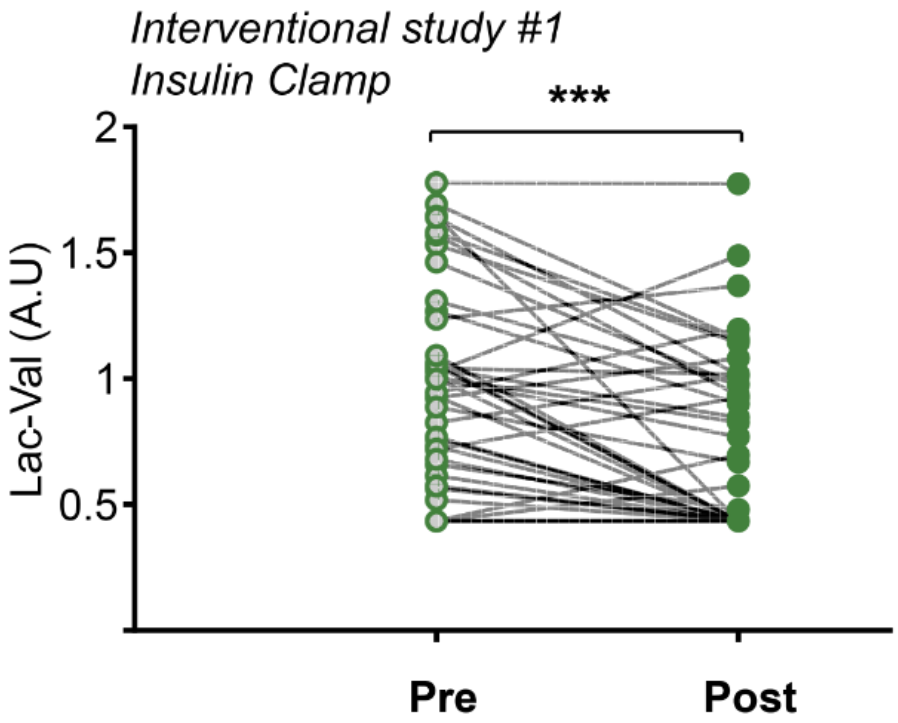

Figure 4.9: No Rise in Lac-Val with Glucose Infusion
N-lactoyl valine (Lac-Val) levels in 47 clinically healthy Arab male subjects, measured after overnight fasting (pre) and 120 minutes after a hyperinsulinemic-euglycemic clamp (post). The subjects were recruited based on specific inclusion criteria to ensure they had no known disease or pathology, normal blood biochemistry, and normal glucose response to OGTT. Venous blood samples were collected before the clamp (pre) and 120 minutes after the start of the clamp procedure (post). The data are presented as individual paired data points. Statistical significance is indicated by ***P < 0.001. Data were analyzed using a paired two-sided t-test.

Contents	per 100ml
Carbohydrate *from glucose syrup*	36.6g
Total Sugars *from glucose and glucose disaccharides*	15.0g
Fructose	0.0g
Sucrose	0.0g
Protein	16.0g
Fat	9.3g
Crude fibre	0.0g

Table 4.1. Nutritional Profile of the Liquid Mixed Meal Containing Glucose Syrup for the BARIA Cohort

Nutritional composition per 100ml of the liquid mixed meal provided to participants in the BARIA cohort. The mixed meal consisted of two Nutridrink Compact 125ml units (Nutricia®). The primary carbohydrate source was glucose syrup. The table details the nutritional breakdown, including carbohydrates, total sugars, protein, fat, and crude fiber.

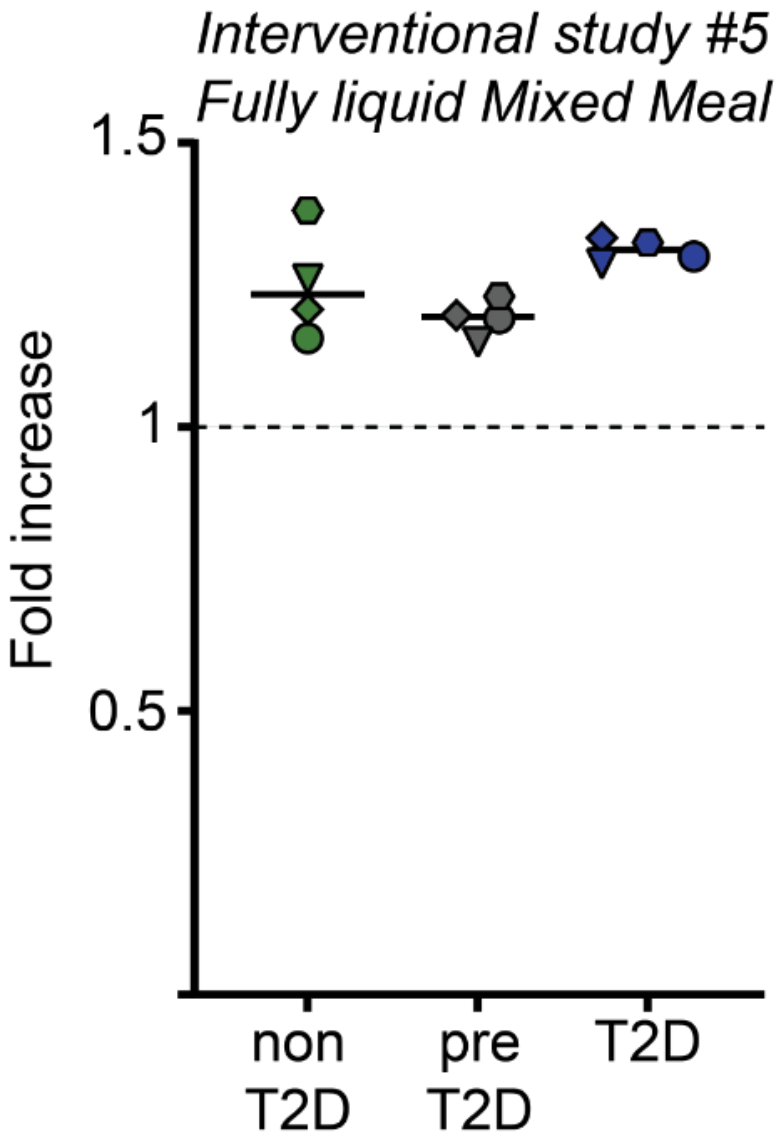

Figure 4.10: Modest Increase in Lac-Phe with Liquid Mixed Meal Containing Glucose as the Exclusive Carbohydrate Source

Comparison of N-lactoyl amino acid levels following consumption of a fully liquid mixed meal in individuals with different glucose tolerance status. The cohort consisted of morbidly obese individuals from the BARIA study, including those with normal glucose tolerance (non-T2D, n = 27), pre-diabetes (pre-T2D, n = 57), and type 2 diabetes (T2D, n = 22). Peripheral plasma samples were collected at fasting (pre) and 2 hours post mixed meal test (MMT; post). The liquid mixed meal used glucose syrup as the carbohydrate source. Fold increases are shown for N-lactoyl phenylalanine (circle), N-lactoyl leucine (triangle), N-lactoyl isoleucine (diamond), and N-lactoyl valine (hexagon). Data are presented as mean values. Error bars were omitted because only mean values, without accompanying measures of variance, were available from the supplemental dataset of the original manuscript.

4.7 Discussion

In this chapter, we sought to investigate additional factors that influence the levels of N-lactoyl amino acids, particularly Lac-Phe. Our analysis of the TwinsUK cohort revealed a notable correlation between elevated Lac-Phe levels and the fed state in T2D volunteers. This finding prompted us to explore further how feeding, as well as the composition of different meals, affects Lac-Phe levels.

Our findings demonstrate that meals consistently induce an increase in Lac-Phe and related N-lactoyl amino acids, highlighting a robust postprandial response across different metabolic statuses, including healthy, pre-diabetic, and T2D individuals. This rise was consistent across a variety of solid meal types, including sugar-dense date fruit, macronutrient-balanced meals, and high-fat meals. By contrast, when glucose was administered in isolation, either through ingestion or infusion, the Lac-Phe response was considerably weaker. In our cohort, liquid meals yielded only a modest response, whereas solid meals consistently led to higher Lac-Phe levels. Moreover, our data suggest that individuals possess distinct set points for Lac-Phe, as evidenced by the consistent baseline and postprandial Lac-Phe levels within individuals across three separate days in a month, with notable differences observed between individuals.

Role of Food Form and Composition in Lac-Phe Response

Our findings indicate that both the form and composition of a meal, not just its caloric content, significantly influence the Lac-Phe response. Across multiple studies, meals containing a solid component consistently triggered a strong increase in Lac-Phe levels. In contrast, three interventions—a standard oral glucose tolerance test, a fully liquid mixed meal, and a glucose infusion—elicited only a modest Lac-Phe response, all of which lacked fiber. Two potential hypotheses could explain this difference: (1) a solid meal component may be required for a strong Lac-Phe response, or (2) fiber may play a critical role in eliciting a robust Lac-Phe response. However, unpublished data from a collaborating group challenge these hypotheses. They observed a strong Lac-Phe response in a cohort study involving a fully liquid meal with only trace fiber content. This suggests that neither solid food nor fiber is strictly necessary for a strong Lac-Phe response. Therefore, the modest response seen in our liquid meal interventions is likely due to other factors, such as the specific nutrient composition, rather than the form or fiber content of the meal alone.

Fructose and Sucrose as Potential Key Contributors

These observations led us to explore alternative hypotheses. The two liquid meal studies we analyzed both had glucose as the primary carbohydrate source. In the oral glucose tolerance test, pure glucose was used, while in the fully liquid mixed meal, glucose syrup served as the sugar source, containing a combination of glucose in mono-, di-, and oligosaccharide forms. In contrast, our collaborator's cohort study utilized a liquid meal containing sucrose—a disaccharide made up of

glucose and fructose—as the main sugar source. A fourth cohort study also included a liquid component with sucrose as the carbohydrate source and elicited a strong Lac-Phe response; however, the meal also included a solid protein bar, complicating direct comparisons[219]. This leads us to speculate that specific sugars, particularly fructose and sucrose, may be key contributors to the Lac-Phe response. Published literature supports this idea, as fructose metabolism differs significantly from glucose metabolism in the intestines[264,265]. Metabolite tracing studies have demonstrated that glucose tends to pass into circulation relatively unchanged, while fructose is metabolized in the intestines into various compounds, including glucose and lactate[264]. This difference is largely due to fructose entering glycolysis through an alternative pathway. Unlike glucose, which is phosphorylated at the 6-position by glucokinase, fructose is phosphorylated at the 1-position by ketohexokinase[266]. This unique phosphorylation allows fructose to bypass the key regulatory step of glycolysis catalyzed by phosphofructokinase, facilitating its rapid metabolism into three-carbon units such as glyceraldehyde and dihydroxyacetone phosphate[267]. Consequently, fructose is more readily converted into lactate within the intestines. At high fructose loads, excess fructose can overflow into the liver and the gut lumen, interacting with the gut microbiota. However, the gut microbiota do not significantly contribute to the conversion of fructose into glucose that appears in the portal vein[264]. Fructose feeding generates a higher lactate concentration in the portal vein of mice compared to glucose feeding[264]. This lactate, produced in the intestines, could serve as a substrate for the synthesis of N-lactoyl amino acids, including Lac-Phe.

The hypothesis that fructose may have a more potent effect on Lac-Phe production is particularly intriguing, as it contrasts with current literature on appetite regulation. Fructose is often implicated in the development of obesity, with the rise of high-fructose corn syrup consumption thought to contribute to the obesity epidemic[268]. Fructose has been associated with increased food-seeking behavior, and human studies have reported differing responses in hypothalamic blood flow—the brain region responsible for regulating feeding—between glucose and fructose consumption[269,270]. Furthermore, glucose and fructose have been shown to have differential effects on satiety-related hormones. Glucose typically elicits a stronger insulin response, which can suppress appetite, and has a more pronounced effect on GLP-1 secretion compared to fructose, although this effect is not universally reported[271–274].

Fructose may have a greater impact on Lac-Phe production than glucose, and dedicated fructose feeding studies would help verify this. Dose-escalation studies with lactate could also provide insight into whether Lac-Phe synthesis has a saturation point. Since fructose is initially metabolized in the intestines, with excess fructose diverted to the liver, the Lac-Phe response may vary with the amount of fructose consumed[264,265]. It is possible that moderate fructose levels, such as those found in fruit, trigger a strong Lac-Phe response, whereas the higher fructose loads common in processed foods may not elicit a substantially larger effect.

Understanding the role of fructose in Lac-Phe production could be valuable in the design and selection of liquid meal replacement drinks, particularly those used in

medical contexts like cachexia, where minimizing appetite-suppressing factors like Lac-Phe might be beneficial. Moreover, these insights could provide a more nuanced understanding of the obesity epidemic, by highlighting how different sugar sources may differentially influence appetite regulation and metabolism.

Intestines likely the site of N-lactoyl Amino Acid Generation

While we do not have direct evidence pinpointing the site of Lac-Phe generation in response to meals, several indirect findings provide strong clues. In the glucose infusion experiments, Lac-Val levels did not increase. Since glucose in this case bypasses the first pass through the intestines—a process typical in meal consumption—this suggests that N-lactoyl amino acids, including Lac-Phe, are likely produced in the intestines in response to meals. This hypothesis aligns with our earlier speculation that lactate metabolism within the intestines plays a key role in triggering Lac-Phe production. Additional support comes from the findings discussed in the previous chapter, where the metformin-driven rise in Lac-Phe was shown to originate from the intestines[236]. Together, these data suggest that the intestines are a central site for the production of Lac-Phe and other N-lactoyl amino acids, potentially preferentially in response to lactate generated by the metabolism of specific sugars, such as fructose and sucrose. To further investigate the role of the intestines in Lac-Phe production in response to feeding, we could use gut-specific CNDP2 knockout mice generated by crossing the conditional Cndp2 allele with the Villin-Cre driver line. This model was used in the parallel metformin-Lac-Phe study[236]. By conducting feeding experiments in these knockout mice and their wild-

type counterparts, we could assess whether the absence of CNDP2 in the intestines eliminates the food-induced rise in Lac-Phe levels. This would confirm the intestines as the primary site for Lac-Phe production in response to food.

Revisiting the Single-Dose Metformin Study in Light of Feeding Data

In the earlier chapters, we demonstrated that metformin administration drives an increase in N-lactoyl amino acids, including Lac-Phe. With feeding also shown to elevate these metabolites, it raises interesting new points for discussion regarding their interplay.

Firstly, it highlights a limitation of the single-dose metformin interventional study[218]. In that study, metformin was given 30 minutes after participants ate a standard meal. This timing likely confounds the observed Lac-Phe increase, as the surge could be attributed to both postprandial effects and metformin's action. This confounding effect complicates the interpretation of a single dose of metformin's impact on Lac-Phe levels. However, it remains likely that metformin exerts an acute effect. In this single-dose metformin cohort, we can assess Lac-Phe levels relative to the meal timing. Lac-Phe appeared to rise from 2.5 hours post-meal (1.5 hours before Cmax) to 4 hours post-meal, when Cmax (the time of peak metformin concentration for an individual) on average occurred. In contrast, the only feeding cohort we studied with time course data was the date fruit study, where Lac-Phe peaked around 90 minutes

after consumption. This suggests that metformin has, at the very least, an additive effect on eating. Additionally, in the metformin Lac-Phe study published concurrently with ours, a single oral gavage of metformin in mice increased Lac-Phe levels, confirming in mice and suggesting in humans that even a single dose of metformin is sufficient to elevate Lac-Phe.

Interestingly, the rise in Lac-Phe following metformin administration parallels the increase seen after meals, suggesting that metformin may mimic natural appetite-suppressing mechanisms typically triggered by feeding. In fasting conditions, metformin might replicate postprandial signals, leading to appetite suppression. This raises the possibility that administering metformin with a meal could lead to elevated, supraphysiological Lac-Phe levels, amplifying appetite suppression. Further investigation into the timing of metformin relative to meals could help optimize therapeutic outcomes, either enhancing or moderating appetite suppression based on clinical needs. Additionally, comparing different formulations—such as immediate-release versus extended-release metformin—may shed light on how drug kinetics influence Lac-Phe responses. For instance, immediate-release metformin might result in a higher peak of Lac-Phe, while extended-release formulations may provide a more sustained, consistent elevation in Lac-Phe levels. A study in children found that metformin reduced food intake in a snack consumed two hours post-meal[275]. This raises the question: could the accumulation of Lac-Phe due to both metformin and food intake contribute to a reduced desire to snack?

Study Limitations

Several limitations must be acknowledged in our study. Firstly, the cohorts we examined were based on pre-existing data from observational and interventional studies, which meant we were unable to standardize experimental conditions across datasets. While the diverse array of meal types studied provided a broad perspective on Lac-Phe response, the lack of replicated studies, constrained our ability to draw more definitive conclusions. For instance, we only had a single oral glucose tolerance test (OGTT) and no trials that exclusively utilized fully fructose- or fully sucrose-based liquid meals, which would have allowed for a clearer understanding of how different carbohydrate sources drive Lac-Phe production. The scarcity of data on Lac-Phe and N-lactoyl metabolites stems from their detection in only a limited number of studies. However, with more companies and research groups adding these metabolites to their analytical platforms, the ability to investigate their role should improve significantly in future research.

Another limitation arises in one of our interventional studies, the 2021 Qatari study involving a hyperinsulinemic-euglycemic clamp with glucose infusion[224]. In this study, Lac-Val was the only N-lactoyl amino acid measured, which limits our ability to infer what happens to Lac-Phe or other N-lactoyl amino acids. However, I've consistently observed strong correlations between N-lactoyl amino acids (e.g., Figure 3.8). Additionally, Lac-Val has shown a similar postprandial response to Lac-Phe in all datasets, such as the date fruit intervention study (Figure 4.7). This strongly suggests that the decrease in Lac-Val during continuous glucose infusion likely applies to Lac-Phe as well.

Another limitation lies in the variation in study designs, particularly in the timing of blood draws following food intake. One study included time-course sampling, while others only provided single time points at varying intervals after meals, making it challenging to directly compare Lac-Phe responses across different conditions. For example, in the Australian habitual and high-fat diet study, comparisons were made between pre-breakfast and post-dinner samples, complicating comparisons with datasets focused on single meals[221]. This variation also raises the possibility of confounding effects if Lac-Phe follows a circadian pattern.

Additionally, certain foods, like Parmigiano cheese[149], contain Lac-Phe. We did not have information on the Lac-Phe content of the meals consumed by participants in the different cohorts, which may have influenced the levels measured in blood. However, given that Lac-Phe is likely synthesized endogenously in response to food intake, it is unlikely that Lac-Phe contained in a meal would significantly affect circulating levels—see further discussion below.

Future Directions

The exact source of serum Lac-Phe elevation in response to food intake has not been conclusively determined, though it is most likely an endogenous response rather than exogenous ingestion. As previously mentioned Lac-Phe is present in foods including parmigiano cheese[149], and indeed Lac-Phe can enhance taste as a

kokumi active compound[150]. The likelihood of Lac-Phe being hydrolyzed in the gastrointestinal tract would challenge a hypothesis that dietary Lac-Phe significantly contributes to circulating levels. Intraperitoneal injection of Lac-Phe in mice suppressed appetite. However, oral administration of Lac-Phe did not suppress appetite, suggesting that exogenous Lac-Phe, when delivered orally, is unlikely to cause a significant rise in serum Lac-Phe levels[142]. This further supports the notion that Lac-Phe is primarily synthesized endogenously in response to feeding rather than absorbed in significant quantities from dietary sources. Feeding experiments using intestine-specific CNDP2 knockout mice could provide valuable insights into the source of serum Lac-Phe. If Lac-Phe levels in these knockout mice rise to the same extent as in wild-type mice after a meal, it would suggest that exogenous dietary Lac-Phe contributes significantly to circulating levels. However, if Lac-Phe levels fail to rise in the knockout mice, this would support the idea that Lac-Phe is primarily synthesized endogenously in the intestines.

Is Lac-Phe a Postprandial Appetite Suppressant?

While Lac-Phe likely functions as an appetite suppressor in the context of food intake, we have not definitively established this. Further experiments are required to confirm its appetite-suppressing role following food consumption. Given that Lac-Phe's role in appetite suppression has been established in both metformin treatment and intense exercise, it seems likely that Lac-Phe also plays a similar role postprandially. Intestine-specific CNDP2 knockout models could provide valuable insights into whether Lac-Phe production in the gut is essential for post-meal

appetite regulation. Identifying meals that maximize Lac-Phe production will be crucial for future studies aimed at optimizing its appetite-suppressing potential.

Lac-Phe Regulation in Response to Macronutrient Intake

This research reveals for the first time that Lac-Phe levels are modulated in response to feeding, similar to the regulatory patterns seen in other appetite-suppressing hormones like ghrelin, leptin, and GLP-1[276–278]. A key direction for future research is to understand how different macronutrients impact Lac-Phe levels and appetite regulation. For example, compared to carbohydrates and fats, protein has stronger satiating effects and is associated with a higher release of peptide YY (PYY) relative to both, and cholecystokinin (CCK) relative to carbohydrates[279–283]. Given Lac-Phe's unique composition—a fusion of lactate and phenylalanine—it may act as an internal signal for the body, efficiently indicating the intake of carbohydrates and proteins.

Data from the Australian cohort, where volunteers were switched to a high-fat diet (lower in carbohydrate and protein sources), offer further insights[221]. A significant rise in Lac-Phe was still observed from pre-breakfast to post-dinner after the switch. However, fasting levels of Lac-Phe (pre-breakfast) appeared to decrease following the switch to the high-fat diet (data not shown), suggesting that fat may provide a weaker stimulus for Lac-Phe production.

Interestingly, our analysis of the date fruit feeding study suggests that significant Lac-Phe increases can occur even with very low-protein meals. Khlas dates, which

contain approximately 1.2% protein and around 70% carbohydrates, still produced a strong post-feeding increase in Lac-Phe levels. This raises the question of whether any protein is necessary for a significant Lac-Phe response, or if a small amount is sufficient. It would be interesting to test whether adding a protein source to the date meal would further increase Lac-Phe levels.

Together, these findings suggest that while both fat and protein may influence Lac-Phe production, carbohydrates could be the primary driver. The lower Lac-Phe levels observed with a high-fat diet, along with the robust increases following carbohydrate-rich, low-protein meals like dates, indicate that carbohydrates may play the dominant role in Lac-Phe responses. Future studies should explore how Lac-Phe reacts to different macronutrients to determine whether specific diets can optimize its appetite-suppressing effects.

Applying the date fruit study model to a broader range of dietary interventions would be valuable. The study's crossover design, in which volunteers participated in three different dietary interventions with time-course metabolomics data (including Lac-Phe), provided rich insights. Extending this approach to explore the effects of different carbohydrate sources (e.g., fructose vs. glucose) as well as protein-, fat-based, and fiber-rich meals could reveal how these nutritional components differentially influence Lac-Phe levels. This would deepen our understanding of how various macronutrients and foods regulate Lac-Phe production.

Summary

In summary, we have demonstrated that Lac-Phe levels consistently rise in response to feeding, reinforcing its potential role in appetite regulation. As discussed in the previous chapter, future work should aim to identify additional factors influencing Lac-Phe levels, such as kidney function and the microbiome. Moreover, there are promising opportunities to develop anti-obesity therapies that exploit the Lac-Phe pathway. The fact that Lac-Phe increases postprandially offers a clear rationale for its use by the body as a signal to regulate appetite.

Chapter 5 - Metformin Drives an Increase of Medium-Chain β-Hydroxy Fatty Acids

Introduction

Our focus in this chapter is to go beyond N-lactoyl amino acids and identify additional metabolites that may be influenced by metformin. Identifying novel metabolites associated with metformin may provide insight into previously unknown mechanisms of its therapeutic effects. To contextualize these findings, we will first reintroduce β-hydroxy fatty acids, highlighting their structural characteristics and role as intermediates in fatty acid metabolism.

β-Hydroxy fatty acids are intermediates formed during the β-oxidation of fatty acids. They are characterized by the presence of a hydroxyl group at the β-carbon position, which is the third carbon in the fatty acid chain[156]. They can be categorized into two structural types: monocarboxylic acids, such as β-OH-C10:0, and dicarboxylic acids, like β-OH-DC-C10:0, which have an additional carboxyl group at the omega position, the final carbon in the chain, formed through ω-oxidation (Figure 1.8). The accumulation of these metabolites in the blood can be influenced by various physiological conditions, such as fasting and mitochondrial dysfunction, where their levels may rise significantly[133,162]. For instance, inborn errors of metabolism, including long-chain 3-hydroxyacyl-CoA dehydrogenase deficiency, can lead to the accumulation of β-hydroxy fatty acids[163]. Moreover, emerging evidence suggests that β-hydroxy fatty acids can function beyond energy metabolism by acting as signaling molecules that engage G-protein-coupled receptors (GPCRs)[167,169].

We begin our analysis by revisiting the TwinsUK dataset.

5.1 β-Hydroxy Fatty Acids Positively Correlate with Metformin in the TwinsUK Cohort

Expanding on our investigation into how metformin affects N-lactoyl amino acids, we used the TwinsUK cohort to explore broader metabolic changes. Through untargeted metabolomics of 885 metabolites in T2D samples, we sought to identify those most strongly correlated with metformin.

We observed that several medium-chain β-hydroxy fatty acids were among the metabolites most positively correlated with serum metformin levels (Table 5.1). This included both monocarboxylic acids (e.g., β-OH-C10:0 Figure 5.1A) and dicarboxylic acids (e.g., β-OH-DC-C10:0 Figure 5.1B) β-hydroxy fatty acids, which possess carboxyl groups at one or both ends, respectively. We have chosen to refer to these metabolites as β-hydroxy fatty acids but they are sometimes alternatively referred to as 3-hydroxy fatty acids.

The consistent positioning of the hydroxy group in these structures suggests a targeted action of metformin on this class of metabolites. Our findings from the TwinsUK cohort suggest that metformin may significantly increase β-hydroxy fatty acid levels.

Metabolite	AltName	Correlation with metformin
3-hydroxysebacate	***β-OH-DC-C10:0***	***61%***
3-hydroxyoctanoate	***β-OH-C8:0***	***61%***
N-lactoyl phenylalanine	Lac-Phe	60%
3-hydroxydecanoate	***β-OH-C10:0***	***58%***
N-lactoyl valine	Lac-Val	51%
phenol sulfate		41%
N,N,N-trimethyl-5-aminovalerate		37%
3-hydroxyhexanoate	***β-OH-C6:0***	***37%***
X - 16580		37%
fumarate		36%
malate		35%

Table 5.1: Medium-Chain β-Hydroxy Fatty Acids Correlated with Metformin in TwinsUK Cohort

Spearman's rank correlation analysis was conducted on T2D samples from the TwinsUK cohort (n = 162), of which 91 contained metformin. This examined the correlation between serum metformin levels and 885 metabolites that passed the threshold of being present in at least 10% of the samples. The table presents metabolites that exhibited significant positive correlations with metformin, with medium-chain β-hydroxy fatty acids highlighted. Metabolon datasets refer to these metabolites as "3-hydroxy," but for consistency, this work will use the convention "β-hydroxy" as shown in the "AltName" column

5.2 β-Hydroxy Fatty Acids are Elevated with Metformin in the Observational ADDITION-Denmark Cohort

A 2021 Danish study, conducted at Aarhus University Hospital, provided an opportunity to further investigate the relationship between metformin and β-hydroxy fatty acids. Conducted within the ADDITION-Denmark cohort, this study employed untargeted metabolomics on plasma samples from 106 volunteers, including volunteers with Type 2 Diabetes (T2D) as well as age- and sex-matched healthy controls. Of the 97 volunteers diagnosed with T2D, 70 were receiving metformin treatment, while 27 were not. Although the original study focused on diabetic polyneuropathy (DPN), our analysis centers on the impact of metformin among the T2D population, with additional comparisons to the healthy control group (Figure 5.1).

To validate our findings from the TwinsUK cohort, we first examined the levels of two β-hydroxy fatty acids—β-OH-C8:0 and β-OH-DC-C10:0—that exhibited the strongest correlation with metformin in the TwinsUK cohort. Although there was a positive trend, neither metabolite showed a statistically significant increase when comparing metformin-treated T2D volunteers (n = 70) to healthy controls (n = 9). This is likely due to the study being underpowered given the small sample size of healthy controls. However, a significant elevation in both metabolites was observed when comparing metformin-treated T2D volunteers (n = 70) to those not on metformin (n = 27), with P-values < 0.001 and < 0.01, respectively (Figure 5.2).

Further analysis within the ADDITION-Denmark cohort, specifically comparing T2D individuals treated with metformin to those without treatment, revealed that several β-hydroxy fatty acids were among the most significantly upregulated metabolites in the metformin-treated group (Figure 5.3). This includes both monocarboxylic acids (e.g., β-OH-C8:0 and β-OH-C10:0) and dicarboxylic acids (e.g., β-OH-DC-C6:0, β-OH-DC-C10:0, and β-OH-DC-C12:0).

To identify which monocarboxylic β-hydroxy fatty acids were most predictive of metformin use, we conducted receiver operating characteristic (ROC) analysis. Among the monocarboxylic acids examined, β-OH-C8:0 and β-OH-C10:0, with chain lengths of 8 and 10 carbons respectively, were the most reliable indicators, with area under the curve (AUC) values of 0.81 and 0.79 (Figure 5.4). These AUC values are substantially higher than those of both shorter and longer chain β-hydroxy fatty acids, such as β-OH-C6:0 (AUC = 0.64) and β-OH-C18:0 (AUC = 0.61), highlighting the strong biomarker potential of β-OH-C8:0 and β-OH-C10:0 for metformin treatment.

These two strong biomarkers, β-OH-C8:0 and β-OH-C10:0, not only effectively distinguish metformin users but also show significant fold increases in those treated with the drug—2.58-fold and 1.99-fold, respectively (Table 5.2). Likewise, the dicarboxylic β-hydroxy fatty acids measured in this cohort— of carbon chain lengths 6, 10, and 12 —are strong indicators of metformin use, with β-OH-DC-C12:0

showing a pronounced 3.54-fold increase in those receiving metformin compared to those without it(Table 5.3).

In contrast, medium-chain β-hydroxy carnitines, such as β-OH-C10:0 carnitine (AUC = 0.50), unlike the monocarboxylic and dicarboxylic β-hydroxy fatty acids, did not exhibit a strong relationship with metformin use in this cohort (Table 5.4).

In summary, the data from the ADDITION-Denmark cohort not only corroborate the findings from the TwinsUK cohort but also provide further evidence that metformin treatment is associated with elevated levels of specific β-hydroxy fatty acids, particularly those with medium-chain lengths.

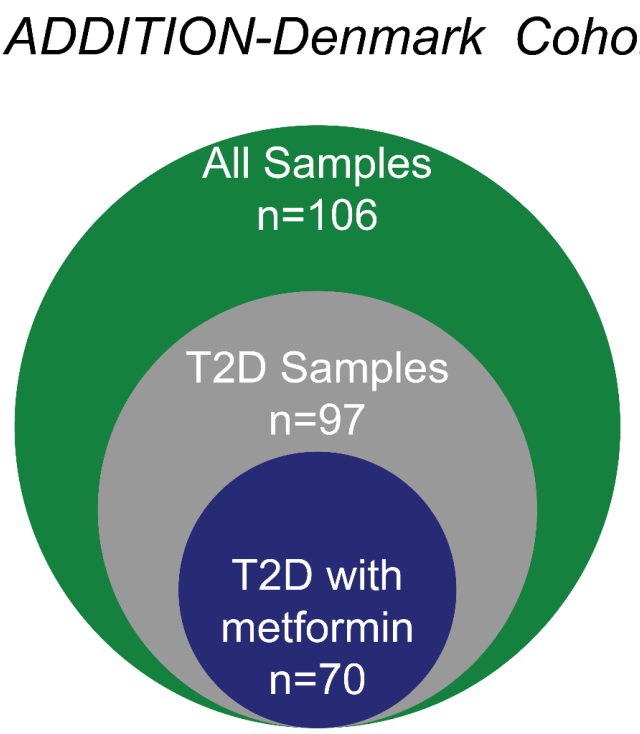

Figure 5.1: ADDITION-Denmark Cohort: Distribution of T2D Volunteers with and without Metformin

The nested circle diagram illustrates the distribution of samples in the ADDITION-Denmark cohort. The largest circle represents all samples (n = 106), the middle circle represents T2D samples (n = 97), and the smallest circle represents T2D samples treated with metformin (n = 70).

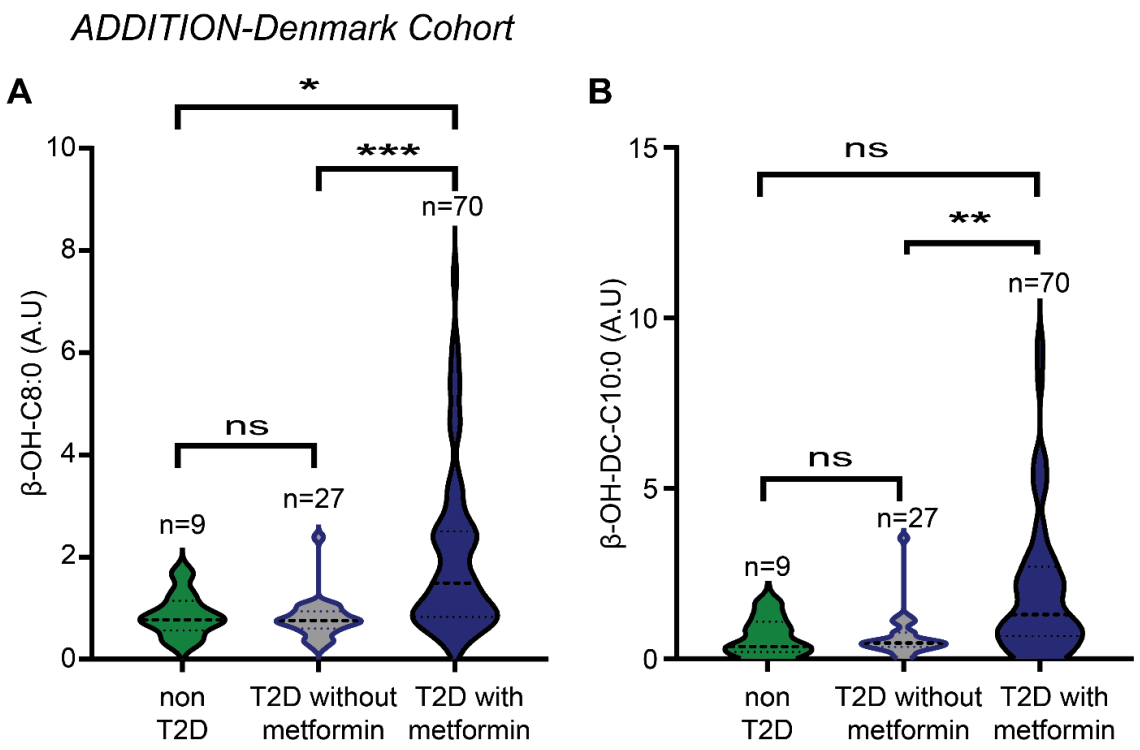

Figure 5.2: β-Hydroxy Fatty Acids and Dicarboxylic Acids Significantly Higher with Metformin in ADDITION-Denmark Cohort

Violin plots showing the levels of two β-hydroxy fatty acids—a monocarboxylic acid (β-OH-C8:0) and a dicarboxylic acid (β-OH-DC-C10:0)—in non-T2D volunteers (n = 9), T2D volunteers without metformin (n = 27), and T2D volunteers with metformin (n = 70) from the ADDITION-Denmark cohort. Data are presented with median (dashed line) and maximum and minimum quartiles (dotted lines).

(A) Levels of the monocarboxylic acid β-OH-C8:0 across the three groups. Statistical comparisons show significant increases in β-OH-C8:0 levels in T2D volunteers with metformin compared to those without (***P < 0.001) and non-T2D volunteers (*P < 0.05).

(B) Levels of the dicarboxylic acid β-OH-DC-C10:0 across the same groups. β-OH-DC-C10:0 levels are significantly higher in T2D volunteers with metformin compared to those without (**P < 0.01). No significant difference was observed between non-T2D volunteers and T2D volunteers without metformin. Statistical comparisons were made using one-way ANOVA with Šídák's post test.

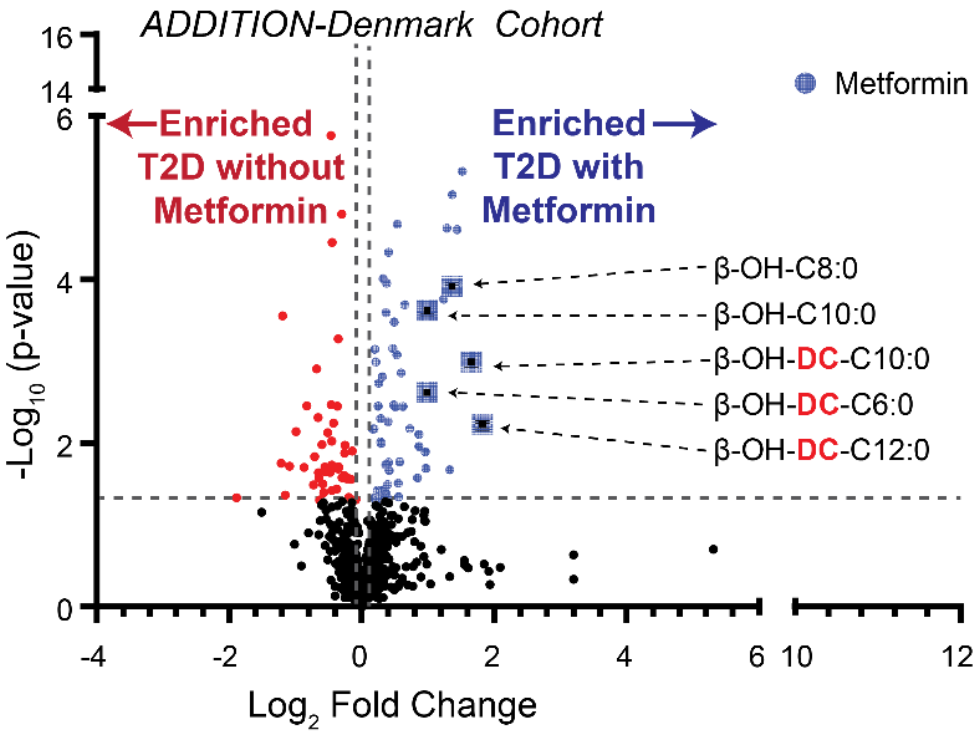

Figure 5.3: β-Hydroxy Fatty Acids Among the Most Significantly Upregulated Metabolites with Metformin Treatment in ADDITION-Denmark Cohort

Volcano plot comparing the plasma metabolomes of T2D individuals with (n = 70) and without (n = 27) metformin treatment from the ADDITION-Denmark cohort. Metabolites significantly ($P < 0.05$) upregulated with metformin treatment are shown in blue, and those downregulated in the absence of metformin are shown in red. Among the most significantly upregulated metabolites in the metformin-treated group are several β-hydroxy fatty acids, including both monocarboxylic acids (e.g., β-OH-C8:0 and β-OH-C10:0) and dicarboxylic acids (e.g., β-OH-DC-C6:0, β-OH-DC-C10:0, and β-OH-DC-C12:0), highlighted in the plot. Each metabolite was independently analyzed using a two-tailed Student's t-test.

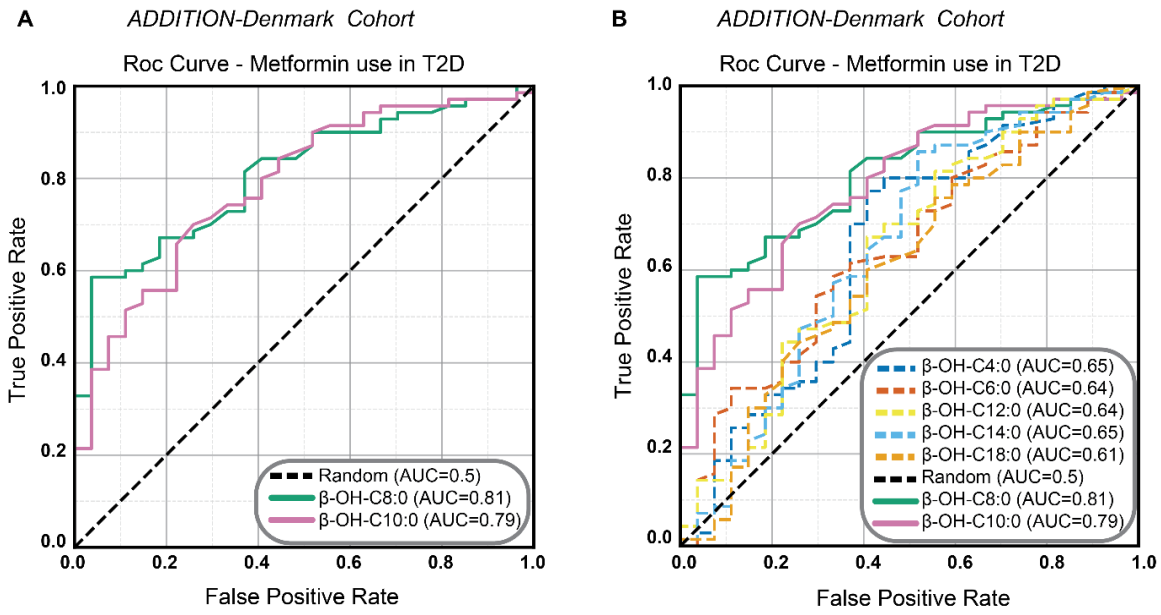

Figure 5.4: β-Hydroxy Fatty Acids with Chain Lengths 8 and 10 Best Differentiate Metformin-Treated T2D Patients in ADDITION-Denmark Cohort

ROC curves comparing the ability of β-hydroxy fatty acids to predict metformin treatment among T2D samples from the ADDITION-Denmark cohort. The cohort includes 97 T2D patients, of which 70 had metformin detected in their plasma, and 27 did not. The analysis evaluates various chain lengths, highlighting the predictive performance of these metabolites.

(A) ROC curves for the two most predictive metabolites, β-OH-C8:0 and β-OH-C10:0, which demonstrate the highest AUCs of 0.81 and 0.79, respectively.

(B) ROC curves comparing additional β-hydroxy fatty acids with chain lengths ranging from C4:0 to C18:0. While β-OH-C8:0 and β-OH-C10:0 maintain the highest predictive values, the other fatty acids show lower AUCs, ranging from 0.61 to 0.65. A random classifier is represented with an AUC of 0.5 in both panels

Metabolite	Fold Change	p-value	Spearman Correlation	ROC AUC
β-OH-C4:0	0.98	0.95	0.23	0.65
β-OH-C6:0	1.23	0.11	0.22	0.64
β-OH-C8:0	***2.58***	***0.0001***	***0.48***	***0.81***
β-OH-C10:0	***1.99***	***0.0002***	***0.44***	***0.79***
β-OH-C12:0	1.27	0.09	0.21	0.64
β-OH-C14:0	1.22	0.10	0.23	0.65
β-OH-C18:0	1.12	0.34	0.17	0.61

Table 5.2: β-Hydroxy Fatty Acids Strongly Associated with Metformin Use in ADDITION-Denmark Cohort

This table presents key metrics comparing mono-hydroxy fatty acids between T2D volunteers with and without metformin treatment in the ADDITION-Denmark cohort. The cohort includes 97 T2D volunteers, of whom 70 had metformin detected in their plasma, and 27 did not. The Fold Change column represents the ratio of metabolite levels between T2D volunteers with and without metformin treatment, with values greater than 1 indicating upregulation with metformin. The p-value column shows the significance of differences in metabolite levels between the two groups, calculated using a two-tailed Student's t-test. The Spearman Correlation column reflects the strength of the association between each mono-hydroxy fatty acid and serum metformin levels. The ROC AUC column displays the area under the ROC curve, representing the ability of each mono-hydroxy fatty acid to predict metformin use, with β-OH-C8:0 and β-OH-C10:0 showing the highest predictive values (AUC = 0.81 and 0.79, respectively). Metabolites with significant p-values are highlighted in red.

Metabolite	Fold Change	p-value	Spearman Correlation	ROC AUC
β-OH-DC-C6:0	***1.98***	***0.002***	***0.42***	***0.77***
β-OH-DC-C10:0	***3.15***	***0.001***	***0.40***	***0.76***
β-OH-DC-C12:0	***3.54***	***0.006***	***0.48***	***0.81***

Table 5.3: β-Hydroxy Dicarboxylic Acids Strongly Associated with Metformin Use in ADDITION-Denmark Cohort

This table presents key metrics comparing β-hydroxy dicarboxylic acids between T2D volunteers with and without metformin treatment in the ADDITION-Denmark cohort. The cohort includes 97 T2D volunteers, of whom 70 had metformin detected in their plasma, and 27 did not. The Fold Change column represents the ratio of metabolite levels between T2D volunteers with and without metformin treatment, with values greater than 1 indicating upregulation with metformin. The p-value column shows the significance of differences in metabolite levels between the two groups, calculated using a two-tailed Student's t-test. The Spearman Correlation column reflects the strength of the association between each β-hydroxy dicarboxylic acid and serum metformin levels. The ROC AUC column displays the area under the ROC curve, representing the ability of each β-hydroxy dicarboxylic acid to predict metformin use, with β-OH-DC-C12:0 showing the highest predictive value (AUC = 0.81). Metabolites with significant p-values are highlighted in red.

Metabolite	Fold Change	p-value	Spearman Correlation	ROC AUC
(R)-β-OH-C4:0 carnitine	1.92	0.08	0.18	0.62
(S)-β-OH-C4:0 carnitine	***1.66***	***0.01***	***0.28***	***0.68***
β-OH-C6:0 carnitine	1.21	0.12	0.09	0.56
β-OH-C10:0 carnitine	0.95	0.75	-0.01	0.50
β-OH-C18:1 carnitine	1.30	0.24	0.10	0.56

Table 5.4: Medium-Chain β-Hydroxy Carnitines Not Strongly Related to Metformin Use in ADDITION-Denmark Cohort

This table presents key metrics comparing medium-chain β-hydroxy carnitines between T2D volunteers with and without metformin treatment in the ADDITION-Denmark cohort. The cohort includes 97 T2D volunteers, of whom 70 had metformin detected in their plasma, and 27 did not. The Fold Change column represents the ratio of metabolite levels between T2D volunteers with and without metformin treatment, with values greater than 1 indicating upregulation with metformin. The p-value column shows the significance of differences in metabolite levels between the two groups, calculated using a two-tailed Student's t-test. The Spearman Correlation column reflects the strength of the association between each β-hydroxy carnitine and serum metformin levels. The ROC AUC column displays the area under the ROC curve, representing the ability of each β-hydroxy carnitine to predict metformin use. The (S)-β-OH-C4:0 carnitine shows a significant p-value but with only moderate correlation (0.28) and predictive value (AUC = 0.68). Metabolites with significant p-values are highlighted in red.

5.3 Reproducible Upregulation of β-Hydroxy Fatty Acids with Metformin Across Multiple Cohorts

A 2023 study conducted in New York provided another opportunity to assess the relationship between metformin and β-hydroxy fatty acids, this time within the Weill Cornell EDRN Prostate Cancer Cohort. The original focus of the study was on prostate cancer and utilized untargeted plasma metabolomics, however we repurposed the dataset to investigate the effects of metformin within the context of T2D.

The cohort included 580 male participants, 61 of whom were diagnosed with T2D. Notably, metformin was detected in the plasma of 35 of these T2D individuals, while the remaining 26 did not have metformin in their plasma (Figure 5.5).

We began by focusing once again on the two β-hydroxy metabolites most strongly correlated with metformin in the TwinsUK cohort: β-OH-C8:0 and β-OH-DC-C10:0. As expected, β-OH-C8:0 levels were higher with metformin treatment, showing significant increases in T2D volunteers treated with metformin compared to both untreated T2D individuals and non-T2D volunteers (Figure 5.6A). β-OH-DC-C10:0 levels were significantly higher in the metformin-treated group when compared to non-T2D participants, however only a trend was observed when comparing metformin-treated T2D volunteers to those not treated with metformin (Figure 5.6B).

In our subsequent analysis, we focused on the differences in metabolite levels between T2D participants on metformin treatment and those not receiving the drug. As expected, β-hydroxy fatty acids were among the most significantly upregulated metabolites in the metformin-treated group (Figure 5.7). Notably, β-OH-C8:0, β-OH-C10:0, and β-OH-DC-C12:0 showed substantial increases, reinforcing the reproducibility of metformin's effects on medium-chain β-hydroxy fatty acids across multiple cohorts.

For the Weill Cornell EDRN Prostate Cancer Cohort, we again employed ROC curve analysis to determine whether β-hydroxy fatty acids replicated as biomarkers. Among the monohydroxy fatty acids, β-OH-C8:0 and β-OH-C10:0 replicated as the strongest biomarkers for metformin treatment, with AUC values of 0.75 and 0.79, respectively (Figure 5.8A). These values highlight the strong biomarker potential of these medium-chain β-hydroxy fatty acids. In contrast, other fatty acids, such as β-OH-C6:0 and β-OH-C18:1, exhibited lower predictive values.

In this cohort, β-OH-C8:0 and β-OH-C10:0 again exhibited considerable fold increases in metformin-treated T2D individuals compared to those not on metformin—2.1 and 2.03 times higher, respectively (Table 5.5). Similarly, one of the dicarboxylic β-hydroxy fatty acids, β-OH-DC-C12:0 showed a substantial fold increase of 2 (Table 5.6).

Conversely, as observed in the ADDITION-Denmark cohort, medium-chain β-hydroxy carnitines, including β-OH-C10:0 carnitine, did not show a significant relationship with metformin treatment (Table 5.7).

In summary, the findings from the Weill Cornell EDRN Prostate Cancer Cohort not only align with those from the TwinsUK and ADDITION-Denmark cohorts but also reinforce the association between metformin treatment and elevated levels of specific β-hydroxy fatty acids, particularly those with medium-chain lengths. The consistency of these results across diverse populations underscores the robustness of these metabolites as biomarkers for metformin use.

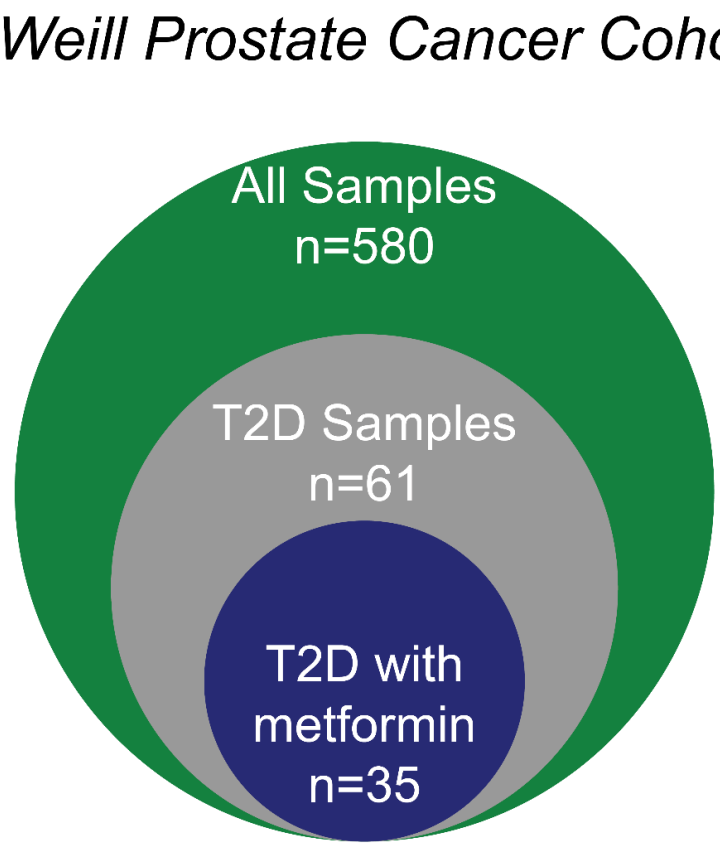

Figure 5.5: Weill Cornell EDRN Prostate Cancer Cohort: Distribution of T2D Volunteers with and without Metformin

The nested circle diagram illustrates the distribution of samples in the Weill Prostate Cancer Cohort. The largest circle represents all samples (n = 580), the middle circle represents T2D samples (n = 61), and the smallest circle represents T2D samples treated with metformin (n = 35)

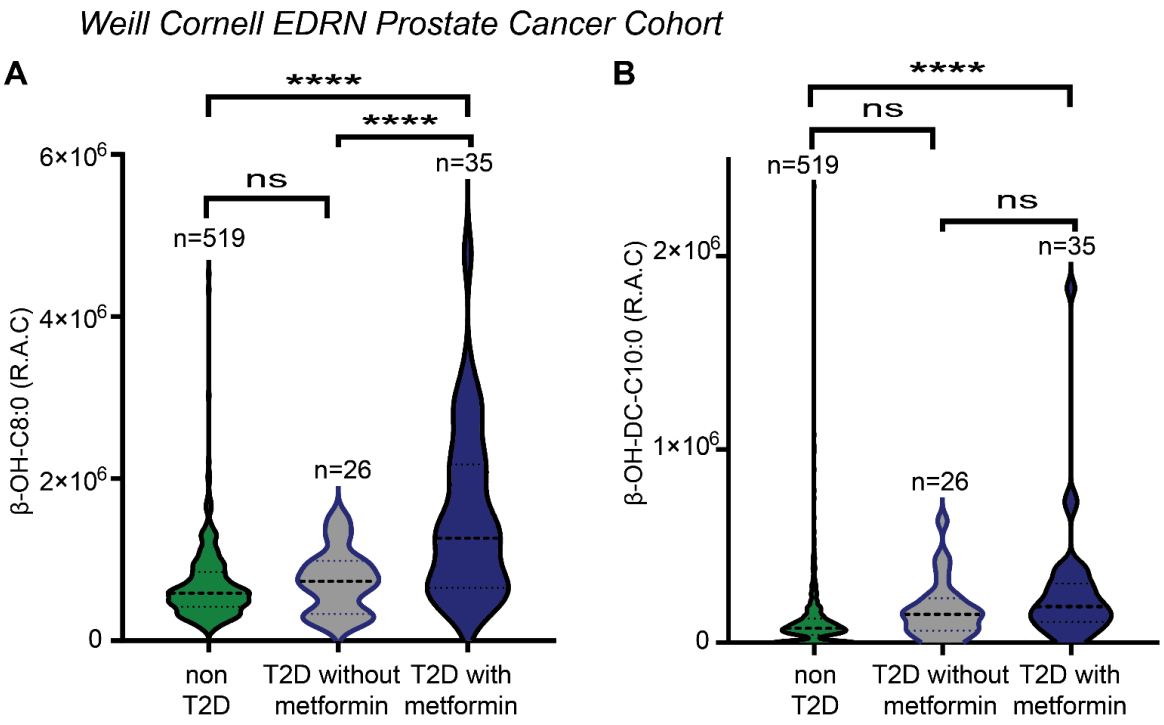

Figure 5.6: β-Hydroxy Fatty Acids and Dicarboxylic Acids Significantly Higher with Metformin in Weill Cornell EDRN Prostate Cancer Cohort

Violin plots showing the levels of two β-hydroxy fatty acids—a monocarboxylic acid (β-OH-C8:0) and a dicarboxylic acid (β-OH-DC-C10:0)—in non-T2D volunteers (n = 519), T2D volunteers without metformin (n = 26), and T2D volunteers with metformin (n = 35) from the Weill Cornell EDRN Prostate Cancer Cohort. Data are presented as Raw Area Counts (R.A.C) with median (dashed line) and maximum and minimum quartiles (dotted lines).

(A) Levels of the monocarboxylic acid β-OH-C8:0 across the three groups. Statistical comparisons show significant increases in β-OH-C8:0 levels in T2D volunteers with metformin compared to those without (****P < 0.0001) and non-T2D volunteers (****P < 0.0001).

(B) Levels of the dicarboxylic acid β-OH-DC-C10:0 across the same groups. β-OH-DC-C10:0 levels are significantly higher in T2D volunteers with metformin compared to those without (****P < 0.0001). No significant difference was observed between non-T2D volunteers and T2D volunteers without metformin. Statistical comparisons were made using one-way ANOVA with Šídák's post test.

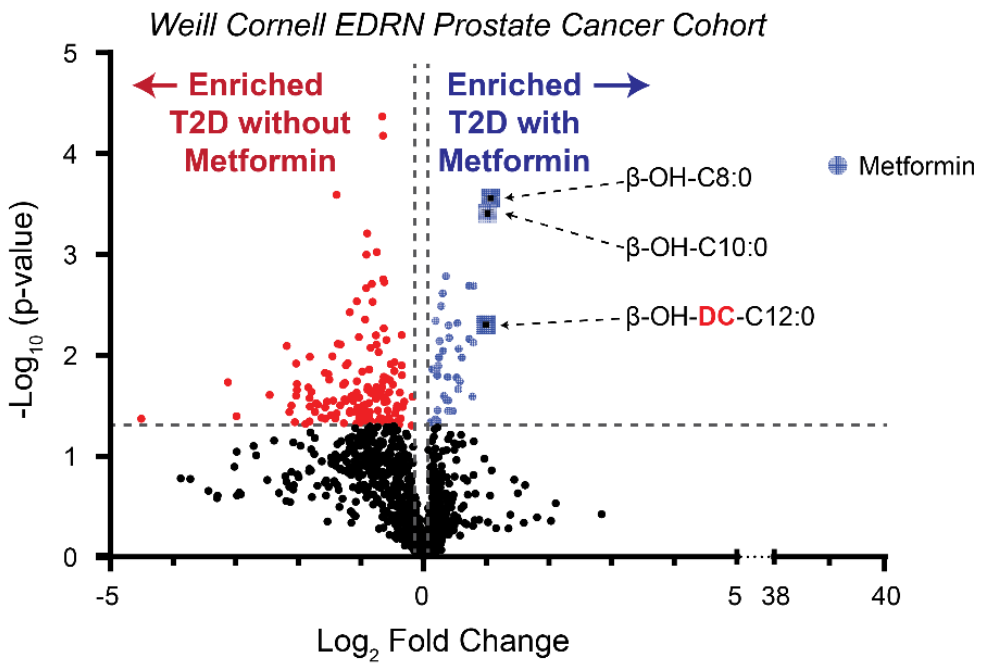

Figure 5.7: β-Hydroxy Fatty Acids Among the Most Significantly Upregulated Metabolites with Metformin Treatment in Weill Cornell EDRN Prostate Cancer Cohort

Volcano plot comparing the plasma metabolomes of T2D individuals with (n = 35) and without (n = 26) metformin treatment from the Weill Cornell EDRN Prostate Cancer Cohort. Metabolites significantly ($P < 0.05$) upregulated with metformin treatment are shown in blue, and those downregulated in the absence of metformin are shown in red. Among the most significantly upregulated metabolites in the metformin-treated group are several β-hydroxy fatty acids, including both monocarboxylic acids (e.g., β-OH-C8:0 and β-OH-C10:0) and dicarboxylic acids (e.g., β-OH-DC-C12:0), highlighted in the plot. Each metabolite was independently analyzed using a two-tailed Student's t-test.

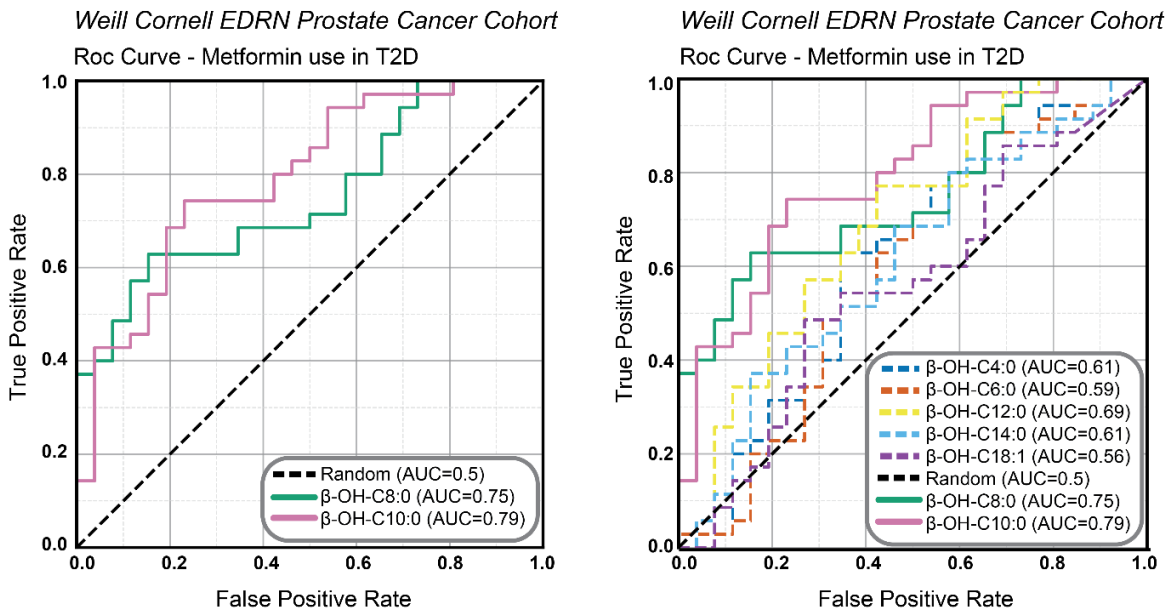

Figure 5.8: β-Hydroxy Fatty Acids with Chain Lengths 8 and 10 Best Differentiate Metformin-Treated T2D Patients in Weill Cornell EDRN Prostate Cancer Cohort

ROC curves comparing the ability of β-hydroxy fatty acids to predict metformin treatment among T2D samples from the Weill Cornell EDRN Prostate Cancer Cohort. The cohort includes 61 diabetic volunteers, of which 35 had metformin detected in their plasma, and 26 did not. The analysis evaluates various chain lengths, highlighting the predictive performance of these metabolites.

(A) ROC curves for the two most predictive metabolites, β-OH-C8:0 and β-OH-C10:0, which demonstrate AUCs of 0.75 and 0.79, respectively.

(B) ROC curves comparing additional β-hydroxy fatty acids with chain lengths ranging from C4:0 to C18:1. While β-OH-C8:0 and β-OH-C10:0 maintain the highest predictive values, the other fatty acids show lower AUCs, ranging from 0.56 to 0.69. A random classifier is represented with an AUC of 0.5 in both panels.

Metabolite	Fold Change	p-value	Spearman Correlatio	ROC AUC
β-OH-C4:0	1.05	0.88	0.19	0.61
β-OH-C6:0	1.13	0.23	0.15	0.59
β-OH-C8:0	***2.10***	***0.0003***	***0.43***	***0.75***
β-OH-C10:0	***2.03***	***0.0004***	***0.50***	***0.79***
β-OH-C12:0	1.34	0.06	0.33	0.69
β-OH-C14:0	1.09	0.47	0.19	0.61
β-OH-C18:1	1.10	0.48	0.10	0.56

Table 5.5: β-Hydroxy Fatty Acids Strongly Associated with Metformin Use in Weill Cornell EDRN Prostate Cancer Cohort

This table presents key metrics comparing mono-hydroxy fatty acids between T2D volunteers with and without metformin treatment in the Weill Cornell EDRN Prostate Cancer Cohort. The cohort includes 61 T2D volunteers, of whom 35 had metformin detected in their plasma, and 26 did not. The Fold Change column represents the ratio of metabolite levels between T2D volunteers with and without metformin treatment, with values greater than 1 indicating upregulation with metformin. The p-value column shows the significance of differences in metabolite levels between the two groups, calculated using a two-tailed Student's t-test. The Spearman Correlation column reflects the strength of the association between each mono-hydroxy fatty acid and serum metformin levels. The ROC AUC column displays the area under the ROC curve, representing the ability of each mono-hydroxy fatty acid to predict metformin use, with β-OH-C8:0 and β-OH-C10:0 showing the highest predictive values (AUC = 0.75 and 0.79, respectively). Metabolites with significant p-values are highlighted in red.

Metabolite	Fold Change	p-value	Spearman Correlation	ROC AUC
β-OH-DC-C6:0	0.92	0.78	0.18	0.61
β-OH-DC-C10:0	1.56	0.17	0.18	0.61
β-OH-DC-C12:0	***2.00***	***0.005***	***0.34***	***0.70***

Table 5.6: β-Hydroxy Dicarboxylic Acids Strongly Associated with Metformin Use in Weill Cornell EDRN Prostate Cancer Cohort

This table presents key metrics comparing β-hydroxy dicarboxylic acids between T2D volunteers with and without metformin treatment in the Weill Cornell EDRN Prostate Cancer Cohort. The cohort includes 61 T2D volunteers, of whom 35 had metformin detected in their plasma, and 26 did not. The Fold Change column represents the ratio of metabolite levels between T2D volunteers with and without metformin treatment, with values greater than 1 indicating upregulation with metformin. The p-value column shows the significance of differences in metabolite levels between the two groups, calculated using a two-tailed Student's t-test. The Spearman Correlation column reflects the strength of the association between each β-hydroxy dicarboxylic acid and serum metformin levels. The ROC AUC column displays the area under the ROC curve, representing the ability of each β-hydroxy dicarboxylic acid to predict metformin use, with β-OH-DC-C12:0 showing the highest predictive value (AUC = 0.70). Metabolites with significant p-values are highlighted in red.

Metabolite	Fold Change	p-value	Spearman Correlation	ROC AUC
(R)-β-OH-C4:0 carnitine	1.28	0.34	0.11	0.56
(S)-β-OH-C4:0 carnitine	1.07	0.68	0.03	0.52
β-OH-C6:0 carnitine	0.71	0.05	-0.28	0.33
β-OH-C8:0 carnitine*	***0.75***	***0.03***	***-0.24***	***0.36***
β-OH-C8:0 carnitine**	0.83	0.11	-0.20	0.39
β-OH-C10:0 carnitine	0.75	0.06	-0.23	0.36
β-OH-C18:1 carnitine	1.11	0.43	0.16	0.60

Table 5.7: Medium-Chain β-Hydroxy Carnitines Not Strongly Related to Metformin Use in Weill Cornell EDRN Prostate Cancer Cohort

This table presents key metrics comparing medium-chain β-hydroxy carnitines between T2D volunteers with and without metformin treatment in the Weill Cornell EDRN Prostate Cancer Cohort. The cohort includes 61 T2D volunteers, of whom 35 had metformin detected in their plasma, and 26 did not. The Fold Change column represents the ratio of metabolite levels between T2D volunteers with and without metformin treatment, with values greater than 1 indicating upregulation with metformin. The p-value column shows the significance of differences in metabolite levels between the two groups, calculated using a two-tailed Student's t-test. The Spearman Correlation column reflects the strength of the association between each β-hydroxy carnitine and serum metformin levels. The ROC AUC column displays the area under the ROC curve, representing the ability of each β-hydroxy carnitine to predict metformin use. Metabolites with significantly lower levels in the metformin group are highlighted in blue.

5.4 Interventional Evidence: β-Hydroxy Fatty Acids Increase in Both Healthy and T2D Volunteers Following Metformin Treatment

To establish a causal relationship between metformin administration and the observed elevations in medium-chain β-hydroxy fatty acids, we reexamined the 2019 Danish metformin interventional study introduced in Chapter 3 to study Lac-Phe. This cohort included 12 healthy volunteers and 12 individuals with recent-onset type 2 diabetes (T2D). The volunteers were administered metformin daily for 12-weeks. Serum metabolomics were conducted pre- and post-intervention to quantify changes in metabolite levels.

β-Hydroxy Fatty Acids: Monocarboxylic Forms

Among the monocarboxylic β-hydroxy fatty acids, β-OH-C8:0 and β-OH-C10:0 have consistently shown the strongest correlation with metformin treatment in previous observational studies, exhibiting the largest fold changes. This pattern was confirmed in this interventional study too. Specifically, β-OH-C8:0 and β-OH-C10:0 displayed the most significant increases, with fold changes of 3.03 and 2.38, respectively, in healthy volunteers, and 2.56 and 2.22, respectively, in T2D volunteers (Table 5.8). These changes were statistically significant in both groups ($P < 0.05$), reinforcing the robust effect of metformin on these medium-chain fatty

acids. The consistent response across both healthy and T2D individuals indicates that metformin elevates these metabolites regardless of diabetic status.

Other monocarboxylic β-hydroxy fatty acids, including β-OH-C6:0, β-OH-C12:0, and β-OH-C14:0, also exhibited significant increases, although with more modest fold changes. For example, β-OH-C12:0 also demonstrated significant increases in both healthy and T2D's, however the fold changes were only 1.45 and 1.34 respectively (Table 5.8). These results highlight the differential impact of metformin on β-hydroxy fatty acids of varying chain lengths.

β-Hydroxy Fatty Acids: Dicarboxylic Forms

We also examined changes in β-hydroxy dicarboxylic acids (Table 5.9). Both metabolites measured, β-OH-DC-C6:0 and β-OH-DC-C10:0, were significantly elevated in response to metformin treatment in both healthy and T2D groups, with substantial fold changes observed in each case. Specifically, β-OH-DC-C10:0 showed the most pronounced increase, with a fold change of 3.65 in healthy volunteers and 3.17 in T2D volunteers. This evidence establishes a causal link between metformin and the elevation of medium-chain dicarboxylic β-hydroxy fatty acids, regardless of diabetic status. These findings confirm and extend the results from our earlier observational datasets.

β-hydroxy carnitines were not assessed in this study, leaving us unable to definitely confirm whether these metabolites remain unaffected by metformin treatment.

In summary, this cohort has allowed us to establish a causal link between metformin treatment and increased blood levels of β-hydroxy fatty acids. Notably, the mono-carboxylic acids β-OH-C8:0 and β-OH-C10:0, along with the dicarboxylic β-OH-DC-C12:0, exhibited the largest fold changes. Significantly, these effects are independent of diabetic status.

Metabolite Name	FC Healthy	Significance Healthy	FC T2D	Significance T2D
β-OH-C6:0	***1.73***	***significant***	1.13	not significant
β-OH-C8:0	***3.03***	***significant***	***2.56***	***significant***
β-OH-C10:0	***2.38***	***significant***	***2.22***	***significant***
β-OH-C12:0	***1.45***	***significant***	***1.34***	***significant***
β-OH-C14:0	**1.3**	**trending**	***1.35***	***significant***
β-OH-C18:1	1.2	not significant	***1.7***	***significant***
β-OH-C18:0	1.49	not significant	1.49	trending

Table 5.8: β-Hydroxy Fatty Acids Significantly Increased in Healthy and T2D Volunteers with Metformin in Danish 12-Week Interventional Study

This table compares the fold changes (FC) of β-hydroxy fatty acids with a single carboxyl group following a 12-week metformin intervention (2000 mg/day) in T2D volunteers and healthy controls (n = 12 per group). Metabolite levels were measured using untargeted metabolomics on serum samples. Fold changes for each fatty acid were calculated relative to pre-treatment levels, with significance assessed independently for the T2D and healthy groups. Statistical significance is indicated as significant ($P < 0.05$) in red or trending ($0.05 < P < 0.10$) in orange. Notably, β-OH-C8:0 and β-OH-C10:0 show significant increases in both groups. Data were analyzed using Welch's two-sided Student's t-test.

Metabolite Name	FC Healthy	Significance Healthy	FC T2D	Significance T2D
β-OH-DC-C6:0	***2.08***	***significant***	***1.94***	***significant***
β-OH-DC-C10:0	***3.65***	***significant***	***3.17***	***significant***

Table 5.9: β-Hydroxy Dicarboxylic Acids Significantly Increased in Healthy and T2D Volunteers with Metformin in Danish 12-Week Interventional Study

This table compares the fold changes (FC) of β-hydroxy dicarboxylic acids following a 12-week metformin intervention (2000 mg/day) in T2D volunteers and healthy controls (n = 12 per group). Metabolite levels were measured using untargeted metabolomics on serum samples. Fold changes for each β-hydroxy dicarboxylic acid were calculated relative to pre-treatment levels, with significance assessed independently for the T2D and healthy groups. Both β-OH-DC-C6:0 and β-OH-DC-C10:0 showed significant increases in both the healthy and T2D groups. Statistical significance is indicated as significant ($P < 0.05$) in red. Data were analyzed using Welch's two-sided Student's t-test.

5.5 Discussion

This chapter builds on our previous work from Chapter 3, where we identified N-lactoyl amino acids as elevated in the blood of humans following metformin treatment. Here, we aimed to explore additional metabolite classes influenced by the drug. Our results demonstrate that medium-chain β-hydroxy fatty acids, particularly β-OH-C8:0 and β-OH-C10:0, consistently increase in the bloodstream following metformin use. This finding was reinforced by multiple observational studies, which revealed a strong association between these metabolites and blood metformin levels. In addition to these monocarboxylic acids, our analysis also identified dicarboxylic β-hydroxy fatty acids, such as β-OH-DC-C10:0, as significantly elevated, suggesting a previously unrecognized role for metformin in regulating specific pathways of fatty acid metabolism. These observations were further validated by a single interventional study, which established a causal relationship between metformin administration and the increase in these blood metabolites. The effects were observed in both healthy and T2D individuals, highlighting that these effects on fatty acid metabolism occur independently of diabetic status. These findings underscore the broad metabolic effects of metformin, demonstrating that while it is typically associated with regulating glucose—a key metabolite—its influence extends to a wider range of metabolites, including those involved in fatty acid metabolism.

Mechanistic Insights into Metformin's Impact on β-Hydroxy Fatty Acid Accumulation

As previously noted, at high concentrations, metformin is known to inhibit mitochondrial Complex I, a key component of the electron transport chain. Complex I oxidizes NADH to NAD+, a critical step that drives proton pumping and sets the electron transport chain in motion. Its inhibition can lead to an increase in the cellular NADH/NAD+ ratio and reduced ATP synthesis. Metformin reaches its highest concentrations in the intestines, and, as discussed in Chapter 3, inhibition of Complex I in the intestines contributes to increases in circulating N-lactoyl amino acids. We propose that a similar mechanism may explain why metformin elevates circulating levels of β-hydroxy fatty acids.

The increase in the cellular NADH/NAD+ ratio driven by metformin likely inhibits β-oxidation, the process by which fatty acids are broken down by removing two carbon units per cycle, with these units subsequently entering the tricarboxylic acid (TCA) cycle for further oxidation. Each cycle of β-oxidation involves four enzymatically catalyzed steps, and one of the critical enzymes, **β-hydroxyacyl-CoA dehydrogenase**, requires NAD+ as a cofactor. This enzyme catalyzes the conversion of **β-hydroxyacyl-CoA to β-ketoacyl-CoA**. When NAD+ is limited due to the elevated NADH/NAD+ ratio induced by metformin, this step is likely inhibited, leading to the accumulation of β-hydroxy fatty acids within the cell. This metabolic bottleneck likely occurs primarily in tissues with high metformin concentrations, such

as the intestines, where the inhibition of β-oxidation results in increased circulation of β-hydroxy fatty acids.

To test whether β-hydroxy fatty acids generated in response to metformin primarily originate from the intestines, an experiment comparing oral gavage and intravenous injection of metformin in mice would be particularly informative. If our hypothesis is correct, we would expect significantly elevated levels of circulating β-hydroxy fatty acids following oral gavage compared to intravenous administration. It is also important to assess the role of the microbiome in this process. While germ-free mice have been shown to have higher baseline levels of β-OH-C10:0, indicating they do not produce it endogenously, the microbiome may still influence its production in the presence of metformin[284]. Cultured gut bacteria have demonstrated the ability to produce β-hydroxy fatty acids, so using germ-free mice treated with metformin would help determine whether the increase in circulating β-hydroxy fatty acids is independent of microbial contributions[285]. This approach would clarify whether the intestines are the primary source of these metabolites in response to metformin, excluding the influence of the microbiome.

Limitations

This study has two primary limitations: small sample sizes that underpowered the analyses and a restricted range of metabolites measured, limiting the scope of the findings.

Underpowered Sample Sizes

The small sample sizes, particularly in the observational datasets, likely reduced our ability to detect significant changes across a broader range of β-hydroxy fatty acid metabolites, especially for those where metformin's effects may be more subtle. In the interventional study, we observed significant increases in multiple β-hydroxy fatty acids. These included chain lengths of 8 and 10, which consistently showed the largest fold changes across all studies. Additionally in this interventional study, we saw increases in chain lengths of 6, 12, and 14 in at least one group (either healthy individuals or T2D volunteers). However, these additional chain lengths did not consistently show statistically significant increases in the observational datasets, with only trends observed, likely due to smaller sample sizes.

In both the ADDITION-Denmark and Weill Cornell cohorts, the relatively small number of T2D participants not on metformin (n = 27 and n = 26, respectively) limited the power of our comparisons. In the ADDITION-Denmark cohort, the control group was especially small (n = 9), complicating comparisons with the T2D groups and possibly explaining why metabolites like β-OH-DC-C10:0 did not show statistically significant differences between metformin-treated T2D individuals and controls. Larger cohorts in future studies would provide the necessary statistical power to confirm trends observed here.

Incomplete List of Metabolites

A second limitation was the restricted range of metabolites measured, which hindered a complete understanding of metformin's effects on fatty acid

metabolism. A subset of saturated β-hydroxy fatty acids was captured, notably β-OH-C16:0 was omitted in both the ADDITION-Denmark and Weill cohorts. The effects of metformin on unsaturated β-hydroxy fatty acids also remain unclear, as only β-OH-C18:1 was included in our analyses, leaving the behavior of other unsaturated β-hydroxy fatty acids unexplored. Furthermore, the dicarboxylic β-hydroxy fatty acids measured were limited to chain lengths 6, 10, and 12, preventing us from drawing broader conclusions about metformin's impact on this class of metabolites. Finally, only a subset of β-hydroxy fatty acid carnitines was measured, and none were included in the interventional study. While our data suggest that metformin does not significantly affect β-hydroxy carnitines, the lack of comprehensive measurements makes it difficult to confirm this definitively. Our findings highlight metformin's impact on fatty acid metabolism, but future interventional studies with expanded metabolite profiling and larger sample sizes will be helpful in providing a more complete picture.

Comparison with Literature

In this chapter, we have demonstrated that β-hydroxy fatty acids (β-OH-FAs) are significantly elevated in response to metformin treatment. This finding complements and expands upon recent literature, published since 2020, the first year of my PhD. Here, we will discuss four key studies relevant to β-hydroxy fatty acids: two focusing on type 2 diabetes (T2D) and two on metformin.

Type 2 Diabetes and β-hydroxy fatty acids studies

In Chapter 4, we utilized data from a mixed meal interventional study conducted in Germany, involving three groups: metabolically healthy, prediabetic, and T2D subjects[219]. The original manuscript from this study, published in 2020, reported an increase in **fasting** β-hydroxy-octanoic acid (β-OH-C8:0) levels between the prediabetic and T2D groups, with higher levels observed in the T2D cohort. While the feeding component of the study was interventional, where participants were tested before and after a mixed meal, this comparison of fasting samples across groups was essentially a small observational study, with 10 participants in each group sampled three times. The observed increase in the T2D cohort is likely attributable to metformin use, despite the fact that T2D participants had discontinued metformin the evening before the fasting sample was collected.

While metformin is rapidly cleared from the blood, it is eliminated much more slowly from other compartments[122,286,287]. Positron emission tomography (PET) scans have shown that increased glucose uptake in the intestines persists for 24 hours but not 48 hours following metformin cessation[288,289]. Although residual transcriptional effects post-clearance cannot be entirely ruled out, we consider this unlikely to cause the observed increase given our hypothesis that the increase in β-hydroxy fatty acids is due to Complex I inhibition by metformin. This suggests that β-hydroxy fatty acids might be a more accurate indicator of intestinal cellular concentrations—specifically within enterocytes—rather than serum metformin levels.

Future studies using mouse models could provide valuable insights into this hypothesis. As previously noted an experiment comparing oral gavage and intravenous injection of metformin would be particularly informative in distinguishing the effects on intestinal versus systemic metformin concentrations. A time-course study, examining the effects of both a single dose of metformin and its cessation following repeated administration, could also be employed. These studies should measure both serum and intestinal concentrations of β-hydroxy fatty acids alongside metformin levels. This approach is motivated by the fact that systemic metformin levels are expected to decline much more rapidly than intestinal concentrations, which could result in different concentrations between the two compartments. Understanding these dynamics is essential to accurately assess the persistence of metformin's effects. Such an approach would help determine whether these β-hydroxy fatty acids are more reflective of local intestinal metformin concentrations than systemic metformin levels, and if they can be used as biomarkers for intestinal metformin exposure specifically. Additionally, it would clarify whether β-hydroxy fatty acid levels correspond more closely to intestinal metformin levels compared to systemic levels.

While conducting this research, a larger 2022 observational study involving volunteers from the Netherlands was published[284]. It reported an increase in β-OH-C8:0 and β-OH-C10:0 levels in individuals with T2D compared to non-diabetics. The study included 84 obese non-diabetic individuals and 22 obese individuals with T2D. Although the study did not account for metformin use, given the widespread use of

metformin among individuals with T2D and our own findings, it is likely that the observed increases in these metabolites are attributable to metformin treatment.

Metformin and β-hydroxy fatty acids studies

A 2020 study conducted in the United States involving patients with Li-Fraumeni syndrome, a hereditary cancer predisposition disorder unrelated to diabetes, was the first to report a relationship between metformin and increased β-hydroxy fatty acids[290]. In this 14-week metformin intervention trial with 26 participants, none of whom were diabetic, the researchers observed a significant increase in β-hydroxy fatty acids, although this was not the main focus of the study. Monocarboxylic β-hydroxy fatty acids with chain lengths between 6 and 12 carbons increased significantly, with the largest fold changes observed in β-OH-C8:0 and β-OH-C10:0, consistent with our findings. Additionally, the dicarboxylic acid β-OH–DC-C10:0 exhibited a fold change greater than four. The levels of these metabolites, measured six weeks after metformin cessation, had returned to baseline, providing additional evidence that metformin influences β-hydroxy fatty acids even in a non-diabetic cohort. This study broadens the context beyond T2D and healthy volunteers by extending the observed effects to a group with a genetic predisposition to cancer.

A very recent study published in 2024, involving volunteers from Qatar, also reported a relationship between metformin and increased β-hydroxy fatty acids[291]. This study utilized an observational dataset of 146 volunteers with T2D, 101 of whom were treated with metformin. Their findings align with ours, showing elevated levels of β-OH-C8:0 and β-OH-C10:0 in the metformin-treated group. However, our research

goes further by examining a more extensive set of cross-sectional cohorts, providing greater confidence in our results and demonstrating that the association holds across a broader range of patient populations. Additionally, we present interventional data, which allows us to establish a causal role for metformin in elevating β-hydroxy fatty acids in both healthy individuals and those with diabetes. Furthermore, we show for the first time an increase in β-hydroxy dicarboxylic acids with metformin treatment in diabetics. Our data suggest that metformin's effects extend beyond just β-OH-C8:0 and β-OH-C10:0, increasing levels of β-hydroxy fatty acids with different chain lengths, though with a lower fold change.

In summary, our findings corroborate and expand on existing literature, providing a more comprehensive understanding of the relationship between metformin and β-hydroxy fatty acids.

Are Medium-Chain β-Hydroxy Fatty Acids Key Signaling Molecules in Metformin's Mechanisms of Action?

The medium-chain β-hydroxy fatty acids β-hydroxyoctanoate (β-OH-C8:0) and β-hydroxydecanoate (β-OH-C10:0), act as signaling molecules by interacting with specific G-protein-coupled receptors. β-OH-C8:0 consistently activates hydroxycarboxylic acid receptor 3 (HCA3), while β-OH-C10:0 primarily activates GPR84 but has been variably reported to activate HCA3 as well[284,285,292]. These receptors are involved in immune regulation and metabolic processes, suggesting a

potential connection between the increased levels of these metabolites and the therapeutic effects of metformin[285].

Immune Modulation by Metformin: Are β-Hydroxy Fatty Acids Important Mediators?

Both HCA3 and GPR84 are expressed on immune cells and have contrasting roles in inflammation[285]. Activation of GPR84 generally promotes pro-inflammatory responses, while HCA3 activation is associated with anti-inflammatory outcomes. For example, β-OH-C10:0, which activates GPR84, has been shown to induce neutrophil recruitment to adipose tissue in mice[284]. This pro-inflammatory effect contrasts with the anti-inflammatory properties of metformin, which include reducing neutrophil extracellular trap (NET) formation, or NETosis[293]. The anti-inflammatory actions of HCA3, particularly in macrophages and neutrophils, align more closely with metformin's known effects, making HCA3 a promising candidate for further investigation.

However, the lack of HCA3 expression in rodents, as it is only expressed in higher primates, poses a challenge for in vivo studies, necessitating alternative approaches such as human cohort studies[169,294]. For example, a placebo-controlled trial in patients with prediabetes demonstrated that metformin treatment reduced neutrophil extracellular trap (NET) components such as elastase, proteinase 3, histones, and double-stranded DNA, independently of its glucose-lowering effects[293]. This

suggests that similar studies could be adapted to investigate the relationship between changes in β-hydroxy fatty acid levels and immune outcomes. Such studies could analyze pre- and post-treatment levels of these metabolites using metabolomics, correlating them with specific immune markers, such as NET components or cytokine profiles, to better understand how these metabolites might mediate the anti-inflammatory effects of metformin. Additionally, assessing how β-hydroxy fatty acids impact other immune cells, such as macrophages or T cells, in the context of metformin treatment could help clarify their specific role in mediating the drug's anti-inflammatory effects.

Appetite Regulation by Metformin: Are Medium-Chain β-Hydroxy Fatty Acids Important Mediators?

GPR84 is highly expressed in the colon and plays a role in nutrient sensing within colonic enteroendocrine cells (EECs), which release gut hormones such as peptide YY (PYY) that regulate satiety[295]. A 2021 study demonstrated that targeted delivery of GPR84 and FFAR4 agonists, specifically 3′3-diindolylmethane and lauric acid, to the colon reduced overall caloric intake and increased postprandial PYY levels in obese adults[295]. Notably, PYY levels also increase with metformin treatment, suggesting a potential overlap in mechanisms[296]. Although this study did not use β-OH-C10:0, which is a natural activator of GPR84, it highlights the receptor's role in appetite regulation. Given that β-OH-C10:0 levels are likely elevated in the intestine

following metformin treatment, it could similarly contribute to the drug's appetite-suppressing effects.

This aligns with findings from another study in rainbow trout, where the GPR84 agonist 3′3-diindolylmethane, administered into cerebrospinal fluid (CSF) via intracerebroventricular injection, also significantly reduced food intake. Additionally, it altered neuropeptide expression in the hypothalamus, increasing the levels of anorexigenic peptides such as the trout homologs of POMC (pomca1) and CART (cartpt), while decreasing orexigenic peptides like the trout homologs of NPY (npy) and AgRP (agrp1)[297]. These results suggest that GPR84 activation can influence appetite both peripherally and centrally. However, a contrasting study in mice with a whole-body knockout of GPR84 found no significant changes in body weight compared to controls, indicating that the regulation of appetite by GPR84 may be more complex and potentially species-specific and further research is needed[298].

Transitioning from GPR84, another receptor of interest is HCA3, which is consistently activated by β-OH-C8:0 and less reliably by β-OH-C10:0[284,285,292]. An initial analysis I conducted using the Type 2 Diabetes Knowledge Portal revealed a highly significant association between HCA3 and body mass index (BMI), as indicated by its high Human Gene E-score (HUGE score), suggesting a potential role in obesity and metabolic regulation. Notably, HCA3 has also been shown to be present in the colon, indicating that β-OH-C8:0 could partially mediate the weight loss effects of metformin in humans[299]. However, since HCA3 is absent in mice, its role in mediating these effects cannot be studied in mouse models. Consequently,

while studies in mice might correctly attribute the appetite and weight loss effects of metformin to Lac-Phe, or other factors such as GDF15, β-OH-C8:0 and HCA3 could also play a contributing role in humans.

Roux-en-Y gastric bypass surgery provides an interesting perspective on the interaction between dietary metabolites and gut receptors. This surgical procedure allows nutrients and metabolites to bypass the upper gastrointestinal tract and reach the lower part of the intestine, where they can more effectively interact with receptors on enteroendocrine cells. This bypass is thought to contribute to the surgery's appetite-suppressing effects[295]. Interestingly, dicarboxylic β-hydroxy fatty acid β-OH-DC-C12:0—one of the metabolites we also observed to be increased with metformin treatment—was identified as one of the most significantly elevated metabolites in urine samples collected after Roux-en-Y surgery. A preliminary re-analysis I conducted of a separate interventional Roux-en-Y surgery study's blood metabolomics data suggests that β-OH-DC-C10:0 levels significantly increased from pre-surgery to several months post-surgery.

Additionally, the consumption of Royal Jelly, which is produced by honeybees, has been shown to increase serum levels of β-OH-DC-C10:0[180]. A recent randomized controlled trial reported that overweight volunteers who were given a Royal Jelly supplement experienced increased satiety compared to a placebo group. This was accompanied by reductions in BMI and body fat percentage, suggesting that β-OH-DC-C10:0 may play a role in these outcomes[300].

Given these findings, it is plausible that β-OH-DC-C10:0 may mediate some of the appetite-suppressing effects observed with metformin treatment, Roux-en-Y surgery, and Royal Jelly supplementation. Future studies should investigate whether β-hydroxy metabolites can impact appetite regulation and metabolic outcomes. Similar to trials involving GPR84 and FFAR4 agonists, capsules containing metformin-induced β-hydroxy fatty acids could be administered to both animal models and humans to assess their effects on appetite and body weight regulation[295]. This approach could help elucidate the role of these metabolites in mediating the therapeutic benefits of metformin and other interventions.

Summary

In conclusion, this chapter has clearly demonstrated that β-hydroxy fatty acids, including both monocarboxylic and dicarboxylic species, are elevated in response to metformin treatment, regardless of diabetic status. This consistent increase highlights a broader metabolic impact of metformin beyond its well-known role in glucose regulation. Future research should focus on determining whether these β-hydroxy fatty acids influence specific actions of metformin, such as its anti-inflammatory properties or appetite-suppressing effects. Unraveling these mechanisms could reveal new therapeutic targets. This study lays a robust foundation for future research to explore the therapeutic potential of β-hydroxy fatty acids and their role in the diverse benefits of metformin.

Chapter 6 - Overall Discussion

General Discussion

Metformin, a widely prescribed drug for type 2 diabetes (T2D), has been reported to exhibit multiple mechanisms of action beyond its primary role in glycemic control[72,127]. Initially developed as a treatment for type 2 diabetes, its therapeutic potential has since been suggested for numerous other conditions, sparking debate on whether it could be universally beneficial to the general population[301–303]. Indeed, metformin has shown promise not only in managing hyperglycemia but also in addressing obesity, cardiovascular disease, and chronic inflammation, which is commonly associated with aging[304–306]. For instance, clinical trials are currently investigating its role in aging and longevity. For example, the Targeting Aging with Metformin (TAME) trial is a large, multi-center study designed to test whether metformin can slow the progression of age-related chronic diseases like heart disease, cancer, and dementia. This landmark study will enroll over 3,000 non-T2D participants aged 65-79 and aims to establish metformin as a potential treatment for aging itself[307]. The broad range of these potential therapeutic effects has sparked discussions on whether metformin could be universally recommended as a preventive therapy.

Despite its multifaceted benefits, metformin remains somewhat unusual in modern pharmacotherapy. Unlike most drugs that interact with specific receptors or enzymes to exert their effects, metformin influences a broad range of cellular processes, many of which are not yet fully elucidated[127]. Its mechanisms of action are complex and appear to involve multiple pathways, such as altering mitochondrial activity, regulating cellular energy balance, and modulating the gut microbiome, all of which

contribute to its diverse physiological effects[115,238,308–310]. A reductionist approach, dissecting these various mechanisms and targeting them individually, could offer a more precise therapeutic strategy. For example, delineating how metformin specifically modulates glucose metabolism, suppresses appetite, reduces inflammation, and potentially extends lifespan could enable the development of targeted treatments for these individual components. In this thesis, our application of untargeted metabolomics has provided novel insights into the metabolic changes induced by metformin, suggesting a potential bridge to such a reductionist approach.

Metabolomics, by capturing a broad spectrum of metabolites, could significantly expand our understanding of metformin's mechanisms of action. It provides a comprehensive overview of the biochemical changes that occur in response to the drug, offering the potential to uncover biomarkers for its effects and perhaps even to identify new targets for therapeutic intervention. For instance, our findings indicate that metformin drives significant increases in two distinct classes of signaling molecules: N-lactoyl amino acids, including the appetite-suppressing N-lactoyl phenylalanine (Lac-Phe) (Figures & Tables Chapter 3), and β-hydroxy fatty acids (Figures & Tables Chapter 5). This highlights the utility of metabolomics of discovering novel metabolites that could serve as direct effectors of action or biomarkers of therapeutic efficacy of metformin. Furthermore, this approach could be extended to uncover additional, previously unidentified metabolites within the human metabolome. Despite significant advances in metabolomics, the full spectrum of human metabolites remains incompletely mapped[311,312]. The discovery

of novel metabolites could pave the way for a deeper understanding of metabolic regulation and drug action, providing new avenues for therapeutic development.

While metformin's pleiotropic effects pose challenges, we will provide two examples of how a reductionist approach—focusing on its impact on metabolites—can enhance our understanding of its biological mechanisms and overall effects.

Metformin: Targeted mitochondrial disease?

In a recent study of MELAS, a mitochondrial disease, interesting parallels emerged between our results on metformin's effects and the blood metabolomics of MELAS patients, suggesting that metformin may phenocopy aspects of mitochondrial disease[133]. MELAS—Mitochondrial Encephalomyopathy, Lactic Acidosis, and Stroke-like episodes—is most frequently caused by the heteroplasmic m.3243A>G mutation in the MT-TL1 gene, which encodes mitochondrial leucyl-tRNA[313]. This mutation accounts for nearly 80% of MELAS cases and presents with a range of symptoms, including lactic acidosis, stroke-like episodes, and multisystem dysfunction[313,314]. MELAS can lead to the disruption of Complex I in the electron transport chain, which provides a rationale for an increased NADH/NAD+ ratio due to defective oxidation of NADH to NAD+[315,316]. Interestingly, mutations in mitochondrial DNA—the typical cause of MELAS—do not affect the primary enzymes involved in FADH2 oxidation, which are nuclear-encoded, including Complex II, ETF (Electron Transfer Flavoprotein), and ETFDH[317]. This could allow

for an alternative pathway to sustain electron transport chain activity by utilizing $FADH_2$ oxidation, thereby bypassing the Complex I defect.

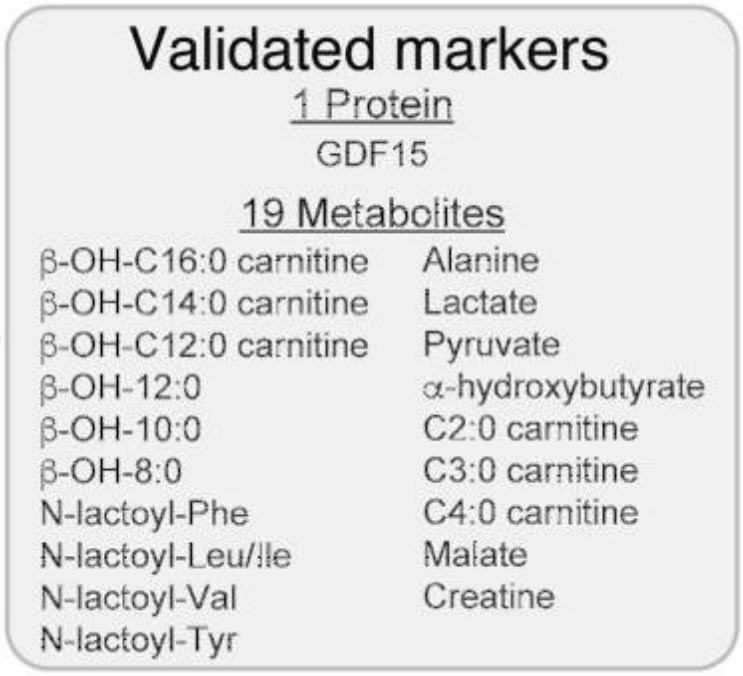

Figure 6.1: MELAS and Metformin Blood Biomarkers Overlap

This figure summarizes biomarkers for MELAS (Mitochondrial Encephalomyopathy, Lactic Acidosis, and Stroke-like episodes). The original study involved two cohorts. The discovery cohort included 134 individuals: 20 with the m.3243A>G mutation and stroke-like episodes (MELAS), 82 with the m.3243A>G mutation without stroke-like events (non-MELAS), and 32 healthy controls. The validation cohort consisted of 7 MELAS patients and 16 controls, resulting in the validation of 20 MELAS biomarkers. The final set of 20 validated biomarkers includes one protein (GDF15) and 19 metabolites, encompassing N-lactoyl amino acids, β-hydroxy fatty acids, carnitines, and others known to be associated with NADH-reductive stress. The study reveals biomarkers closely linked to mitochondrial dysfunction and parallels with metformin treatment effects, notably in increased N-lactoyl amino acids, β-hydroxy fatty acids, and serum malate.

Source: Adapted from Sharma et al., 2021[133]

The MELAS study identified 20 validated biomarkers associated with the disease, many of which were linked to NADH-reductive stress[133]. Notably, this included

elevated N-lactoyl amino acids and β-hydroxy fatty acids, which mirror our findings related to metformin (Figures and Tables Chapters 3 & 5). Additionally, the study observed increased levels of markers such as GDF15 and serum malate, both of which have been reported to increase with metformin treatment[86,87,318]. Lactate was also elevated in MELAS, and similarly, lactate levels have been shown to increase in T2D cohorts with metformin use, though the effect tends to be modest and not universal[106]. A comprehensive study would be useful to investigate all MELAS biomarkers to determine which might also serve as biomarkers for metformin treatment. The fact that the blood metabolomic profile of metformin treatment closely phenocopies that of MELAS is likely due to NADH-reductive stress[133]. This supports the idea that Complex I inhibition by metformin, even at physiological doses, plays a significant role in driving its metabolic effects.

Metabolomics of MELAS and Metformin: Similarities and Differences

While there are significant overlaps between the metabolites elevated in MELAS and those influenced by metformin treatment, important distinctions exist. For example, although N-lactoyl amino acids are increased in both conditions, lactate is markedly elevated in MELAS but only modestly increased with metformin[106]. This discrepancy may be attributed to a phenomenon we might call “targeted mitochondrial dysfunction” potentially occurring primarily in the intestines in response to metformin, allowing the rest of the body to effectively buffer and rapidly clear excess lactate. Lactate is known for its high turnover rate and ability to inhibit lipolysis during

exercise, likely serving as a strategy to prioritize its utilization as an oxidative fuel[139,319]. Conversely, there appears to be no equally robust mechanism for clearing excess Lac-Phe produced in response to metformin, resulting in its sustained higher levels in the bloodstream (Figure and Tables Chapter 3). Allowing a greater dynamic range may also enable Lac-Phe to function as a more effective signaling molecule.

Expanding this comparison to β-hydroxy fatty acids, a similar pattern of divergence emerges. While β-hydroxy fatty acids are elevated in both MELAS and metformin treatment, the specific patterns differ. In MELAS, medium- and long-chain β-hydroxy fatty acids show significant increases[133], whereas in metformin-treated subjects, only medium-chain β-hydroxy fatty acids—specifically chain lengths 8 and 10—demonstrate high fold increases (Tables 5.2, 5.5 and 5.8). The MELAS study did not appear to examine dicarboxylic fatty acids, leaving open questions about their potential involvement[133]. Moreover, β-hydroxy carnitines were elevated in MELAS but showed no strong relationship with metformin treatment in our datasets. We propose two mechanisms that could account for the observed differences:

1. **Metformin and MELAS drive subtly different processes:** Different species of β-hydroxy fatty acids, such as those with varying chain lengths, are synthesized at different rates in metformin treatment compared to MELAS.
2. **Metformin and MELAS drive the same processes. However the body can better cope with targeted mitochondrial disease:** The body's ability to clear specific subsets of β-hydroxy metabolites from the blood may vary significantly between the two conditions**.**

Tissue-Specific Variability in β-Hydroxy Fatty Acid Production?

Complex I inhibition is most pronounced in the intestines with metformin treatment, whereas MELAS likely manifests a more widespread effect on mitochondrial Complex I function across various tissues[95,320,321]. Elevated β-hydroxy carnitine levels in mitochondrial diseases affecting muscle are correlated with the muscle mutation load, indicating a potential link between these metabolites and the extent of mtDNA mutations in muscle tissue[322]. This suggests that muscle tissue may be the primary source of these metabolites in MELAS. This could explain why β-hydroxy carnitines are consistently elevated in MELAS but do not seem to be elevated with metformin treatment (Tables 5.4 and 5.7).

Two hypotheses could account for the lack of a significant metformin-driven increase in β-hydroxy carnitines:

1. **Excess Production and Clearance:** In response to metformin treatment the intestines produce excess β-hydroxy carnitines, which are subsequently cleared by other tissues—possibly muscle—in which metformin concentrations are not high enough to inhibit Complex I, allowing these tissues to utilize the metabolites as an oxidative fuel source.

2. **Stable Levels and Flux:** The absolute levels and flux of β-hydroxy carnitines remain unchanged with metformin treatment, potentially because the tissues that produce excess β-hydroxy carnitines in MELAS, such as muscle, do not experience sufficiently high metformin concentrations to inhibit Complex I.

To test these hypotheses, we could administer metformin via oral gavage in mice and assess β-hydroxy carnitine levels in blood samples from the portal vein, comparing them to systemic circulation. Additionally, this analysis could be extended to assess blood samples across muscle tissue, looking at arterio-venous differences. If β-hydroxy carnitine concentrations increase in the portal vein relative to systemic circulation after metformin administration, it would support the first hypothesis, indicating intestinal production and clearance by other tissues.If no change is observed, the second hypothesis is more likely, indicating that excess β-hydroxy carnitine production is not primarily driven by the intestines.

Mitochondrial β-Oxidation: A Cell-Specific Response to Metformin vs. MELAS?

A potential differential effect of metformin treatment and MELAS on medium-chain versus longer-chain fatty acids could be explained by variations in metabolite production at the cellular level.

β-oxidation of MCFAs and LCFAs involves distinct enzymes, which may respond differently to treatment with metformin[24]. The β-oxidation metabolism of LCFAs

involves very-long-chain acyl-CoA dehydrogenase (VLCAD) and the mitochondrial trifunctional protein (MTP), a multi-enzyme complex embedded in the inner mitochondrial membrane that facilitates the hydration, dehydrogenation, and thiolysis of LCFAs. All of these enzymes are embedded in the inner mitochondrial membrane[24]. MTP needs NAD+ to catalyze the reaction of β-hydroxyacyl-CoA to β-ketoacyl-CoA. By contrast MCFAs are likely metabolized by enzymes primarily located in the mitochondrial matrix, such as medium-chain acyl-CoA dehydrogenase (MCAD), crotonase, and β-ketothiolase[24]. However, there is a suggestion that MTP can catalyze the dehydrogenation of L-β-hydroxyacyl-CoA during MCFA oxidation[25]. Metformin inhibits Complex I of the electron transport chain, leading to NADH accumulation and a lower NAD+/NADH ratio[323]. Specifically Complex I is the enzyme complex of the electron transport chain that regenerates NAD+ from NADH. Complex I - like the enzymes involved in long chain fatty acid beta-oxidation - is embedded in the mitochondrial membrane. MCFA metabolism could be more vulnerable to disruption by metformin. Given that metformin's inhibition of Complex I is relatively mild and reversible, the residual activity may still generate enough NAD+ to support the activity of the matrix bound enzyme MTP in close proximity to Complex I[73]. In contrast, MELAS may result in a more profound deficiency of Complex I activity in certain tissues. Consequently, the selective availability of NAD+ might enable the continued processing of LCFAs by MTP, while MCFA metabolism becomes more disrupted due to their reliance on matrix-localized enzymes that are more sensitive to changes in the NAD+/NADH ratio and further from the site of production. This hypothesis suggests that the differential impact of metformin on β-

hydroxy fatty acids could be attributed to the distinct mitochondrial localization of the enzymes responsible for MCFA and LCFA β-oxidation.

Fatty acid transport into mitochondria

Another crucial difference between long-chain and medium-chain fatty acid oxidation lies in the transport mechanisms for their entry into the mitochondrial matrix. Saturated medium-chain fatty acids (MCFAs) with a chain length of up to at least eight carbons, such as octanoic acid (C8), can freely diffuse across the mitochondrial membranes in their non esterified form[18–20]. In contrast, long-chain fatty acids (LCFAs) require the carnitine shuttle system to cross the mitochondrial membrane and undergo β-oxidation. The carnitine shuttle, mediated by carnitine palmitoyltransferase 1 (CPT1) and carnitine palmitoyltransferase 2 (CPT2), is essential for the transport of LCFAs into the mitochondrial matrix, where β-oxidation occurs[17].

In the context of metformin treatment, this distinction in transport mechanisms may play a significant role. Given the easier diffusion of MCFAs, it is conceivable that these fatty acids could preferentially accumulate in the mitochondrial matrix under metformin treatment, independent of the carnitine shuttle. This differential transport could result in altered processing and accumulation patterns, with medium-chain β-hydroxy fatty acids accumulating due to the simpler diffusion of MCFAs, while long-

chain β-hydroxy fatty acids, which depend on the carnitine shuttle for LCFA transport, may be affected differently.

Proposed Cell Line Experiments to Investigate the Differential Impact of Metformin on Fatty Acid Metabolism

We could use cell lines to test competing hypotheses. HT-29 are an example of intestinal cell lines that could be used[324]. These experiments aim to determine whether the observed differences in β-hydroxy fatty acid accumulation of various chain lengths between metformin treatment and MELAS are due to differences in cellular production. To model the mitochondrial dysfunction seen in MELAS, HT-29 cells could be treated with rotenone, a known Complex I inhibitor that has been shown to increase β-hydroxy fatty acid production[325]. The doses should be calibrated so that both drugs have similar impacts on cellular respiration for a direct comparison. If medium-chain and long-chain β-hydroxy fatty acids accumulate at similar rates under both metformin and rotenone treatment, this would indicate that the differing patterns observed between MELAS and metformin are less likely to be attributed to a specific cellular phenotype. Conversely, if the accumulation rates differ, further investigation would be warranted to elucidate the underlying mechanisms.

To test the source of medium-chain β-hydroxy fatty acids, we could use isotope tracing experiments. Cells can be supplemented with labeled long-chain (e.g., ^{13}C-palmitic acid) and compare this to supplementation with medium-chain fatty acids (e.g., ^{13}C-octanoic acid) to trace their incorporation into β-hydroxy fatty acids. If labeled β-hydroxy medium-chain fatty acids are predominantly derived from medium-chain precursors, this would indicate that metformin does not impair the transport of medium-chain fatty acids into the mitochondria. Conversely, if the medium-chain β-hydroxy fatty acids are primarily derived from long-chain precursors, it would suggest that long-chain fatty acids are transported into the mitochondria and undergo initial rounds of β-oxidation, but that β-oxidation is selectively impaired for medium-chain fatty acids.

In summary, these experiments would aim to establish if the observed differential effects of metformin treatment on medium-chain versus long-chain β-hydroxy fatty acids could be driven by differences in transport mechanisms or differences in their oxidation via β-oxidation.

Hypothesis: Preferential Oxidation of Long Chain β-Hydroxy Fatty Acids

Another possible explanation for the differential regulation of medium chain β-hydroxy fatty acids, long chain β-hydroxy fatty acids and β-hydroxy carnitines involves the hypothesis of a metabolite shuttle mechanism. In this model, fatty acids are partially oxidised to β-hydroxy fatty acids in tissues with high metformin concentrations, such as the intestines, and then exported to other tissues for further

oxidation. This partial oxidation would generate FADH2,in the first step of β-oxidation, feeding into the electron transport chain. However, in the absence of sufficient NAD+, the process may stall at the third step of β-oxidation, leading to the export of β-hydroxy intermediates.

Long-chain β-hydroxy fatty acids, such as β-OH-C16:0, have been reported to be toxic. Acute fatty liver of pregnancy (AFLP), which can be caused by long-chain 3-hydroxy-acyl-CoA dehydrogenase (LCHAD) deficiency in the **fetus**, leads to the accumulation of long chain β-hydroxy fatty acids in the **maternal** circulation[326]. This buildup of long-chain β-hydroxy fatty acids is proposed to be a causal factor in the often fatal liver injury observed in the **mother**[327]. Additionally, long-chain β-hydroxy fatty acids have been shown to be cytotoxic to muscle mitochondria, potentially contributing to the muscle condition rhabdomyolysis in patients with long-chain LCHAD deficiencies[328]. This provides a rationale for why the body would preferentially uptake and oxidize these longer chain intermediates rapidly to avoid toxicity. Perhaps longer chain β-hydroxy fatty acids could be preferentially oxidized. This mechanism aligns with the observation that medium-chain β-hydroxy fatty acids naturally have higher concentrations in serum compared to their long-chain counterparts[329]. Additionally, medium-chain β-hydroxy fatty acids are known to function as signaling molecules, which might suggest a role as longer-lived metabolites for signaling purposes[285,294]. To test this hypothesis, an experiment could be conducted to measure the decay rates of isotope-labeled β-hydroxy fatty acids of different chain lengths. If the longer chain β-hydroxy fatty acids are cleared

more rapidly, it would indicate a preferential oxidation pathway, consistent with their higher toxicity and the body's need to eliminate them swiftly. This would further support the idea that medium-chain β-hydroxy fatty acids are more stable and potentially serve a signaling function in the body. This would suggest that the body could cope with “targeted mitochondrial disease” induced by metformin and clear toxic molecules. But the body might get overwhelmed by systematic mitochondrial disease like MELAS.

In conclusion, we began with the observation that metformin largely phenocopies the blood metabolomics profile of MELAS. We propose a reductionist approach to dissect this phenomenon and gain a deeper understanding of the molecular effects of metformin.

Metformin: Providing Insight into How Metabolites Influence Appetite

The findings of this thesis significantly advance our understanding of metformin's role in appetite suppression and weight loss. While metformin is widely used to treat type 2 diabetes and is known to cause modest weight loss, it has not been approved as an anti-obesity drug due to its limited efficacy in this area[304]. However, a reductionist approach to further understanding its molecular mechanisms could aid in the development of targeted therapies for obesity. Obesity is a growing public health crisis, and understanding the mechanisms that regulate appetite at the molecular level is a critical step toward combating this issue.

The present work, along with findings from the Long group, shows that Lac-Phe, contributes to the appetite suppressing effect of metformin in both mice and potentially in humans[230,236]. We have also speculated the increases in medium chain β-hydroxy fatty acids may influence appetite through receptor signaling, specifically via HCA3 and GPR84. It is also possible that the increase in β-hydroxy fatty acids highlight pathways through which metformin treatment leads to wasted energy expenditure. Each time fatty acids undergo β-oxidation, they need to be activated by being converted into acyl-CoA derivatives, a process that consumes two ATP molecules[21]. If this activation happens multiple times—such as through the shuttling of β-hydroxy intermediates between cells or tissues—it becomes energetically costly, leading to inefficient fat utilization. Additionally, evidence suggests that dicarboxylic β-hydroxy fatty acid derivatives, such as β-OH-DC-C10:0, are excreted in the urine, providing a route for carbon loss through excessive excretion[176,177]. This may further contribute to energy loss and help explain some of metformin's metabolic effects.

Further research is needed to understand how metformin-induced metabolites might interact with the body's satiety signals. Metformin's effects on appetite and satiety likely involve complex interactions between gut-derived signaling molecules and brain centers that regulate hunger. Satiety, the feeling of fullness that stops eating, and appetite, the desire to eat, are influenced by a variety of signaling molecules produced by enteroendocrine cells in the gut, including ghrelin, PYY, CCK, and GLP-1[330]. These molecules communicate with two major regions of the brain: the hypothalamus and the brainstem[330]. The arcuate nucleus (ARC) of the

hypothalamus integrates hunger signals and contains both orexigenic neurons, which promote appetite, and anorexigenic neurons, which promote satiety[331]. The gut communicates with the brainstem via neural signaling through the vagus nerve, which relays signals to the hypothalamus to regulate food intake[332].

One hypothesis we propose is that enteroendocrine cells in the intestine may "taste" metformin-boosted metabolites like Lac-Phe and β-hydroxy fatty acids, which are likely present in high concentrations in the intestines following metformin treatment. Lac-Phe has been shown to possess taste-like properties and enhance kokumi sensations, with molecular docking studies suggesting it activates specific taste receptors[150,151]. Similarly, medium-chain β-hydroxy fatty acids are known to bind to receptors in the gut[299]. This interaction could trigger neural signaling to the brainstem via the vagus nerve, contributing to satiety. In Metabolon datasets, both N-lactoyl amino acids and medium-chain β-hydroxy fatty acids have been detected in cerebrospinal fluid, suggesting that metformin-derived metabolites may also function as long-lasting humoral signals, influencing satiety by signaling through the hypothalamus[333].

A recent preprint (September 2024) demonstrated that pharmacological administration of Lac-Phe to mice led to neuronal activation in both the hypothalamus and brainstem, offering valuable insights into how Lac-Phe may influence appetite regulation[334]. However, the precise signaling mechanism remains unclear. Medium-chain β-hydroxy fatty acids signal through GPCRs, and it has been suggested that Lac-Phe may also act via GPCR signaling[152,285,294]. It will be important to explore whether Lac-Phe receptors are located in the intestines,

signaling through the vagus nerve, or directly within the hypothalamus, as this could clarify the pathways involved in its appetite regulation.

In summary, this thesis has revealed novel insights into metformin's effects on metabolic regulation, particularly via gut-derived metabolites like N-lactoyl amino acids and β-hydroxy fatty acids. A reductionist approach to further study these pathways could help uncover specific mechanisms that can be directly targeted with dedicated anti-obesity treatments.

Chapter 7 - Bibliography

1. Berg, J. M. *et al. Biochemistry*. (Macmillan Learning, Austin Boston New York Plymouth, 2023).
2. Levin, R. Digestion and absorption of carbohydrates”” from molecules and membranes to humans. *Am. J. Clin. Nutr.* **59**, 690S-698S (1994).
3. Bar-Even, A., Flamholz, A., Noor, E. & Milo, R. Rethinking glycolysis: on the biochemical logic of metabolic pathways. *Nat. Chem. Biol.* **8**, 509–517 (2012).
4. Liu, S. *et al.* Insights into Mechanism of Glucokinase Activation: OBSERVATION OF MULTIPLE DISTINCT PROTEIN CONFORMATIONS. *J. Biol. Chem.* **287**, 13598–13610 (2012).
5. Lee, Y.-H., Li, Y., Uyeda, K. & Hasemann, C. A. Tissue-specific Structure/Function Differentiation of the Liver Isoform of 6-Phosphofructo-2-kinase/Fructose-2,6-bisphosphatase*. *J. Biol. Chem.* **278**, 523–530 (2003).
6. Chandel, N. S. Glycolysis. *Cold Spring Harb. Perspect. Biol.* **13**, a040535 (2021).
7. Moussaieff, A. *et al.* Glycolysis-Mediated Changes in Acetyl-CoA and Histone Acetylation Control the Early Differentiation of Embryonic Stem Cells. *Cell Metab.* **21**, 392–402 (2015).
8. Krebs, H. A. The History of the Tricarboxylic Acid Cycle. *Perspect. Biol. Med.* **14**, 154–172 (1970).
9. Mitchell, P. Keilin’s Respiratory Chain Concept and Its Chemiosmotic Consequences. *Science* **206**, 1148–1159 (1979).
10. Lunt, S. Y. & Heiden, M. G. V. Aerobic Glycolysis: Meeting the Metabolic

Requirements of Cell Proliferation. *Annu. Rev. Cell Dev. Biol.* **27**, 441–464 (2011).

11. Cheetham, M. E., Boobis, L. H., Brooks, S. & Williams, C. Human muscle metabolism during sprint running. *J. Appl. Physiol.* **61**, 54–60 (1986).

12. Luengo, A. *et al.* Increased demand for NAD+ relative to ATP drives aerobic glycolysis. *Mol. Cell* **81**, 691-707.e6 (2021).

13. McArdle, W. D., Katch, F. I. & Katch, V. L. *Exercise Physiology: Nutrition, Energy, and Human Performance*. (Wolters Kluwer Health, Philadelphia Baltimore New York London Buenos Aires Hong Kong Sydney Tokyo, 2015).

14. Ding, L. *et al.* Peroxisomal β-oxidation acts as a sensor for intracellular fatty acids and regulates lipolysis. *Nat. Metab.* **3**, 1648–1661 (2021).

15. Rao, M. S. & Reddy, J. K. Peroxisomal β-Oxidation and Steatohepatitis. *Semin. Liver Dis.* **21**, 43–56 (2001).

16. Rinaldo, P., Matern, D. & Bennett, M. J. Fatty Acid Oxidation Disorders. *Annu. Rev. Physiol.* **64**, 477–502 (2002).

17. McGarry, J. D. & Brown, N. F. The Mitochondrial Carnitine Palmitoyltransferase System — From Concept to Molecular Analysis. *Eur. J. Biochem.* **244**, 1–14 (1997).

18. Bonnefont, J.-P. *et al.* Carnitine palmitoyltransferases 1 and 2: biochemical, molecular and medical aspects. *Mol. Aspects Med.* **25**, 495–520 (2004).

19. Chase, J. F. A. The substrate specificity of carnitine acetyltransferase. *Biochem. J.* **104**, 510 (1967).

20. Short- and medium-chain fatty acids in energy metabolism: the cellular

perspective - Journal of Lipid Research. https://www.jlr.org/article/S0022-2275(20)35173-7/fulltext.

21. Schulz, H. Beta oxidation of fatty acids. *Biochim. Biophys. Acta BBA - Lipids Lipid Metab.* **1081**, 109–120 (1991).

22. Houten, S. M., Violante, S., Ventura, F. V. & Wanders, R. J. A. The Biochemistry and Physiology of Mitochondrial Fatty Acid β-Oxidation and Its Genetic Disorders. *Annu. Rev. Physiol.* **78**, 23–44 (2016).

23. Xia, C., Fu, Z., Battaile, K. P. & Kim, J.-J. P. Crystal structure of human mitochondrial trifunctional protein, a fatty acid β-oxidation metabolon. *Proc. Natl. Acad. Sci.* **116**, 6069–6074 (2019).

24. Ranea-Robles, P. & Houten, S. M. The biochemistry and physiology of long-chain dicarboxylic acid metabolism. *Biochem. J.* **480**, 607–627 (2023).

25. Adeva-Andany, M. M., Carneiro-Freire, N., Seco-Filgueira, M., Fernández-Fernández, C. & Mouriño-Bayolo, D. Mitochondrial β-oxidation of saturated fatty acids in humans. *Mitochondrion* **46**, 73–90 (2019).

26. Wakabayashi, K. & Shimazono, N. Studies *in vitro* on the mechanism of ω-oxidation of fatty acids. *Biochim. Biophys. Acta* **48**, 615–617 (1961).

27. Robbins: Enzymatic omega oxidation of fatty acids - Google Scholar. https://scholar.google.com/scholar_lookup?journal=Fed.+Proc&title=Enzymatic+omega+oxidation+of+fatty+acids&author=KC+Robbins&volume=20&issue=272&publication_year=1961&.

28. Robbins, K. C. *In vitro* enzymic omega oxidation of medium-chain fatty acids in mammalian tissue. *Arch. Biochem. Biophys.* **123**, 531–538 (1968).

29. Pettersen, J. E. Formation of *n*-hexanedioic acid from hexadecanoic acid by an initial ω oxidation in ketotic rats. *Clin. Chim. Acta* **41**, 231–237 (1972).

30. Passi, S., Nazzaro-Porro, M., Picardo, M., Mingrone, G. & Fasella, P. Metabolism of straight saturated medium chain length (C9 to C12) dicarboxylic acids. *J. Lipid Res.* **24**, 1140–1147 (1983).

31. Wada, F. & Usami, M. Studies on fatty acid ω-oxidation antiketogenic effect and gluconeogenicity of dicarboxylic acids. *Biochim. Biophys. Acta BBA - Lipids Lipid Metab.* **487**, 261–268 (1977).

32. Martínez-Reyes, I. & Chandel, N. S. Mitochondrial TCA cycle metabolites control physiology and disease. *Nat. Commun.* **11**, 102 (2020).

33. Lambeth, D. O., Tews, K. N., Adkins, S., Frohlich, D. & Milavetz, B. I. Expression of Two Succinyl-CoA Synthetases with Different Nucleotide Specificities in Mammalian Tissues *. *J. Biol. Chem.* **279**, 36621–36624 (2004).

34. Hosler, J. P., Ferguson-Miller, S. & Mills, D. A. Energy Transduction: Proton Transfer Through the Respiratory Complexes. *Annu. Rev. Biochem.* **75**, 165–187 (2006).

35. Wittig, I. & Schägger, H. Supramolecular organization of ATP synthase and respiratory chain in mitochondrial membranes. *Biochim. Biophys. Acta BBA - Bioenerg.* **1787**, 672–680 (2009).

36. Mráček, T., Drahota, Z. & Houštěk, J. The function and the role of the mitochondrial glycerol-3-phosphate dehydrogenase in mammalian tissues. *Biochim. Biophys. Acta BBA - Bioenerg.* **1827**, 401–410 (2013).

37. Gnaiger, E. Complex II ambiguities—FADH2 in the electron transfer system.

J. Biol. Chem. **300**, 105470 (2024).

38. Goetzman, E. S. Modeling Disorders of Fatty Acid Metabolism in the Mouse. in *Progress in Molecular Biology and Translational Science* vol. 100 389–417 (Elsevier, 2011).

39. Schultz, B. E. & Chan, S. I. Structures and Proton-Pumping Strategies of Mitochondrial Respiratory Enzymes. *Annu. Rev. Biophys.* **30**, 23–65 (2001).

40. Henriques, B. J., Katrine Jentoft Olsen, R., Gomes, C. M. & Bross, P. Electron transfer flavoprotein and its role in mitochondrial energy metabolism in health and disease. *Gene* **776**, 145407 (2021).

41. White, R. A., Dowler, L. L., Angeloni, S. V. & Koeller, D. M. Assignment of*Etfdh, Etfb,*and*Etfa*to Chromosomes 3, 7, and 13: The Mouse Homologs of Genes Responsible for Glutaric Acidemia Type II in Human. *Genomics* **33**, 131–134 (1996).

42. El-Hattab, A. W., Adesina, A. M., Jones, J. & Scaglia, F. MELAS syndrome: Clinical manifestations, pathogenesis, and treatment options. *Mol. Genet. Metab.* **116**, 4–12 (2015).

43. Ahmad, E., Lim, S., Lamptey, R., Webb, D. R. & Davies, M. J. Type 2 diabetes. *The Lancet* **400**, 1803–1820 (2022).

44. Field, A. E. *et al.* Impact of Overweight on the Risk of Developing Common Chronic Diseases During a 10-Year Period. *Arch. Intern. Med.* **161**, 1581–1586 (2001).

45. Golay, A. & Ybarra, J. Link between obesity and type 2 diabetes. *Best Pract. Res. Clin. Endocrinol. Metab.* **19**, 649–663 (2005).

46. Sarma, S., Sockalingam, S. & Dash, S. Obesity as a multisystem disease: Trends in obesity rates and obesity-related complications. *Diabetes Obes. Metab.* **23**, 3–16 (2021).

47. Prior, I. A. & Davidson, F. The epidemiology of diabetes in Polynesians and Europeans in New Zealand and the Pacific. *N. Z. Med. J.* **65**, 375–383 (1966).

48. Boulton, A. J. Guidelines for diagnosis and outpatient management of diabetic peripheral neuropathy. European Association for the Study of Diabetes, Neurodiab. *Diabetes Metab.* **24 Suppl 3**, 55–65 (1998).

49. Laakso, M. Cardiovascular disease in type 2 diabetes: challenge for treatment and prevention. *J. Intern. Med.* **249**, 225–235 (2001).

50. Ruta, L. M. *et al.* Prevalence of diabetic retinopathy in Type 2 diabetes in developing and developed countries. *Diabet. Med.* **30**, 387–398 (2013).

51. Seuring, T., Archangelidi, O. & Suhrcke, M. The Economic Costs of Type 2 Diabetes: A Global Systematic Review. *PharmacoEconomics* **33**, 811–831 (2015).

52. Mahrouseh, N. *et al.* How the European Union legislations are tackling the burden of diabetes mellitus: A legal surveillance study. *Front. Public Health* **10**, 1002265 (2022).

53. Mehnert, H. Metformin, the rebirth of a biguanide: mechanism of action and place in the prevention and treatment of insulin resistance. *Exp. Clin. Endocrinol. Diabetes* **109**, S259–S264 (2001).

54. The vegetable system [...] Vol. XXI. https://bibdigital.rjb.csic.es/en/records/item/14480-the-vegetable-system-vol-

xxi?offset=1.

55. Untersuchungen über die chemischen Beziehungen zwischen Guanin, Xanthin, Theobromin, Caffeïn und Kreatinin - Strecker - 1861 - Justus Liebigs Annalen der Chemie - Wiley Online Library. https://chemistry-europe.onlinelibrary.wiley.com/doi/abs/10.1002/jlac.18611180203.

56. Watanabe, C. K. STUDIES IN THE METABOLISM CHANGES INDUCED BY ADMINISTRATION OF GUANIDINE BASES: I. INFLUENCE OF INJECTED GUANIDINE HYDROCHLORIDE UPON BLOOD SUGAR CONTENT. *J. Biol. Chem.* **33**, 253–265 (1918).

57. Werner, E. A. & Bell, J. CCXIV.—The preparation of methylguanidine, and of ββ-dimethylguanidine by the interaction of dicyanodiamide, and methylammonium and dimethylammonium chlorides respectively. *J. Chem. Soc. Trans.* **121**, 1790–1794 (1922).

58. Slotta, K. H. & Tschesche, R. Über Biguanide, II.: Die blutzucker-senkende Wirkung der Biguanide. *Berichte Dtsch. Chem. Ges. B Ser.* **62**, 1398–1405 (1929).

59. Hesse, E. & Taubmann, G. Die Wirkung des Biguanids und seiner Derivate auf den Zuckerstoffwechsel. *Naunyn-Schmiedebergs Arch. Für Exp. Pathol. Pharmakol.* **142**, 290–308 (1929).

60. Sterne, J. Du nouveau dans les antidiabétiques. La NN diméthylamino guanyl guanidine (NNDG). *Maroc Méd.* **36**, 1295–1296 (1957).

61. Lactic acidosis in biguanide-treated diabetics | Diabetologia. https://link.springer.com/article/10.1007/BF01263444.

62. DeFronzo, R., Fleming, G. A., Chen, K. & Bicsak, T. A. Metformin-associated lactic acidosis: Current perspectives on causes and risk. *Metabolism* **65**, 20–29 (2016).

63. Clinical and biochemical aspects of lactic acidosis. https://febs.onlinelibrary.wiley.com/doi/epdf/10.1016/0014-5793%2876%2980789-2.

64. Schäfer, G. Biguanides. A review of history, pharmacodynamics and therapy. *Diabete Metab.* **9**, 148–163 (1983).

65. Bailey, C. J. Metformin: historical overview. *Diabetologia* **60**, 1566–1576 (2017).

66. Effect of intensive blood-glucose control with metformin on complications in overweight patients with type 2 diabetes (UKPDS 34). *The Lancet* **352**, 854–865 (1998).

67. Bodmer, M., Meier, C., Krähenbühl, S., Jick, S. S. & Meier, C. R. Metformin, Sulfonylureas, or Other Antidiabetes Drugs and the Risk of Lactic Acidosis or Hypoglycemia: A nested case-control analysis. *Diabetes Care* **31**, 2086–2091 (2008).

68. Maruthur, N. M. *et al.* Diabetes Medications as Monotherapy or Metformin-Based Combination Therapy for Type 2 Diabetes. *Ann. Intern. Med.* **164**, 740–751 (2016).

69. Clarke, B. F. & Duncan, L. J. P. COMPARISON OF CHLORPROPAMIDE AND METFORMIN TREATMENT ON WEIGHT AND BLOOD-GLUCOSE RESPONSE OF UNCONTROLLED OBESE DIABETICS. *The Lancet* **291**, 123–

126 (1968).

70. The Diabetes Prevention Program Research Group. Long-Term Safety, Tolerability, and Weight Loss Associated With Metformin in the Diabetes Prevention Program Outcomes Study. *Diabetes Care* **35**, 731–737 (2012).

71. Yerevanian, A. & Soukas, A. A. Metformin: Mechanisms in Human Obesity and Weight Loss. *Curr. Obes. Rep.* **8**, 156–164 (2019).

72. Bailey, C. J. Metformin: Therapeutic profile in the treatment of type 2 diabetes. *Diabetes Obes. Metab.* **26**, 3–19 (2024).

73. LaMoia, T. E. & Shulman, G. I. Cellular and Molecular Mechanisms of Metformin Action. *Endocr. Rev.* **42**, 77–96 (2021).

74. Hundal, R. S. *et al.* Mechanism by which metformin reduces glucose production in type 2 diabetes. *Diabetes* **49**, 2063–2069 (2000).

75. Inzucchi, S. E. *et al.* Efficacy and Metabolic Effects of Metformin and Troglitazone in Type II Diabetes Mellitus. *N. Engl. J. Med.* **338**, 867–873 (1998).

76. Perriello, G. *et al.* Acute Antihyperglycemic Mechanisms of Metformin in NIDDM: Evidence for Suppression of Lipid Oxidation and Hepatic Glucose Production. *Diabetes* **43**, 920–928 (1994).

77. Morita, Y. *et al.* Enhanced Release of Glucose Into the Intraluminal Space of the Intestine Associated With Metformin Treatment as Revealed by [18F]Fluorodeoxyglucose PET-MRI. *Diabetes Care* **43**, 1796–1802 (2020).

78. Zhou, G. *et al.* Role of AMP-activated protein kinase in mechanism of metformin action. *J. Clin. Invest.* **108**, 1167–1174 (2001).

79. Fontaine, E. Metformin-Induced Mitochondrial Complex I Inhibition: Facts,

Uncertainties, and Consequences. *Front. Endocrinol.* **9**, (2018).

80. Madiraju, A. K. *et al.* Metformin suppresses gluconeogenesis by inhibiting mitochondrial glycerophosphate dehydrogenase. *Nature* **510**, 542–546 (2014).

81. LaMoia, T. E. *et al.* Metformin, phenformin, and galegine inhibit complex IV activity and reduce glycerol-derived gluconeogenesis. *Proc. Natl. Acad. Sci.* **119**, e2122287119 (2022).

82. Ma, T. *et al.* Low-dose metformin targets the lysosomal AMPK pathway through PEN2. *Nature* **603**, 159–165 (2022).

83. Wu, H. *et al.* Metformin alters the gut microbiome of individuals with treatment-naive type 2 diabetes, contributing to the therapeutic effects of the drug. *Nat. Med.* **23**, 850–858 (2017).

84. Lee, A. & Morley, J. E. Metformin Decreases Food Consumption and Induces Weight Loss in Subjects with Obesity with Type II Non-Insulin-Dependent Diabetes. *Obes. Res.* **6**, 47–53 (1998).

85. Klein, A. B. *et al.* The GDF15-GFRAL pathway is dispensable for the effects of metformin on energy balance. *Cell Rep.* **40**, 111258 (2022).

86. Day, E. A. *et al.* Metformin-induced increases in GDF15 are important for suppressing appetite and promoting weight loss. *Nat. Metab.* **1**, 1202–1208 (2019).

87. Coll, A. P. *et al.* GDF15 mediates the effects of metformin on body weight and energy balance. *Nature* **578**, 444–448 (2020).

88. GDF15: emerging biology and therapeutic applications for obesity and cardiometabolic disease | Nature Reviews Endocrinology.

https://www.nature.com/articles/s41574-021-00529-7.

89. Zhang, S.-Y. *et al.* Metformin triggers a kidney GDF15-dependent area postrema axis to regulate food intake and body weight. *Cell Metab.* **35**, 875-886.e5 (2023).

90. Kincaid, J. W. R. *et al.* The gastrointestinal tract is a major source of the acute metformin-stimulated rise in GDF15. *Sci. Rep.* **14**, 1899 (2024).

91. Napolitano, A. *et al.* Novel Gut-Based Pharmacology of Metformin in Patients with Type 2 Diabetes Mellitus. *PLOS ONE* **9**, e100778 (2014).

92. Zubiaga, L. *et al.* Oral metformin transiently lowers post-prandial glucose response by reducing the apical expression of sodium-glucose co-transporter 1 in enterocytes. *iScience* **26**, (2023).

93. Borg, M. J. *et al.* Comparative effects of proximal and distal small intestinal administration of metformin on plasma glucose and glucagon-like peptide-1, and gastric emptying after oral glucose, in type 2 diabetes. *Diabetes Obes. Metab.* **21**, 640–647 (2019).

94. Once-daily delayed-release metformin lowers plasma glucose and enhances fasting and postprandial GLP-1 and PYY: results from two randomised trials | Diabetologia. https://link.springer.com/article/10.1007/s00125-016-3992-6.

95. Bailey, C. J., Wilcock, C. & Scarpello, J. H. B. Metformin and the intestine. *Diabetologia* **51**, 1552–1553 (2008).

96. Gormsen, L. C. *et al.* In Vivo Imaging of Human 11C-Metformin in Peripheral Organs: Dosimetry, Biodistribution, and Kinetic Analyses. *J. Nucl.*

Med. **57**, 1920–1926 (2016).

97. El-Mir, M.-Y. *et al.* Dimethylbiguanide Inhibits Cell Respiration via an Indirect Effect Targeted on the Respiratory Chain Complex I. *J. Biol. Chem.* **275**, 223–228 (2000).

98. Owen, M. R., Doran, E. & Halestrap, A. P. Evidence that metformin exerts its anti-diabetic effects through inhibition of complex 1 of the mitochondrial respiratory chain. *Biochem. J.* **348**, 607–614 (2000).

99. Pentikäinen, P. J., Neuvonen, P. J. & Penttilä, A. Pharmacokinetics of metformin after intravenous and oral administration to man. *Eur. J. Clin. Pharmacol.* **16**, 195–202 (1979).

100. Liang, X. & Giacomini, K. M. Transporters Involved in Metformin Pharmacokinetics and Treatment Response. *J. Pharm. Sci.* **106**, 2245–2250 (2017).

101. Scheen, A. J. Clinical Pharmacokinetics of Metformin. *Clin. Pharmacokinet.* **30**, 359–371 (1996).

102. Heaf, J. Metformin in Chronic Kidney Disease: Time for a Rethink. *Perit. Dial. Int.* **34**, 353–357 (2014).

103. Ito, J. *et al.* Dose-dependent accumulation of glucose in the intestinal wall and lumen induced by metformin as revealed by 18F-labelled fluorodeoxyglucose positron emission tomography-MRI. *Diabetes Obes. Metab.* **23**, 692–699 (2021).

104. Koffert, J. P. *et al.* Metformin treatment significantly enhances intestinal glucose uptake in patients with type 2 diabetes: Results from a randomized

clinical trial. *Diabetes Res. Clin. Pract.* **131**, 208–216 (2017).

105. Luengo, A. *et al.* Increased demand for NAD+ relative to ATP drives aerobic glycolysis. *Mol. Cell* **81**, 691-707.e6 (2021).

106. Huang, W., Castelino, R. L. & Peterson, G. M. Lactate Levels with Chronic Metformin Use: A Narrative Review. *Clin. Drug Investig.* **37**, 991–1007 (2017).

107. Rittig, N. *et al.* Metformin Stimulates Intestinal Glycolysis and Lactate Release: A single-Dose Study of Metformin in Patients With Intrahepatic Portosystemic Stent. *Clin. Pharmacol. Ther.* **110**, 1329–1336 (2021).

108. Tobar, N. *et al.* Metformin acts in the gut and induces gut-liver crosstalk. *Proc. Natl. Acad. Sci.* **120**, e2211933120 (2023).

109. Andrzejewski, S., Gravel, S.-P., Pollak, M. & St-Pierre, J. Metformin directly acts on mitochondria to alter cellular bioenergetics. *Cancer Metab.* **2**, 12 (2014).

110. Shin, N.-R. *et al.* An increase in the Akkermansia spp. population induced by metformin treatment improves glucose homeostasis in diet-induced obese mice. *Gut* **63**, 727–735 (2014).

111. Silamiķele, L. *et al.* Metformin Strongly Affects Gut Microbiome Composition in High-Fat Diet-Induced Type 2 Diabetes Mouse Model of Both Sexes. *Front. Endocrinol.* **12**, (2021).

112. Bhansali, S., Bhansali, A. & Dhawan, V. Metformin promotes mitophagy in mononuclear cells: a potential in vitro model for unraveling metformin's mechanism of action. *Ann. N. Y. Acad. Sci.* **1463**, 23–36 (2020).

113. Metformin Is Associated With Higher Relative Abundance of Mucin-Degrading Akkermansia muciniphila and Several Short-Chain Fatty Acid–

Producing Microbiota in the Gut | Diabetes Care | American Diabetes Association. https://diabetesjournals.org/care/article/40/1/54/37183/Metformin-Is-Associated-With-Higher-Relative.

114. Bharath, L. P. *et al.* Metformin Enhances Autophagy and Normalizes Mitochondrial Function to Alleviate Aging-Associated Inflammation. *Cell Metab.* **32**, 44-55.e6 (2020).

115. Hung, W.-W. *et al.* Gut microbiota compositions and metabolic functions in type 2 diabetes differ with glycemic durability to metformin monotherapy. *Diabetes Res. Clin. Pract.* **174**, 108731 (2021).

116. Bonnet, F. & Scheen, A. Understanding and overcoming metformin gastrointestinal intolerance. *Diabetes Obes. Metab.* **19**, 473–481 (2017).

117. Kim, H. W. Metabolomic Approaches to Investigate the Effect of Metformin: An Overview. *Int. J. Mol. Sci.* **22**, 10275 (2021).

118. Mueller, N. T. *et al.* Metformin Affects Gut Microbiome Composition and Function and Circulating Short-Chain Fatty Acids: A Randomized Trial. *Diabetes Care* **44**, 1462–1471 (2021).

119. Breier, M. *et al.* Immediate reduction of serum citrulline but no change of steroid profile after initiation of metformin in individuals with type 2 diabetes. *J. Steroid Biochem. Mol. Biol.* **174**, 114–119 (2017).

120. Xu, T. *et al.* Effects of Metformin on Metabolite Profiles and LDL Cholesterol in Patients With Type 2 Diabetes. *Diabetes Care* **38**, 1858–1867 (2015).

121. Nordlie, R. C., Foster, J. D. & Lange, A. J. REGULATION OF GLUCOSE PRODUCTION BY THE LIVER. *Annu. Rev. Nutr.* **19**, 379–406 (1999).

122. Sundelin, E., Jensen, J. B., Jakobsen, S., Gormsen, L. C. & Jessen, N. Metformin Biodistribution: A Key to Mechanisms of Action? *J. Clin. Endocrinol. Metab.* **105**, 3374–3383 (2020).

123. Gormsen, L. C. *et al.* Metformin increases endogenous glucose production in non-diabetic individuals and individuals with recent-onset type 2 diabetes. *Diabetologia* **62**, 1251–1256 (2019).

124. Madiraju, A. K. *et al.* Metformin inhibits gluconeogenesis via a redox-dependent mechanism in vivo. *Nat. Med.* **24**, 1384–1394 (2018).

125. Reczek, C. R. *et al.* Metformin targets mitochondrial complex I to lower blood glucose levels. *Sci. Adv.* **10**, eads5466 (2024).

126. Foretz, M. *et al.* Metformin inhibits hepatic gluconeogenesis in mice independently of the LKB1/AMPK pathway via a decrease in hepatic energy state. *J. Clin. Invest.* **120**, 2355–2369 (2010).

127. Foretz, M., Guigas, B. & Viollet, B. Metformin: update on mechanisms of action and repurposing potential. *Nat. Rev. Endocrinol.* **19**, 460–476 (2023).

128. Tobar, N. *et al.* Metformin acts in the gut and induces gut-liver crosstalk. *Proc. Natl. Acad. Sci.* **120**, e2211933120 (2023).

129. Rogatzki, M. J., Ferguson, B. S., Goodwin, M. L. & Gladden, L. B. Lactate is always the end product of glycolysis. *Front. Neurosci.* **9**, (2015).

130. Leija, R. G. *et al.* Enteric and systemic postprandial lactate shuttle phases and dietary carbohydrate carbon flow in humans. *Nat. Metab.* **6**, 670–677 (2024).

131. Jorfeldt, L., Juhlin-Dannfelt, A. & Karlsson, J. Lactate release in relation to

tissue lactate in human skeletal muscle during exercise. *J. Appl. Physiol.* **44**, 350–352 (1978).

132. Nolt, B. *et al.* Lactate and Immunosuppression in Sepsis. *Shock* **49**, 120 (2018).

133. Sharma, R. *et al.* Circulating markers of NADH-reductive stress correlate with mitochondrial disease severity. *J. Clin. Invest.* **131**, (2021).

134. Madaan, A. *et al.* Lactate produced during labor modulates uterine inflammation via GPR81 (HCA1). *Am. J. Obstet. Gynecol.* **216**, 60.e1-60.e17 (2017).

135. Ahmed, K. *et al.* An Autocrine Lactate Loop Mediates Insulin-Dependent Inhibition of Lipolysis through GPR81. *Cell Metab.* **11**, 311–319 (2010).

136. McCarthy, S. F., Islam, H. & Hazell, T. J. The emerging role of lactate as a mediator of exercise-induced appetite suppression. *Am. J. Physiol.-Endocrinol. Metab.* **319**, E814–E819 (2020).

137. O'Neill, L. A. J., Kishton, R. J. & Rathmell, J. A guide to immunometabolism for immunologists. *Nat. Rev. Immunol.* **16**, 553–565 (2016).

138. Stanley, W. C. *et al.* Lactate extraction during net lactate release in legs of humans during exercise. *J. Appl. Physiol.* **60**, 1116–1120 (1986).

139. Rabinowitz, J. D. & Enerbäck, S. Lactate: the ugly duckling of energy metabolism. *Nat. Metab.* **2**, 566–571 (2020).

140. Halestrap, A. P. The monocarboxylate transporter family—Structure and functional characterization. *IUBMB Life* **64**, 1–9 (2012).

141. N-lactoyl-amino acids are ubiquitous metabolites that originate from

CNDP2-mediated reverse proteolysis of lactate and amino acids | PNAS. https://www.pnas.org/doi/10.1073/pnas.1424638112.

142. Li, V. L. *et al.* An exercise-inducible metabolite that suppresses feeding and obesity. *Nature* **606**, 785–790 (2022).

143. Kim, J. T., Li, V. L., Terrell, S. M., Fischer, C. R. & Long, J. Z. Family-wide Annotation of Enzymatic Pathways by Parallel In Vivo Metabolomics. *Cell Chem. Biol.* **26**, 1623-1629.e3 (2019).

144. Moya-Garzon, M. D. *et al.* A secondary β-hydroxybutyrate metabolic pathway linked to energy balance. 2024.09.09.612087 Preprint at https://doi.org/10.1101/2024.09.09.612087 (2024).

145. Kobayashi, S. *et al.* Carnosine dipeptidase II (CNDP2) protects cells under cysteine insufficiency by hydrolyzing glutathione-related peptides. *Free Radic. Biol. Med.* **174**, 12–27 (2021).

146. Blau, N., Spronsen, F. J. van & Levy, H. L. Phenylketonuria. *The Lancet* **376**, 1417–1427 (2010).

147. Metabolites | Free Full-Text | Exercise-Induced N-Lactoylphenylalanine Predicts Adipose Tissue Loss during Endurance Training in Overweight and Obese Humans. https://www.mdpi.com/2218-1989/13/1/15.

148. SLC17A1/3 transporters mediate renal excretion of Lac-Phe in mice and humans | Nature Communications. https://www.nature.com/articles/s41467-024-51174-3.

149. Sforza, S., Cavatorta, V., Galaverna, G., Dossena, A. & Marchelli, R. Accumulation of non-proteolytic aminoacyl derivatives in Parmigiano-Reggiano

cheese during ripening. *Int. Dairy J.* **19**, 582–587 (2009).

150. Wu, J. *et al.* Preparation and Taste Characteristics of Kokumi N-Lactoyl Phenylalanine in the Presence of Phenylalanine and Lactate. *J. Agric. Food Chem.* **70**, 5396–5407 (2022).

151. Wu, J. *et al.* Discovery of N-l-Lactoyl-l-Trp as a Bitterness Masker via Structure-Based Virtual Screening and a Sensory Approach. *J. Agric. Food Chem.* **71**, 2082–2093 (2023).

152. Lund, J., Clemmensen, C. & Schwartz, T. W. Outrunning obesity with Lac-Phe? *Cell Metab.* **34**, 1085–1087 (2022).

153. Bremer, J. & Wojtczak, A. B. Factors controlling the rate of fatty acid β-oxidation in rat liver mitochondria. *Biochim. Biophys. Acta BBA - Lipids Lipid Metab.* **280**, 515–530 (1972).

154. Gander, J. *et al.* Metabolic Impairment in Coronary Artery Disease: Elevated Serum Acylcarnitines Under the Spotlights. *Front. Cardiovasc. Med.* **8**, (2021).

155. Violante, S. *et al.* Carnitine palmitoyltransferase 2: New insights on the substrate specificity and implications for acylcarnitine profiling. *Biochim. Biophys. Acta BBA - Mol. Basis Dis.* **1802**, 728–732 (2010).

156. Hull, F. E., Waugh, R. A., Malone, M., Albers-Schönberg, G. & Smith, J. Synthesis of ordinary and β-hydroxy fatty acids by heart mitochondria. *Arch. Biochem. Biophys.* **149**, 69–90 (1972).

157. Bartlett, K. & Eaton, S. Mitochondrial β-oxidation. *Eur. J. Biochem.* **271**, 462–469 (2004).

158. Lopes-Cardozo, M., Klazinga, W. & van den BERGH, S. G. Accumulation of

Carnitine Esters of β-Oxidation Intermediates during Palmitate Oxidation by Rat-Liver Mitochondria. *Eur. J. Biochem.* **83**, 629–634 (1978).

159. Jones, P. M., Tjoa, S., Fennessey, P. V., Goodman, S. I. & Bennett, M. J. Addition of Quantitative 3-Hydroxy-Octadecanoic Acid to the Stable Isotope Gas Chromatography-Mass Spectrometry Method for Measuring 3-Hydroxy Fatty Acids. *Clin. Chem.* **48**, 176–179 (2002).

160. Jones, P. M. *et al.* Improved stable isotope dilution-gas chromatography-mass spectrometry method for serum or plasma free 3-hydroxy-fatty acids and its utility for the study of disorders of mitochondrial fatty acid β-oxidation. *Clin. Chem.* **46**, 149–155 (2000).

161. Costa, C. G. *et al.* Simultaneous analysis of plasma free fatty acids and their 3-hydroxy analogs in fatty acid β-oxidation disorders. *Clin. Chem.* **44**, 463–471 (1998).

162. Jones, P. M. & Bennett, M. J. Clinical applications of 3-hydroxy fatty acid analysis by gas chromatography–mass spectrometry. *Biochim. Biophys. Acta BBA - Mol. Cell Biol. Lipids* **1811**, 657–662 (2011).

163. Costa, C. G. *et al.* Simultaneous analysis of plasma free fatty acids and their 3-hydroxy analogs in fatty acid β-oxidation disorders. *Clin. Chem.* **44**, 463–471 (1998).

164. Southwell, N. *et al.* A coordinated multiorgan metabolic response contributes to human mitochondrial myopathy. *EMBO Mol. Med.* **15**, e16951 (2023).

165. Jin, S. J., Hoppel, C. L. & Tserng, K. Y. Incomplete fatty acid oxidation. The

production and epimerization of 3-hydroxy fatty acids. *J. Biol. Chem.* **267**, 119–125 (1992).

166. Stanley, K. K. & Tubbs, P. K. The role of intermediates in mitochondrial fatty acid oxidation. *Biochem. J.* **150**, 77–88 (1975).

167. Natural biased signaling of hydroxycarboxylic acid receptor 3 and G protein-coupled receptor 84 | Cell Communication and Signaling | Full Text. https://biosignaling.biomedcentral.com/articles/10.1186/s12964-020-0516-2.

168. Offermanns, S. *et al.* International Union of Basic and Clinical Pharmacology. LXXXII: Nomenclature and Classification of Hydroxy-carboxylic Acid Receptors (GPR81, GPR109A, and GPR109B). *Pharmacol. Rev.* **63**, 269–290 (2011).

169. Deorphanization of GPR109B as a Receptor for the β-Oxidation Intermediate 3-OH-octanoic Acid and Its Role in the Regulation of Lipolysis* - Journal of Biological Chemistry. https://www.jbc.org/article/S0021-9258(18)49399-4/fulltext.

170. Hydroxy-Carboxylic Acid Receptor Actions in Metabolism: Trends in Endocrinology & Metabolism. https://www.cell.com/trends/endocrinology-metabolism/abstract/S1043-2760(16)30167-9?_returnURL=https%3A%2F%2Flinkinghub.elsevier.com%2Fretrieve%2Fpii%2FS1043276016301679%3Fshowall%3Dtrue.

171. Suzuki, M. *et al.* Medium-chain Fatty Acid-sensing Receptor, GPR84, Is a Proinflammatory Receptor. *J. Biol. Chem.* **288**, 10684–10691 (2013).

172. Peters, A. *et al.* Hydroxycarboxylic acid receptor 3 and GPR84 – Two

metabolite-sensing G protein-coupled receptors with opposing functions in innate immune cells. *Pharmacol. Res.* **176**, 106047 (2022).

173. Tawfik, D. M. *et al.* Comparison of host immune responses to LPS in human using an immune profiling panel, in vivo endotoxemia versus ex vivo stimulation. *Sci. Rep.* **10**, 9918 (2020).

174. Weil, D. *et al.* Circulating levels of 3-hydroxymyristate, a direct quantification of endotoxaemia in noninfected cirrhotic patients. *Liver Int.* **39**, 106–114 (2019).

175. Tserng, K.-Y., Jin, S.-J., Kerr, D. S. & Hoppel, C. L. Urinary 3-hydroxydicarboxylic acids in pathophysiology of metabolic disorders with dicarboxylic aciduria. *Metab. - Clin. Exp.* **40**, 676–682 (1991).

176. Tserng, K. Y. & Jin, S. J. Metabolic origin of urinary 3-hydroxydicarboxylic acids. *Biochemistry* **30**, 2508–2514 (1991).

177. Omega oxidation of 3-hydroxy fatty acids by the human CYP4F gene subfamily enzyme CYP4F11 - Journal of Lipid Research. https://www.jlr.org/article/S0022-2275(20)42420-4/fulltext.

178. Martins, E. *et al.* Short-chain 3-hydroxyacyl-CoA dehydrogenase deficiency: the clinical relevance of an early diagnosis and report of four new cases. *J. Inherit. Metab. Dis.* **34**, 835–842 (2011).

179. Li, J. V. *et al.* Roux-en-Y gastric bypass-induced bacterial perturbation contributes to altered host-bacterial co-metabolic phenotype. *Microbiome* **9**, 139 (2021).

180. Yamaga, M., Tani, H., Yamaki, A., Tatefuji, T. & Hashimoto, K. Metabolism and pharmacokinetics of medium chain fatty acids after oral administration of

royal jelly to healthy subjects. *RSC Adv.* **9**, 15392–15401 (2019).

181. 10- hydroxy decanoic acid, trans- 10- hydroxy- 2- decanoic acid, and sebacic acid: Source, metabolism, and potential health functionalities and nutraceutical applications - Liao - 2024 - Journal of Food Science - Wiley Online Library. https://ift.onlinelibrary.wiley.com/doi/full/10.1111/1750-3841.17143.

182. Liu, X. & Locasale, J. W. Metabolomics: A Primer. *Trends Biochem. Sci.* **42**, 274–284 (2017).

183. Emwas, A.-H. M. The Strengths and Weaknesses of NMR Spectroscopy and Mass Spectrometry with Particular Focus on Metabolomics Research. in *Metabonomics: Methods and Protocols* (ed. Bjerrum, J. T.) 161–193 (Springer, New York, NY, 2015). doi:10.1007/978-1-4939-2377-9_13.

184. Emwas, A.-H. *et al.* NMR Spectroscopy for Metabolomics Research. *Metabolites* **9**, 123 (2019).

185. Ren, J.-L., Zhang, A.-H., Kong, L. & Wang, X.-J. Advances in mass spectrometry-based metabolomics for investigation of metabolites. *RSC Adv.* **8**, 22335–22350 (2018).

186. Nagana Gowda, G. A. & Raftery, D. Can NMR solve some significant challenges in metabolomics? *J. Magn. Reson.* **260**, 144–160 (2015).

187. Griffiths, W. J. *et al.* Targeted Metabolomics for Biomarker Discovery. *Angew. Chem. Int. Ed.* **49**, 5426–5445 (2010).

188. Gertsman, I. & Barshop, B. A. Promises and pitfalls of untargeted metabolomics. *J. Inherit. Metab. Dis.* **41**, 355–366 (2018).

189. Holčapek, M., Jirásko, R. & Lísa, M. Recent developments in liquid

chromatography–mass spectrometry and related techniques. *J. Chromatogr. A* **1259**, 3–15 (2012).

190. Žuvela, P. *et al.* Column Characterization and Selection Systems in Reversed-Phase High-Performance Liquid Chromatography. *Chem. Rev.* **119**, 3674–3729 (2019).

191. Horvath, Csaba., Melander, Wayne. & Molnar, Imre. Liquid chromatography of ionogenic substances with nonpolar stationary phases. *Anal. Chem.* **49**, 142–154 (1977).

192. Guo, Y. & Gaiki, S. Retention and selectivity of stationary phases for hydrophilic interaction chromatography. *J. Chromatogr. A* **1218**, 5920–5938 (2011).

193. Bruins, A. P. Mechanistic aspects of electrospray ionization. *J. Chromatogr. A* **794**, 345–357 (1998).

194. Zeleny, J. Instability of Electrified Liquid Surfaces. *Phys. Rev.* **10**, 1–6 (1917).

195. Eliuk, S. & Makarov, A. Evolution of Orbitrap Mass Spectrometry Instrumentation. *Annu. Rev. Anal. Chem.* **8**, 61–80 (2015).

196. Kingdon, K. H. A Method for the Neutralization of Electron Space Charge by Positive Ionization at Very Low Gas Pressures. *Phys. Rev.* **21**, 408–418 (1923).

197. Ceglarek, U. *et al.* Challenges and developments in tandem mass spectrometry based clinical metabolomics. *Mol. Cell. Endocrinol.* **301**, 266–271 (2009).

198. de Hoffmann, E. Tandem mass spectrometry: A primer. *J. Mass Spectrom.*

31, 129–137 (1996).

199. McLafferty, F. W. Tandem Mass Spectrometry. *Science* **214**, 280–287 (1981).

200. Thomas, S. N., French, D., Jannetto, P. J., Rappold, B. A. & Clarke, W. A. Liquid chromatography–tandem mass spectrometry for clinical diagnostics. *Nat. Rev. Methods Primer* **2**, 1–14 (2022).

201. Schymanski, E. L. *et al.* Identifying Small Molecules via High Resolution Mass Spectrometry: Communicating Confidence. *Environ. Sci. Technol.* **48**, 2097–2098 (2014).

202. Clarke, G. S., Page, A. J. & Eldeghaidy, S. The gut–brain axis in appetite, satiety, food intake, and eating behavior: Insights from animal models and human studies. *Pharmacol. Res. Perspect.* **12**, e70027 (2024).

203. Yang, M. *et al.* Separate orexigenic hippocampal ensembles shape dietary choice by enhancing contextual memory and motivation. *Nat. Metab.* **7**, 276–296 (2025).

204. Azevedo, E. P., Ivan, V. J., Friedman, J. M. & Stern, S. A. Higher-Order Inputs Involved in Appetite Control. *Biol. Psychiatry* **91**, 869–878 (2022).

205. Li, S. *et al.* The Mechanism of the Gut-Brain Axis in Regulating Food Intake. *Nutrients* **15**, 3728 (2023).

206. Deem, J. D., Faber, C. L. & Morton, G. J. AgRP neurons: Regulators of feeding, energy expenditure, and behavior. *FEBS J.* **289**, 2362–2381 (2022).

207. Millington, G. W. The role of proopiomelanocortin (POMC) neurones in feeding behaviour. *Nutr. Metab.* **4**, 18 (2007).

208. Grill, H. J. & Hayes, M. R. The nucleus tractus solitarius: a portal for visceral afferent signal processing, energy status assessment and integration of their combined effects on food intake. *Int. J. Obes.* **33**, S11–S15 (2009).

209. Leptin and insulin pathways in POMC and AgRP neurons that modulate energy balance and glucose homeostasis. https://www.embopress.org/doi/epdf/10.1038/embor.2012.174 doi:10.1038/embor.2012.174.

210. A Preprandial Rise in Plasma Ghrelin Levels Suggests a Role in Meal Initiation in Humans | Diabetes | American Diabetes Association. https://diabetesjournals.org/diabetes/article/50/8/1714/11298/A-Preprandial-Rise-in-Plasma-Ghrelin-Levels.

211. Little, T. J., Horowitz, M. & Feinle-Bisset, C. Role of cholecystokinin in appetite control and body weight regulation. *Obes. Rev.* **6**, 297–306 (2005).

212. Fakhry, J. *et al.* Distribution and characterisation of CCK containing enteroendocrine cells of the mouse small and large intestine. *Cell Tissue Res.* **369**, 245–253 (2017).

213. Batterham, R. L. & Bloom, S. R. The Gut Hormone Peptide YY Regulates Appetite. *Ann. N. Y. Acad. Sci.* **994**, 162–168 (2003).

214. Näslund, E. *et al.* Energy intake and appetite are suppressed by glucagon-like peptide-1 (GLP-1) in obese men. *Int. J. Obes.* **23**, 304–311 (1999).

215. Rozengurt, N. *et al.* Colocalization of the α-subunit of gustducin with PYY and GLP-1 in L cells of human colon. *Am. J. Physiol.-Gastrointest. Liver Physiol.* **291**, G792–G802 (2006).

216. Moayyeri, A., Hammond, C. J., Hart, D. J. & Spector, T. D. The UK Adult Twin Registry (TwinsUK Resource). *Twin Res. Hum. Genet.* **16**, 144–149 (2013).

217. Cirulli, E. T. *et al.* Profound Perturbation of the Metabolome in Obesity Is Associated with Health Risk. *Cell Metab.* **29**, 488-500.e2 (2019).

218. Dahabiyeh, L. A. *et al.* A Metabolic Pattern in Healthy Subjects Given a Single Dose of Metformin: A Metabolomics Approach. *Front. Pharmacol.* **12**, (2021).

219. Agueusop, I., Musholt, P. B., Klaus, B., Hightower, K. & Kannt, A. Short-term variability of the human serum metabolome depending on nutritional and metabolic health status. *Sci. Rep.* **10**, 16310 (2020).

220. Mathew, S. *et al.* Metabolic changes of the blood metabolome after a date fruit challenge. *J. Funct. Foods* **49**, 267–276 (2018).

221. Moholdt, T. *et al.* The effect of morning vs evening exercise training on glycaemic control and serum metabolites in overweight/obese men: a randomised trial. *Diabetologia* **64**, 2061–2076 (2021).

222. Rumora, A. E. *et al.* Plasma lipid metabolites associate with diabetic polyneuropathy in a cohort with type 2 diabetes. *Ann. Clin. Transl. Neurol.* **8**, 1292–1307 (2021).

223. Benedetti, E. *et al.* Plasma metabolomics profiling of 580 patients from an Early Detection Research Network prostate cancer cohort. *Sci. Data* **10**, 830 (2023).

224. Halama, A. *et al.* The metabolic footprint of compromised insulin sensitivity

under fasting and hyperinsulinemic-euglycemic clamp conditions in an Arab population. *Sci. Rep.* **10**, 17164 (2020).

225. Li, P. *et al.* Systems analysis of metabolic responses to a mixed meal test in an obese cohort reveals links between tissue metabolism and the gut microbiota. 2022.04.26.489057 Preprint at https://doi.org/10.1101/2022.04.26.489057 (2022).

226. Van Olden, C. C. *et al.* A systems biology approach to understand gut microbiota and host metabolism in morbid obesity: design of the BARIA Longitudinal Cohort Study. *J. Intern. Med.* **289**, 340–354 (2021).

227. Evans, A. M., DeHaven, C. D., Barrett, T., Mitchell, M. & Milgram, E. Integrated, Nontargeted Ultrahigh Performance Liquid Chromatography/Electrospray Ionization Tandem Mass Spectrometry Platform for the Identification and Relative Quantification of the Small-Molecule Complement of Biological Systems. *Anal. Chem.* **81**, 6656–6667 (2009).

228. Ford, L. *et al.* Precision of a Clinical Metabolomics Profiling Platform for Use in the Identification of Inborn Errors of Metabolism. *J. Appl. Lab. Med.* **5**, 342–356 (2020).

229. DeHaven, C. D., Evans, A. M., Dai, H. & Lawton, K. A. Organization of GC/MS and LC/MS metabolomics data into chemical libraries. *J. Cheminformatics* **2**, 9 (2010).

230. Scott, B. *et al.* Metformin and feeding increase levels of the appetite-suppressing metabolite Lac-Phe in humans. *Nat. Metab.* **6**, 651–658 (2024).

231. Rena, G., Pearson, E. R. & Sakamoto, K. Molecular mechanism of action of

metformin: old or new insights? *Diabetologia* **56**, 1898–1906 (2013).

232. Salpeter, S. R., Greyber, E., Pasternak, G. A. & Salpeter (posthumous), E. E. Risk of fatal and nonfatal lactic acidosis with metformin use in type 2 diabetes mellitus. *Cochrane Database Syst. Rev.* (2010) doi:10.1002/14651858.CD002967.pub3.

233. Klein, A. B. *et al.* The GDF15-GFRAL pathway is dispensable for the effects of metformin on energy balance. 21.

234. Long, J. *et al.* Metabolite biomarkers of type 2 diabetes mellitus and pre-diabetes: a systematic review and meta-analysis. *BMC Endocr. Disord.* **20**, 174 (2020).

235. Xu, T. *et al.* Effects of Metformin on Metabolite Profiles and LDL Cholesterol in Patients With Type 2 Diabetes. *Diabetes Care* **38**, 1858–1867 (2015).

236. Xiao, S. *et al.* Lac-Phe mediates the effects of metformin on food intake and body weight. *Nat. Metab.* **6**, 659–669 (2024).

237. Wheaton, W. W. *et al.* Metformin inhibits mitochondrial complex I of cancer cells to reduce tumorigenesis. *eLife* **3**, e02242 (2014).

238. Bridges, H. R. *et al.* Structural basis of mammalian respiratory complex I inhibition by medicinal biguanides. *Science* **379**, 351–357 (2023).

239. Wilcock, C. & Bailey, C. J. Accumulation of metformin by tissues of the normal and diabetic mouse. *Xenobiotica* **24**, 49–57 (1994).

240. The Primary Glucose-Lowering Effect of Metformin Resides in the Gut, Not the Circulation: Results From Short-term Pharmacokinetic and 12-Week Dose-Ranging Studies | Diabetes Care | American Diabetes Association.

https://diabetesjournals.org/care/article/39/2/198/37205/The-Primary-Glucose-Lowering-Effect-of-Metformin.

241. McCreight, L. J., Bailey, C. J. & Pearson, E. R. Metformin and the gastrointestinal tract. *Diabetologia* **59**, 426–435 (2016).

242. Rittig, N. *et al.* Metformin Stimulates Intestinal Glycolysis and Lactate Release: A single-Dose Study of Metformin in Patients With Intrahepatic Portosystemic Stent. *Clin. Pharmacol. Ther.* **110**, 1329–1336 (2021).

243. Metformin acts in the gut and induces gut-liver crosstalk | PNAS. https://www.pnas.org/doi/full/10.1073/pnas.2211933120.

244. Wang, S. *et al.* Intestinal monocarboxylate transporter 1 mediates lactate transport in the gut and regulates metabolic homeostasis of mouse in a sex-dimorphic pattern. *Life Metab.* **3**, load041 (2024).

245. Forslund, K. *et al.* Disentangling type 2 diabetes and metformin treatment signatures in the human gut microbiota. *Nature* **528**, 262–266 (2015).

246. Pavlo Petakh, Kamyshna, I. & Kamyshnyi, A. Effects of metformin on the gut microbiota: A systematic review. *Mol. Metab.* **77**, 101805 (2023).

247. Metformin Triggers PYY Secretion in Human Gut Mucosa | The Journal of Clinical Endocrinology & Metabolism | Oxford Academic. https://academic.oup.com/jcem/article/104/7/2668/5315430?login=false.

248. Mannucci, E. *et al.* Effect of Metformin on Glucagon-Like Peptide 1 (GLP-1) and Leptin Levels in Obese Nondiabetic Subjects. *Diabetes Care* **24**, 489–494 (2001).

249. Plomgaard, P. *et al.* GDF15 is an exercise-induced hepatokine regulated by

glucagon and insulin in humans. *Front. Endocrinol.* **13**, (2022).

250. Naja, K., Anwardeen, N., Al-Hariri, M., Al Thani, A. A. & Elrayess, M. A. Pharmacometabolomic Approach to Investigate the Response to Metformin in Patients with Type 2 Diabetes: A Cross-Sectional Study. *Biomedicines* **11**, 2164 (2023).

251. Nabrdalik, K. *et al.* Gastrointestinal adverse events of metformin treatment in patients with type 2 diabetes mellitus: A systematic review, meta-analysis and meta-regression of randomized controlled trials. *Front. Endocrinol.* **13**, (2022).

252. Bouchoucha, M., Uzzan, B. & Cohen, R. Metformin and digestive disorders. *Diabetes Metab.* **37**, 90–96 (2011).

253. van der Burgh, A. C. *et al.* Circulating metabolites associated with kidney function decline and incident CKD: a multi-platform population-based study. *Clin. Kidney J.* **17**, sfad286 (2024).

254. Fino, N. F. *et al.* Evaluation of novel candidate filtration markers from a global metabolomic discovery for glomerular filtration rate estimation. *Kidney Int.* **105**, 582–592 (2024).

255. Rogers, R. S. *et al.* Circulating N-lactoyl-amino acids and N-formyl-methionine reflect mitochondrial dysfunction and predict mortality in septic shock. *Metabolomics* **20**, 36 (2024).

256. Angus, D. C. & Poll, T. van der. Severe Sepsis and Septic Shock. *N. Engl. J. Med.* **369**, 840–851 (2013).

257. Krawczyk, C. M. *et al.* Toll-like receptor–induced changes in glycolytic metabolism regulate dendritic cell activation. *Blood* **115**, 4742–4749 (2010).

258. Yao, H., Shen, S., Gao, X., Song, X. & Xiang, W. The causal relationship between blood metabolites and rosacea: A Mendelian randomization. *Skin Res. Technol.* **30**, e13796 (2024).

259. Akin Belli, A., Ozbas Gok, S., Akbaba, G., Etgu, F. & Dogan, G. The relationship between rosacea and insulin resistance and metabolic syndrome. *Eur. J. Dermatol. EJD* **26**, 260–264 (2016).

260. Metformin as an anti-inflammatory agent: a short review in: Journal of Endocrinology Volume 251 Issue 2 (2021). https://joe.bioscientifica.com/view/journals/joe/251/2/JOE-21-0194.xml.

261. Metformin Inhibits Proinflammatory Responses and Nuclear Factor-κB in Human Vascular Wall Cells | Arteriosclerosis, Thrombosis, and Vascular Biology. https://www.ahajournals.org/doi/10.1161/01.ATV.0000201938.78044.75?url_ver=Z39.88-2003&rfr_id=ori:rid:crossref.org&rfr_dat=cr_pub%20%200pubmed.

262. Astrup, A. *et al.* Safety, tolerability and sustained weight loss over 2 years with the once-daily human GLP-1 analog, liraglutide. *Int. J. Obes.* **36**, 843–854 (2012).

263. Once-Weekly Semaglutide in Adults with Overweight or Obesity | New England Journal of Medicine. https://www.nejm.org/doi/full/10.1056/NEJMoa2032183.

264. Jang, C. *et al.* The Small Intestine Converts Dietary Fructose into Glucose and Organic Acids. *Cell Metab.* **27**, 351-361.e3 (2018).

265. Jang, C. *et al.* The small intestine shields the liver from fructose-induced

steatosis. *Nat. Metab.* **2**, 586–593 (2020).

266. JCI - Enzymes of fructose metabolism in human liver. https://www.jci.org/articles/view/105872.

267. Mor, I., Cheung, E. C. & Vousden, K. H. Control of Glycolysis through Regulation of PFK1: Old Friends and Recent Additions. *Cold Spring Harb. Symp. Quant. Biol.* **76**, 211–216 (2011).

268. Tappy, L. & Lê, K.-A. Metabolic Effects of Fructose and the Worldwide Increase in Obesity. *Physiol. Rev.* **90**, 23–46 (2010).

269. Effects of Fructose vs Glucose on Regional Cerebral Blood Flow in Brain Regions Involved With Appetite and Reward Pathways | Radiology | JAMA | JAMA Network. https://jamanetwork.com/journals/jama/article-abstract/1555133.

270. Payant, M. A. & Chee, M. J. Neural mechanisms underlying the role of fructose in overfeeding. *Neurosci. Biobehav. Rev.* **128**, 346–357 (2021).

271. Lee, B. M. & Woleve, T. M. S. Effect of glucose, sucrose and fructose on plasma glucose and insulin responses in normal humans: comparison with white bread. *Eur. J. Clin. Nutr.* **52**, 924–928 (1998).

272. Woods, S. C., Lotter, E. C., McKay, L. D. & Porte, D. Chronic intracerebroventricular infusion of insulin reduces food intake and body weight of baboons. *Nature* **282**, 503–505 (1979).

273. Benedict, C., Kern, W., Schultes, B., Born, J. & Hallschmid, M. Differential Sensitivity of Men and Women to Anorexigenic and Memory-Improving Effects of Intranasal Insulin. *J. Clin. Endocrinol. Metab.* **93**, 1339–1344 (2008).

274. Kong, M.-F. *et al.* Effects of oral fructose and glucose on plasma GLP-1 and

appetite in normal subjects. *Peptides* **20**, 545–551 (1999).

275. Effects of metformin on energy intake and satiety in obese children - Adeyemo - 2015 - Diabetes, Obesity and Metabolism - Wiley Online Library. https://dom-pubs.pericles-prod.literatumonline.com/doi/10.1111/dom.12426.

276. Lim, G. E. & Brubaker, P. L. Glucagon-Like Peptide 1 Secretion by the L-Cell: The View From Within. *Diabetes* **55**, S70–S77 (2006).

277. JCI - Nutritional and insulin regulation of fatty acid synthetase and leptin gene expression through ADD1/SREBP1. https://www.jci.org/articles/view/1411.

278. Koliaki, C., Kokkinos, A., Tentolouris, N. & Katsilambros, N. The Effect of Ingested Macronutrients on Postprandial Ghrelin Response: A Critical Review of Existing Literature Data. *Int. J. Pept.* **2010**, 710852 (2010).

279. Batterham, R. L. *et al.* Critical role for peptide YY in protein-mediated satiation and body-weight regulation. *Cell Metab.* **4**, 223–233 (2006).

280. Comparative Study of the Effects of Equal Amounts of Fat, Protein, and Starch on Plasma Cholecystokinin in Man: Scandinavian Journal of Gastroenterology: Vol 20, No 7. https://www.tandfonline.com/doi/abs/10.3109/00365528509088832.

281. Latner, J. & Schwartz, M. The Effects of a High-carbohydrate, High-protein or Balanced Lunch upon Later Food Intake and Hunger Ratings. *Appetite* **33**, 119–128 (1999).

282. Porrini, M., Crovetti, R., Testolin, G. & Silva, S. Evaluation of Satiety Sensations and Food Intake After Different Preloads. *Appetite* **25**, 17–30 (1995).

283. Marmonier, C., Chapelot, D. & Louis-Sylvestre, J. Effects of macronutrient

content and energy density of snacks consumed in a satiety state on the onset of the next meal. *Appetite* **34**, 161–168 (2000).

284. Mikkelsen, R. B. *et al.* Type 2 diabetes is associated with increased circulating levels of 3-hydroxydecanoate activating GPR84 and neutrophil migration. *iScience* **25**, 105683 (2022).

285. Peters, A. *et al.* Hydroxycarboxylic acid receptor 3 and GPR84 – Two metabolite-sensing G protein-coupled receptors with opposing functions in innate immune cells. *Pharmacol. Res.* **176**, 106047 (2022).

286. Tucker, G. *et al.* Metformin kinetics in healthy subjects and in patients with diabetes mellitus. *Br. J. Clin. Pharmacol.* **12**, 235–246 (1981).

287. Clinical Pharmacokinetics of Metformin | Clinical Pharmacokinetics. https://link.springer.com/article/10.2165/11534750-000000000-00000#Tab1.

288. Oh, J.-R. *et al.* Impact of Medication Discontinuation on Increased Intestinal FDG Accumulation in Diabetic Patients Treated With Metformin. *Am. J. Roentgenol.* **195**, 1404–1410 (2010).

289. Hamidizadeh, R. *et al.* Metformin Discontinuation prior to FDG PET/CT: A Randomized Controlled Study to Compare 24- and 48-hour Bowel Activity. *Radiology* **289**, 418–425 (2018).

290. Walcott, F. L. *et al.* Pilot Study Assessing Tolerability and Metabolic Effects of Metformin in Patients With Li-Fraumeni Syndrome. *JNCI Cancer Spectr.* **4**, pkaa063 (2020).

291. Frontiers | Metformin increases 3-hydroxy medium chain fatty acids in patients with type 2 diabetes: a cross-sectional pharmacometabolomic study.

https://www.frontiersin.org/journals/endocrinology/articles/10.3389/fendo.2024.1313597/full.

292. Schulze, A. S. *et al.* Evolutionary analyses reveal immune cell receptor GPR84 as a conserved receptor for bacteria-derived molecules. *iScience* **25**, (2022).

293. Menegazzo, L. *et al.* The antidiabetic drug metformin blunts NETosis in vitro and reduces circulating NETosis biomarkers in vivo. *Acta Diabetol.* **55**, 593–601 (2018).

294. Peters, A. *et al.* Metabolites of lactic acid bacteria present in fermented foods are highly potent agonists of human hydroxycarboxylic acid receptor 3. *PLOS Genet.* **15**, e1008145 (2019).

295. Peiris, M. *et al.* Decoy bypass for appetite suppression in obese adults: role of synergistic nutrient sensing receptors GPR84 and FFAR4 on colonic endocrine cells. *Gut* **71**, 928–937 (2022).

296. Metformin Triggers PYY Secretion in Human Gut Mucosa | The Journal of Clinical Endocrinology & Metabolism | Oxford Academic. https://academic.oup.com/jcem/article/104/7/2668/5315430?login=false.

297. Role of the G protein-coupled receptors GPR84 and GPR119 in the central regulation of food intake in rainbow trout | Journal of Experimental Biology | The Company of Biologists. https://journals.biologists.com/jeb/article/224/13/jeb242360/270772/Role-of-the-G-protein-coupled-receptors-GPR84-and.

298. Du Toit, E. *et al.* Effect of GPR84 deletion on obesity and diabetes

development in mice fed long chain or medium chain fatty acid rich diets. *Eur. J. Nutr.* **57**, 1737–1746 (2018).

299. Thangaraju, M. *et al.* GPR109A Is a G-protein–Coupled Receptor for the Bacterial Fermentation Product Butyrate and Functions as a Tumor Suppressor in Colon. *Cancer Res.* **69**, 2826–2832 (2009).

300. Petelin, A. *et al.* Effects of Royal Jelly Administration on Lipid Profile, Satiety, Inflammation, and Antioxidant Capacity in Asymptomatic Overweight Adults. *Evid. Based Complement. Alternat. Med.* **2019**, 4969720 (2019).

301. Bannister, C. A. *et al.* Can people with type 2 diabetes live longer than those without? A comparison of mortality in people initiated with metformin or sulphonylurea monotherapy and matched, non-diabetic controls. *Diabetes Obes. Metab.* **16**, 1165–1173 (2014).

302. Keys, M. T. *et al.* Reassessing the evidence of a survival advantage in Type 2 diabetes treated with metformin compared with controls without diabetes: a retrospective cohort study. *Int. J. Epidemiol.* **51**, 1886–1898 (2022).

303. Metformin as Anti-Aging Therapy: Is It for Everyone?: Trends in Endocrinology & Metabolism. https://www.cell.com/trends/endocrinology-metabolism/abstract/S1043-2760(19)30147-X.

304. Masarwa, R. *et al.* Efficacy and Safety of Metformin for Obesity: A Systematic Review. *Pediatrics* **147**, e20201610 (2021).

305. Saisho, Y. Metformin and Inflammation: Its Potential Beyond Glucose-lowering Effect. *Endocr. Metab. Immune Disord. - Drug TargetsFormerly Curr. Drug Targets - Immune Endocr. Metab. Disord.* **15**, 196–205 (2015).

306. Goldberg, R. B. *et al.* Effect of Long-Term Metformin and Lifestyle in the Diabetes Prevention Program and Its Outcome Study on Coronary Artery Calcium. *Circulation* **136**, 52–64 (2017).

307. Barzilai, N., Crandall, J. P., Kritchevsky, S. B. & Espeland, M. A. Metformin as a Tool to Target Aging. *Cell Metab.* **23**, 1060–1065 (2016).

308. El-Mir, M.-Y. *et al.* Dimethylbiguanide Inhibits Cell Respiration via an Indirect Effect Targeted on the Respiratory Chain Complex I *. *J. Biol. Chem.* **275**, 223–228 (2000).

309. Duca, F. A. *et al.* Metformin activates a duodenal Ampk–dependent pathway to lower hepatic glucose production in rats. *Nat. Med.* **21**, 506–511 (2015).

310. Howell, J. J. *et al.* Metformin Inhibits Hepatic mTORC1 Signaling via Dose-Dependent Mechanisms Involving AMPK and the TSC Complex. *Cell Metab.* **25**, 463–471 (2017).

311. Mitchell Crow, J. Canada's scientists are elucidating the dark metabolome. *Nature* **599**, S14–S15 (2021).

312. Jones, O. A. H. Illuminating the dark metabolome to advance the molecular characterisation of biological systems. *Metabolomics* **14**, 101 (2018).

313. Goto, Y., Nonaka, I. & Horai, S. A mutation in the tRNALeu(UUR) gene associated with the MELAS subgroup of mitochondrial encephalomyopathies. *Nature* **348**, 651–653 (1990).

314. Pavlakis, S. G., Phillips, P. C., DiMauro, S., De Vivo, D. C. & Rowland, L. P. Mitochondrial myopathy, encephalopathy, lactic acidosis, and strokelike

episodes: A distinctive clinical syndrome. *Ann. Neurol.* **16**, 481–488 (1984).

315. Nishizawa, M. *et al.* A mitochondrial encephalomyopathy with cardiomyopathy: A case revealing a defect of complex I in the respiratory chain. *J. Neurol. Sci.* **78**, 189–201 (1987).

316. Kobayashi, M. *et al.* Two cases of NADH-coenzyme Q reductase deficiency: Relationship to MELAS syndrome. *J. Pediatr.* **110**, 223–227 (1987).

317. Mandavilli, B. S., Santos, J. H. & Van Houten, B. Mitochondrial DNA repair and aging. *Mutat. Res. Mol. Mech. Mutagen.* **509**, 127–151 (2002).

318. Harada, M. *et al.* Bidirectional modulation of TCA cycle metabolites and anaplerosis by metformin and its combination with SGLT2i. *Cardiovasc. Diabetol.* **23**, 199 (2024).

319. Brooks, G. A. Lactate as a fulcrum of metabolism. *Redox Biol.* **35**, 101454 (2020).

320. Kobayashi, M. *et al.* Two cases of NADH-coenzyme Q reductase deficiency: Relationship to MELAS syndrome. *J. Pediatr.* **110**, 223–227 (1987).

321. El-Hattab, A. W., Adesina, A. M., Jones, J. & Scaglia, F. MELAS syndrome: Clinical manifestations, pathogenesis, and treatment options. *Mol. Genet. Metab.* **116**, 4–12 (2015).

322. Vissing, C. R., Dunø, M., Wibrand, F., Christensen, M. & Vissing, J. Hydroxylated Long-Chain Acylcarnitines are Biomarkers of Mitochondrial Myopathy. *J. Clin. Endocrinol. Metab.* **104**, 5968–5976 (2019).

323. Gui, D. Y. *et al.* Environment Dictates Dependence on Mitochondrial Complex I for NAD+ and Aspartate Production and Determines Cancer Cell

Sensitivity to Metformin. *Cell Metab.* **24**, 716–727 (2016).

324. Khodaei, F., Hosseini, S. M., Omidi, M., Hosseini, S. F. & Rezaei, M. Cytotoxicity of metformin against HT29 colon cancer cells contributes to mitochondrial Sirt3 upregulation. *J. Biochem. Mol. Toxicol.* **35**, e22662 (2021).

325. Jin, S. J., Hoppel, C. L. & Tserng, K. Y. Incomplete fatty acid oxidation. The production and epimerization of 3-hydroxy fatty acids. *J. Biol. Chem.* **267**, 119–125 (1992).

326. Ibdah, J. A. Acute fatty liver of pregnancy: An update on pathogenesis and clinical implications. *World J. Gastroenterol. WJG* **12**, 7397–7404 (2006).

327. Natarajan, S. K. & Ibdah, J. A. Role of 3-Hydroxy Fatty Acid-Induced Hepatic Lipotoxicity in Acute Fatty Liver of Pregnancy. *Int. J. Mol. Sci.* **19**, 322 (2018).

328. Cecatto, C., Godoy, K. dos S., da Silva, J. C., Amaral, A. U. & Wajner, M. Disturbance of mitochondrial functions provoked by the major long-chain 3-hydroxylated fatty acids accumulating in MTP and LCHAD deficiencies in skeletal muscle. *Toxicol. In Vitro* **36**, 1–9 (2016).

329. Jones, P. M., Burlina, A. B. & Bennett, M. J. Quantitative measurement of total and free 3-hydroxy fatty acids in serum or plasma samples: short-chain 3-hydroxy fatty acids are not esterified. *J. Inherit. Metab. Dis.* **23**, 745–750 (2000).

330. Cummings, D. E. & Overduin, J. Gastrointestinal regulation of food intake. *J. Clin. Invest.* **117**, 13–23 (2007).

331. Jais, A. & Brüning, J. C. Arcuate Nucleus-Dependent Regulation of Metabolism—Pathways to Obesity and Diabetes Mellitus. *Endocr. Rev.* **43**, 314–

328 (2022).

332. Suzuki, K., Simpson, K. A., Minnion, J. S., Shillito, J. C. & Bloom, S. R. The role of gut hormones and the hypothalamus in appetite regulation. *Endocr. J.* **57**, 359–372 (2010).

333. Brown, A. L. *et al.* Cerebrospinal Fluid Metabolomic Profiles Associated With Fatigue During Treatment for Pediatric Acute Lymphoblastic Leukemia. *J. Pain Symptom Manage.* **61**, 464–473 (2021).

334. Moya-Garzon, M. D. *et al.* A secondary β-hydroxybutyrate metabolic pathway linked to energy balance. 2024.09.09.612087 Preprint at https://doi.org/10.1101/2024.09.09.612087 (2024).